CHALMERS
UNIVERSITY OF TECHNOLOGY

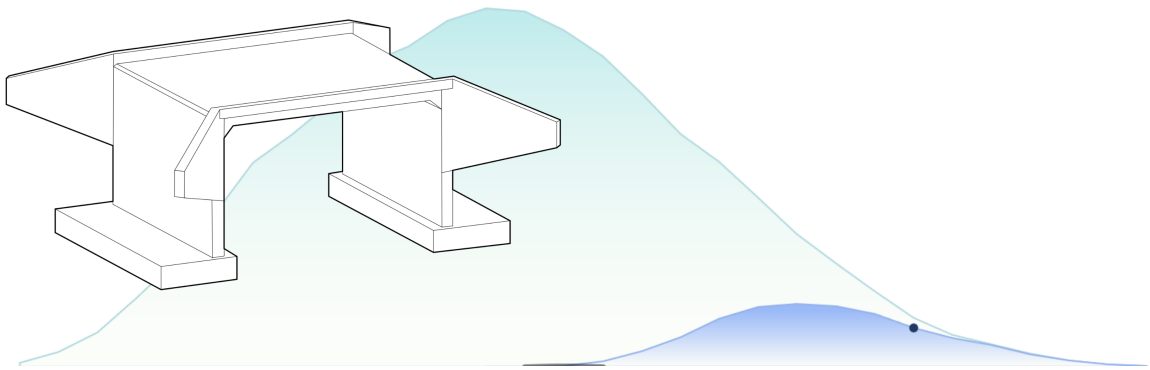

Set-Based Multi-Criteria Optimization of Slab Frame Bridges

A Study on the Implementation of a Set-Based Multi-Criteria Optimization Algorithm on Slab Frame Bridges, considering Investment Cost, Environmental Impact and Buildability

Master's thesis in Structural Engineering and Building Technology

FELICIA BERGENRAM, SIGRID ULANDER

DEPARTMENT OF ARCHITECTURE AND CIVIL ENGINEERING
CHALMERS UNIVERSITY OF TECHNOLOGY
Gothenburg, Sweden 2023
www.chalmers.se

Master's thesis 2023

Set-Based Multi-Criteria Optimization of Slab Frame Bridges

A Study on the Implementation of a Set-Based Multi-Criteria Optimization Algorithm on Slab Frame Bridges, considering Investment Cost, Environmental Impact and Buildability

FELICIA BERGENRAM, SIGRID ULANDER

CHALMERS
UNIVERSITY OF TECHNOLOGY

Department of Architecture and Civil Engineering
Division of Structural Engineering
Chalmers University of Technology
Gothenburg, Sweden 2023

Set-Based Multi-Criteria Optimization of Slab Frame Bridges
A Study on the Implementation of a Set-Based Multi-Criteria Optimization Algorithm on Slab Frame Bridges, considering Investment Cost, Environmental Impact and Buildability
FELICIA BERGENRAM AND SIGRID ULANDER

Industrial supervisors: Structural engineer Alexander Kjellgren and structural engineer specialist Per Kettil, Department of Bridge and Infrastructure projects at Skanska
Examiner and academic supervisor: Senior researcher Rasmus Rempling, Department of Architecture and Civil Engineering

Master's Thesis 2023
Department of Architecture and Civil Engineering
Division of Structural Engineering
Chalmers University of Technology
SE-412 96 Gothenburg
Telephone +46 31 772 1000

Cover: A visualization of the principal structure of a slab frame bridge, together with a normalized probability density distribution representing the environmental impact criterion for design solutions emerging from the optimization algorithm implemented.

Typeset in LaTeX
Printed by Chalmers Reproservice
Gothenburg, Sweden 2023

Set-Based Multi-Criteria Optimization of Slab Frame Bridges
A Study on the Implementation of a Set-Based Multi-Criteria Optimization Algorithm on Slab Frame Bridges, considering Investment Cost, Environmental Impact and Buildability
FELICIA BERGENRAM, SIGRID ULANDER
Department of Architecture and Civil Engineering
Chalmers University of Technology

Abstract

This master's thesis presents research performed on parametric multi-criteria optimization in early stage design of slab frame bridges, using set-based design. As a result of immense CO_2-emissions emerging from concrete production- and usage, there is a need for methods mitigating the volume of concrete without affecting the function of the structure. Set-based design was implemented in order to enable a wide design space during the design process, constituting a basis for facilitated negotiation in planning processes. Previous research suggests a general correlation between curtailed CO_2-footprint and cost reduction, due to minimized material use. However, the aspect of buildability may conflict with lessened material, as slim designs might simultaneously entail a more time consuming production. This research aimed to develop an optimization method with respect to investment cost and environmental impact, while concurrently considering the potentially contradictory criterion of buildability. Possible quantitative measurements of the buildability criterion were thus explored. In addition, the method focused on generating large data sets of possible bridge designs, increasing the potential of obtaining statistical significance in the optimization results. An algorithm was created using Python-programming within the Grasshopper interface, connected to the 3D modelling software Rhino. The results demonstrated the buildability criterion to be decisive when finding optimal bridge designs in the multi-criteria optimization. In relation to the reference project, it was concluded that the most optimal design was predominantly governed by buildability aspects, resulting in limited environmental impact reductions. Therefore, a geometrically optimized design with the lowest environmental impact was also sought, yielding slightly increased costs for the client, caused by buildability costs related to the slimmed design. Conclusively, there is considerable incentive for implementing set-based optimization procedures in the everyday work of bridge engineers. Thereby, far-fetched optimal solutions can be identified in an early stage providing a basis for negotiation during tendering procedures, and risks related to unforeseen costs are mitigated.

Keywords: multi-criteria optimization, parametric design, set-based design, automation, slab frame bridge, concrete, investment cost, environmental impact, buildability

Set-Baserad Multikriterieoptimering av Plattrambroar
En Studie på Tillämpningen av Set-Baserad Multikriterieoptimering på Plattrambroar med hänsyn till Investeringskostnad, Miljöpåverkan och Byggbarhet
FELICIA BERGENRAM, SIGRID ULANDER
Institutionen för Arkitektur och Samhällsbyggnad
Chalmers Tekniska Högskola

Sammanfattning

Denna masteruppsats presenterar en studie på tillämpningen av parametrisk multikriterieoptimering i det preliminära designskedet av plattrambroar, genom setbaserad design. Till följd av enorma koldioxidutsläpp orsakade av betongproduktion- och användning, finns ett behov av metoder som begränsar betongkonstruktioners volym utan att påverka deras strukturella funktion. Setbaserad design implementerades för att möjliggöra en öppen designrymd utmed designprocessen, vilket utgör en grund för förenklad förhandling i projekteringsprocesser. Tidigare studier påvisar en generell korrelation mellan minimerade materielmängder och såväl minskat koldioxidavtryck som avtagande kostnader. Däremot har byggbarhetskriteriet visat motstridiga effekter relaterade till minskad materialåtgång, eftersom slimmade utformningar i flera avseenden kan kopplas till mer tidskrävande produktion. Studien syftade till att skapa en optimeringsmetod med hänsyn till investeringskostnad och miljöpåverkan, samtidigt som det potentiellt motstridiga byggbarhetskriteriet togs i beaktning. Vidare undersöktes möjliga kvantifierbara mått på byggbarhetskriteriet. Ett fokusområde i optimeringsmetoden var att generera stora data-set av möjliga broutformningar för att öka potentialen till statistisk signifikans i optimeringsresultatet. En algoritm skapades i Python, implementerat i programvaran Grasshoppers gränssnitt, kopplat till modelleringsprogrammet Rhino. Resultatet belyste byggbarhetskriteriets avgörande inverkan på de optimala broutformningarna. I relation till ett referensprojekt kunde slutsatsen dras att den mest optimala broutformningen i stor utsträckning styrdes av byggbarhetsaspekter, vilket begränsade nedskärningen av miljöpåverkan. Därför söktes även en geometriskt optimerad broutformning med minimerad miljöpåverkan, vilken demonstrerade något ökade kostnader för kunden, orsakade av byggbarhetskostnader relaterade till den slimmade utformningen. Sammanfattningsvis finns incitament för att införa setbaserade multikriterieoptimeringsmetoder i det vardagliga arbetet som utförs av brokonstruktörer. Därigenom kan osannolika optimala lösningar identifieras i ett tidigt skede, vilket kan användas som förhandlingsunderlag i anbudsprocesser, samtidigt som risken för oförutsedda kostnader minskas.

Nyckelord: multikriterieoptimering, parametrisk design, setbaserad design, automation, plattrambro, betong, investeringskostnad, miljöpåverkan, byggbarhet

Acknowledgements

This research project was carried out at the department of *Structural Engineering and Building Technology* at Chalmers University of Technology, bringing an end to a five year long educational journey. Additionally, the research was performed in close cooperation with the *Bridge and Infrastructure Department* at Skanska, in Gothenburg, during the spring of 2023.

An initial interest for the topic of parametric design appeared during the early years of our studies at the bachelors program *Architecture and Engineering*, ever growing since then. The design philosophy enables effective generation and comparison of design alternatives, allowing for considering sustainability on multiple societal levels simultaneously. With parametric design and environmental awareness being two topical fields of development within the construction industry, in combination with our growing interests, the choice of subject was rather given. Also, a newly found curiosity for the possibilities related to Python-programming spiked the interest for parametric optimization.

We want to direct a special thanks to our supervisors at Skanska, Alexander Kjellgren and Per Kettil, for all the inputs and the constant support throughout the completion of this thesis. Also, the continuous enthusiasm shown by our supervisor and examiner at Chalmers, Rasmus Rempling, has been highly motivating throughout the entire process.

I, Felicia Bergenram, would like to give a special thanks to my grandparents for the constant support and shown interest throughout my studies, especially during the completion of this thesis.

I, Sigrid Ulander, would like to give thanks to my supportive family, especially for the wise advise that I have received from my brother during my studies.

Felicia Bergenram and Sigrid Ulander, Gothenburg, June 2023

List of Acronyms

Below is the list of acronyms that have been used throughout this thesis listed in alphabetical order:

AI	Artificial Intelligence
BIM	Building Information Modelling
FEM	Finite Element Modelling
FLS	Fatigue Limit State
GHG	Green House Gas
GWP	Global Warming Potential
LCC	Life Cycle Cost
PBD	Point-Based Design
SBD	Set-Based Design
SLS	Serviceability Limit State
ULS	Ultimate Limit State

Nomenclature

This chapter presents the main nomenclature of indices, sets, parameters, and variables referred to in this thesis.

Input parameters

L	Span length of bridge deck
H	Structural height of bridge
W	Width of bridge deck, transverse to span direction
bc	Boundary condition between frame leg and foundation slab

Indices

i	Index for cross-section within a bridge design
j	Index for tensile reinforcement layer within a cross-section i

Variable parameters

h_i	Cross-sectional height of cross-section i
$n_{i,j}$	Number of tensile reinforcement bars in row j in cross-section i
f_{ck_i}	Characteristic compression concrete strength in cross-section i
ϕ_i	Reinforcement diameter in cross-section i

Optimization elements

x	One bridge design alternative
$F_{eq}(x)$	Objective function (the equivalent cost of all optimization criteria)
$f_{inv}(x)$	Partial objective function (the investment cost criterion)
$f_{env}(x)$	Partial objective function (the environmental impact cost criterion)
$f_{build}(x)$	Partial objective function (the buildability cost criterion)
$\mu_{ULS,i}(x)$	ULS-utilization ratio constraints set on all cross-sections
$\mu_{SLS,i}(x)$	SLS-utilization ratio constraint set on all cross-sections

Design spaces

Design space $\mathcal{A}$	Set of feasible and non-feasible bridge design solutions, regardless of input parameters
Design space $\mathcal{B}$	Set of feasible and non-feasible bridge design solutions, for specified input parameters
Design space $\mathcal{C}$	Set of feasible bridge design solutions, for specified input parameters
Design space $\mathcal{D}$	Set of most optimized bridge design solutions, for specified input parameters

Contents

List of Figures

List of Tables

1
Introduction

This chapter introduces the thesis background, aim, limitations, research questions and the methodology applied.

1.1 Background

In 2018, the Swedish parliament established new environmental laws as a result of the Paris agreement made in 2015. The goal is to reduce the carbon dioxide emissions by 50% by 2030 and eventually achieve climate neutrality in 2045. An action plan has been developed under the leadership of Skanska, signed by the main contractors within the industry, to ensure necessary changes within the construction field (*Färdplan för fossilfri konkurrenskraft*, n.d.).

Today's construction industry is responsible for a vast environmental impact regarding its extensive emissions of greenhouse gases (GHG). Concrete in particular contributes to considerable amounts of greenhouse gases during production, maintenance and demolition (Kim et al., 2016). The cement production alone is accountable for approximately 8% of the global carbon dioxide (CO_2) emissions (Cosentino et al., 2020). In order to reach the goals set by the Swedish legislation, it is of immense importance to take measures for mitigating the use of construction material in general, and concrete in particular. Such measures can be taken by challenging traditional design approaches and developing optimization algorithms for minimizing the material usage.

The construction industry is characterized by a large amount of repetitive work in designing well-known and commonly used construction types, leaving a demand for parametric models to save time (Girardet & Boton, 2021). Bridge engineers would benefit from having access to such models for the most commonly used bridge types in Sweden, being the slab frame bridge, slab bridge and girder bridge (Olsson McDowell, 2021).

Parametric design is a method where modelling is controlled by a set of connected variables, which enables efficient generation of different solutions. As presented by Khairulzaman, H. A., and Usman, F. (2018), automation within the construction industry is an increasingly developing field with potential of significant gains. As less repetitive work is needed, time and resources can instead be used for development and innovation or working creatively with smart solutions. By creating parametric

models there is a potential for enhancing the structural efficiency and to implement algorithms that optimize the structures on criteria such as cost (Solat Yavari et al., 2016) and environmental impact (Solat Yavari et al., 2017), without compromising buildability (Rempling et al., 2019). Furthermore, parametric design can be extended to a decision based multi-criteria decision analysis in which the evaluation and decision making of generated design alternatives is automated. Decision based design entails opportunities for enhancing the creativity of the design process (Lee & Ostwald, 2020).

Different research projects have been carried out on the subject of structural optimization of concrete bridges, resulting in somewhat differing conclusions. In general, the observed trend is that there is a close correlation between cost mitigation and minimized carbon footprint (Mathern et al., n.d.). Some studies show that the final optimized design ends up being the same in both cases, no matter if optimizing towards economics or carbon dioxide emissions (Rempling et al., 2019). Others show diverging results in terms of the cross-sectional design when optimizing on the two criteria separately (Solat Yavari et al., 2017), making the client having to prioritize economical or environmental sustainability when moving forward with the project.

Despite existing research on the topic, newly developed methods have not yet been implemented in large scale. As the design of different bridge structures is still based on traditional methods that have been adopted for many years, there is potential for using optimization routines to a greater extent than what is currently being done (*Färdplan för fossilfri konkurrenskraft*, n.d.). Producing preliminary design proposals with environmental aspects as the starting point would be a step towards preventing unnecessary climate impact. A way of integrating the environmental aspects early on could be by adjusting the assessment procedure of tendering proposals.

Today's traditional design procedure is governed by point-based design (PBD) (Fernández Luis Santiago & Tarazona Rams David, 2014), in which decisions need to be made for every step in the design process (Parrish et al., 2007). The methodology of set-based design (SBD), on the contrary, maintains a wide design space for as long as possible. Consequently, information can be provided during a project's progress when there is still a possibility to adjust the design without major additional costs, thus maintaining the assigned budget (Mathern, 2019). Implementing SBD can facilitate optimization procedures of concrete structures, contributing to the work towards achieving the climate goals added to the Swedish legislation (Rempling et al., 2019).

The tendering process regarding infrastructural investments is generally governed by economic aspects (Boverket, 2022a), by using the *Lowest price-* or *Lowest total cost- method*. In some cases the tendering proposal can be evaluated using the so called *Most economically advantageous- method*, where additional profits are given to the contractor based on other criteria related to sustainability on different

societal levels. One such criteria could be the extent of environmental focus shown in the tendering proposal (Boverket, 2022b). Necessary changes within the field entail making sustainability considerations an essential aspect in the tendering offers, for both clients and contractors.

Additionally, ethical sustainability should be acknowledged in parametric optimization. An important ethical dilemma arising when developing an automated design process is the possible consequences from not being in control of every design step. In many cases, input parameters for the parametric model are defined by the user, followed by an output of the optimized structural design without any transparency of the process in between. This *black box - phenomenon*, where the user is not in control of the processes occurring between input and output, is important to consider (Kenton, 2022).

Moreover, it is important to keep buildability in mind when developing structurally optimized designs, as the final design has to be feasible in practice ("Constructability in Construction and Issues at Design and Execution", 2023). Buildability is, from a corporate perspective, foremost a matter of worker safety and efficiency, thereby cost. Efficient productions entail less time required, being of economical advantage for the contractor and the client. In other terms, optimization towards buildability is not only valuable in a societal sense, concerning manufacturers, construction workers and adjacent society. From a corporate point of view, cost efficiency from effective production is an economic incentive (Chigozie Osuizugbo et al., 2022).

Consequently, considering the potential environmental-, time- and cost gain, it can be of vast advantage to develop efficient methods for parametric optimization of bridge structures. Implementing such procedures can be a step towards achieving the climate goals added to the Swedish legislation in 2018. Considering the various findings in previous projects, further development of optimization methods is required, contributing to the existing research. One necessary improvement is further implementation of the buildability aspect within structural optimization, as means of generating feasible designs and lowering the overall construction costs. Multi-criteria optimization towards investment cost, environmental impact and buildability can be an economic incentive for including environmental considerations in the tendering process.

1.2 Aim

This master's thesis aimed to challenge today's ways of working within the structural engineering field, focusing on the early design process of bridge structures. The study sought to evaluate the possibilities of implementing parametric optimization algorithms in early design as means of finding cost- and environment optimized solutions that take buildability into consideration. The goal was thus to develop an automated set-based parametric model, containing a multi-criteria decision analysis, for early design of slab frame bridges.

1.3 Limitations

The research was performed using 2D linear-elastic analysis, as means of minimizing the computational complexity, enabling production of large sets of design alternatives. A limitation made on the scope was to implement the optimization algorithm on one specific bridge construction type – slab frame bridges. Moreover, the optimization was conducted solely for the bridge deck and frame legs, disregarding foundation slabs and wing walls. Design verifications were further limited to ultimate limit state (ULS) and deflections within serviceability limit state (SLS), excluding fatigue limit state (FLS).

1.4 Research questions

By creating the multi-criteria optimization procedure for slab frame bridges, the goal was to answer the following research questions:

- Is linear-elastic 2D analysis sufficient for the preliminary design of slab frame bridges in order to mitigate the computational complexity, to ultimately achieve statistical significance?
- Is Grasshopper a suitable software for parametric optimization using Python-programming?
- How can buildability be defined in measurable quantities, to enable the implementation of the criterion within an optimization algorithm?
- Are there gains to be made by implementing optimization procedures considering investment cots, environmental impact and buildability for slab frame bridges?
- What are the major aspects affecting the outcome of the optimization algorithm?
- What are the future prospects of implementing optimization procedures during the preliminary design phase of slab frame bridges?

1.5 Methodology

The initial phase of the work consisted of a literature study, evaluating existing research of parametric models and optimization algorithms, in order to gain knowledge on the current developments observed within the field. Additionally, national requirements on the structural performance of slab frame bridges were examined and compiled, to ease the calculation procedure. Furthermore, a study was performed on the conventional preliminary design procedure of slab frame bridges and possible interpretations of the buildability criterion. Dialogues were held with employees at Skanska, specialized within structural engineering and cost calculation, in order to understand the practice implemented today.

The principal method applied consisted of developing a parametric optimization algorithm for the chosen bridge type. As basis for the optimization, the parametric

design software Grasshopper, supported by the 3D modelling tool Rhinoceros 3D™ (commonly referred to as Rhino), was utilized. The algorithm itself was developed as a Python script within the Grasshopper software, which enabled instant visualization of results via Rhino.

The main focus was the development of a set-based multi-criteria optimization algorithm, including generation of design alternatives, structural verification and evaluation of optimization criteria – investment cost, environmental impact and buildability. The load effects calculated within the algorithm were verified by comparison to a reference project. As output, the model provided multiple optimized solutions, which were compared and analysed in comparison to another reference project. The possibilities of implementing parametric optimization algorithms as means of minimizing costs and environmental impact, while considering the cost effects of buildability, were then concluded and discussed.

2
Theory

This chapter presents the theory behind the environmental impact caused by the construction industry, different design approaches, slab frame bridges, parametric optimization and the software used. Additionally, possible interpretations of the investment cost-, environmental impact- and buildability criteria are explored.

2.1 Environmental impact of the construction industry

The annual outlet of green house gases in Sweden caused by the construction sector reaches about the same levels as the emissions due to car-transportation and exceeds the levels representing emissions from busses and trucks, as shown in Figure 2.1 (Westlund et al., 2021). Looking further into the construction field, around 80% of the emissions originate from material production – mainly cement and steel –, while the last 20% is due to tasks performed on the production site, as well as the transportation of construction materials (*Färdplan för fossilfri konkurrenskraft*, n.d.).

Furthermore, concrete is the most versatile construction material, being used in 90% of cases while steel and timber together constitutes the last 10% (*Färdplan cement för ett klimatneutralt betongbyggande*, 2018). This results in, from a global perspective, that approximately 8% of CO_2-emissions originate from cement-production (Cosentino et al., 2020). For context, the industry sector as a whole constitutes approximately 21% of the global CO_2-emissions (Intergovernmental Panel on Climate Change. Working Group III & Edenhofer, n.d.), as shown in Figure 2.2. The cement production process involves heating limestone ($CaCO_3$) in a rotary kiln, subjected to a temperature of approximately 1400 C°. The chemical reaction – calcination – produces CO_2 and lime (CaO), the latter being the cement clinker which is then ground into cement (Lea & Mason, 2022). 50% of the emissions due to cement production originate from the actual calcination procedure, while 40% comes from the fuel used to heat the rotating kiln. The last 10% is due to electricity and transportation of materials (Anand, 2013). To reduce the CO_2-emissions due to cement production, one possibility is to minimize the use of cement by either focusing on structural efficiency or by implementing cement-replacement materials. Another way would be to neglect using fossil fuels as the main source of heat for the rotating kiln.

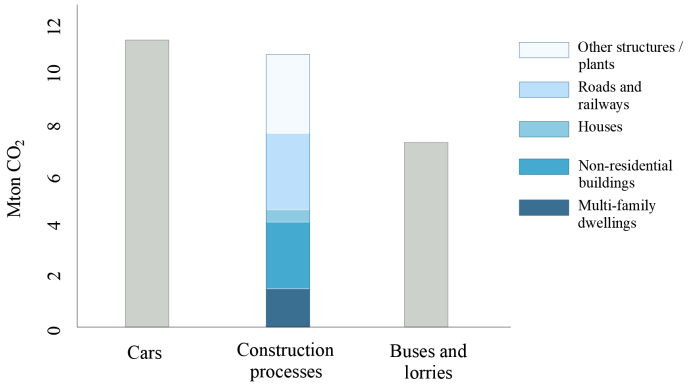

Figure 2.1: Annual green house gas emissions in Sweden according to Westlund et al. (2021)

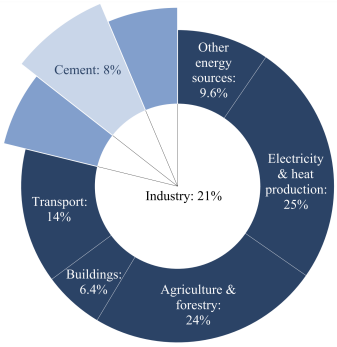

Figure 2.2: Global CO_2 emissions from the industry sector (Intergovernmental Panel on Climate Change. Working Group III & Edenhofer, n.d.), of which 8% of global emissions come from cement (Cosentino et al., 2020)

Moreover, as an effect of the current climate crisis, which the construction sector has highly contributed to, an agreement was made in Paris in 2015 to stop global warming. 196 parties conciliated on the matter (United Nations, 2023). As a result of the Paris agreement the Swedish parliament formulated goals and implemented new environmental laws during 2018, in line with the agreed terms. The general goal is to half the carbon dioxide emissions by 2030, to eventually be able to reach net zero emissions by 2045. An action plan has been developed under the leadership of Skanska, *Färdplan för fossilfri konkurrenskraft*, signed by the main contractors within the industry, to ensure necessary changes within the construction field. Many of the recommended improvements are related to the early design phase, where possibilities to influence the end product are large without major economical costs. One recommendation is to increasingly present environmental considerations in the tendering proposals, even if it is not asked for. Another recommendation is to implement digital models of the design and the construction process to a larger extent, to be able to foresee design problems and minimize waste products on the construction site (*Färdplan för fossilfri konkurrenskraft*, n.d.).

Research projects performed indicate that there is a possibility to achieve a 50% reduction of emissions within bridge construction by implementing the technologies that we already have today. Even if the technology exists, a vast challenge lies in implementing the new findings in the everyday work performed by bridge engineers. Additionally the design norms used in Sweden often result in over-dimensioning, hence causing unnecessary use of materials. Further research is needed on the integration of new technology in the common practice of bridge engineers, being a vital part in realizing necessary changes within the construction field. The action plan recognizes that the development within the field has to occur in consonance with what the market wants and what is feasible, since the final designs also have to be constructed in reality (*Färdplan för fossilfri konkurrenskraft*, n.d.).

An environmental focus needs to be adopted at all levels of the construction process, amongst all stakeholders, in order to avoid the status quo phenomenon. To impact the current situation there has to be a change in mindset amongst people within the field, where the focus is partly shifted from economical gains to environmental gains (*Färdplan för fossilfri konkurrenskraft*, n.d.). In a small scale, steps towards the environmental transition have been taken, however still leaving considerable potential for further development. In today's construction industry, environmental impact is not a direct corporate cost. However, demands on climate action are increasing. In 2022, a new Swedish law entered into force, stating that construction companies are responsible of publishing a climate declaration for building construction projects (SFS2021:787). Moreover, the Swedish Transport Administration as a client has developed a process of demanding specific environmental goals to be met by the contractor, where additional profits are given if the emissions are decreased further than what is specified. By adopting such ways of working and by introducing legislations regulating the climate impact of all new infrastructural projects, the awareness of environmental improvements can be spread amongst the different stakeholders (*Färdplan för fossilfri konkurrenskraft*, n.d.).

By finding means of implementing new technologies minimizing the use of materials, the construction field can be a vital part of the necessary changes needed to achieve the climate goals stated in the Paris agreement.

2.2 Design procedures

In a design procedure, different approaches in developing and selecting alternatives can be adopted. A distinction can then be made between *point-based design* (PBD) and *set-based design* (SBD). Design processes within the construction industry are today predominantly governed by PBD (Parrish et al., 2007). Furthermore, the Swedish Transport Administration has established a planning-process which is to be followed for all larger infrastructural projects in Sweden. The aim of the procedure is to ensure that a certain design methodology is followed, to ensure quality and environmental awareness (Miliutenko, 2022). The difference between PBD and SBD, as well as the planning-process implemented by the Swedish Transport Administration are presented in the following sections.

2.2.1 Point-based and set-based design

The traditional design approach that has been adopted by structural engineers for decades is based on a step-wise chronology, referred to as point-based design, visualised in Figure 2.3. The methodology of PBD is based on initially choosing a plausible design for every step in the process, after which the design is refined as the detailing is developing. A characteristic of PBD is that the design tends to be obtained from a base design uninformed about buildability aspects involving rebar fabricators, concrete suppliers and construction site. In other terms, PBD risks excluding a broader production perspective in the generation and choice of designs. (Parrish et al., 2007)

Set-based design refers to procedures that, as opposed to PBD, maintain a broad *design space* for as long as possible. Therefore, a specific solution is not decided in every design step. Rather, a set of possible solutions is narrowed down as information is established by the stakeholders involved, visualised in Figure 2.3 (Levandowski et al., 2014). The progression of SBD is thus characterized by decreasing the design space as alternatives are deselected. Thereby, information can be provided during the progression of a project when there is still a possibility to change the design, as absolute decisions have been avoided by instead narrowing down the design space. Thus, a parametric SBD allows for an automatic generation of design alternatives (Parrish et al., 2007). By implementing SBD, all design solutions within the sets are continuously accessible, enabling a constant comparison of alternatives and the possibility of tracing back, facilitating negotiation (Parrish et al., 2007). Moreover, the criterion of environmental impact can be used as basis for the decision making during early-stage design (Penadés-Plà et al., 2016), ultimately challenging the traditional approach of tendering procedures which are governed by economical aspects (Ek et al., 2019).

To further concretize the issue of PBD, complex problems arise from only considering one design alternative simultaneously, illustrated in Figure 2.4. When learning points occur along the project execution, in the shape of new information, the current design solution needs modification according to the new circumstances. When additional learning points emerge further down the project time-line, the new information might be too comprehensive resulting in the need to completely reconsider the current design in order to fulfill the newly set demands. When instead applying the SBD-procedure, learning points such as changes in dimensions or new information regarding the construction site can provide useful information needed to limit the design space. As a result of multiple learning points, the design space can be limited down to one optimal solution. Hence, working with SBD provides an economical safety-net to avoid extensive design changes due to unforeseeable changes of conditions resulting in increasing expenditure.

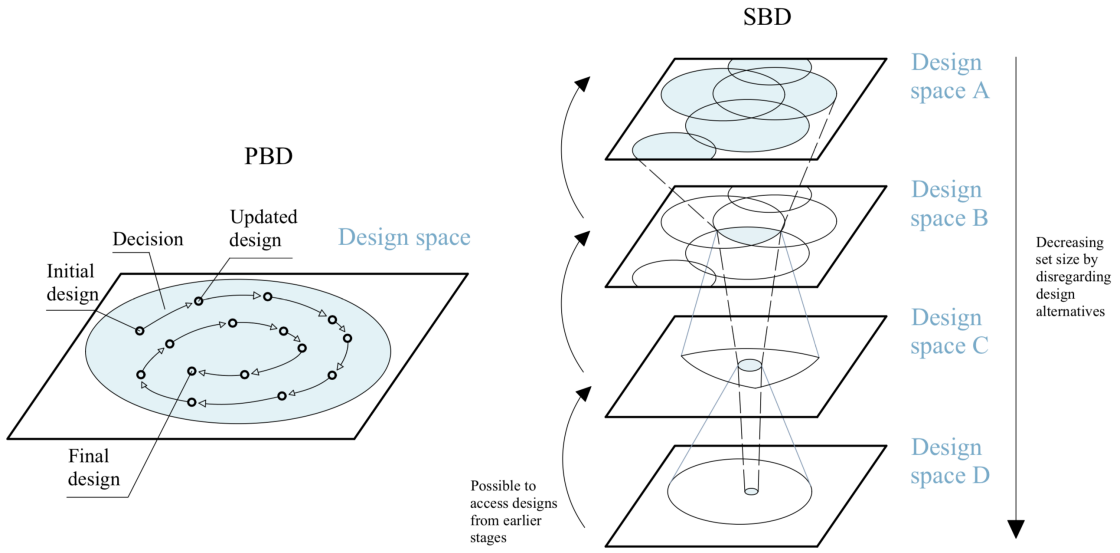

Figure 2.3: A visual representation of the design process following SBD, in comparison to the more traditional PBD procedure.

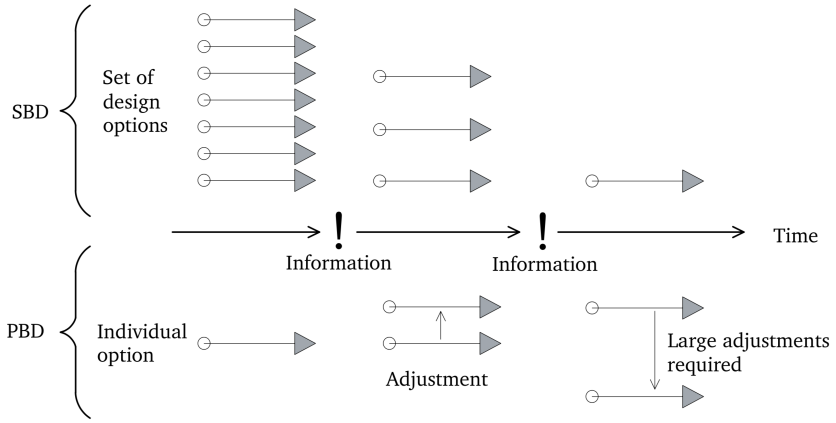

Figure 2.4: The difference between SBD and PBD related to the information gain throughout the progression of a planning-process.

2.2.2 Planning process

The Swedish Transport Administration has established a planning process for large infrastructural projects (>50 million SEK) in order to specify when certain deliverables are expected to ensure economical and environmental sustainability throughout the whole project lifetime. The established methodology was implemented in consonance with the newly developed action plan aiming at climate neutrality within the construction field by 2045. The planning process is further aspired to ensure consistency in the evaluation and documentation of the climate impact caused by infrastructural projects to enable the comparison of different solutions in order to strive for further improvements.

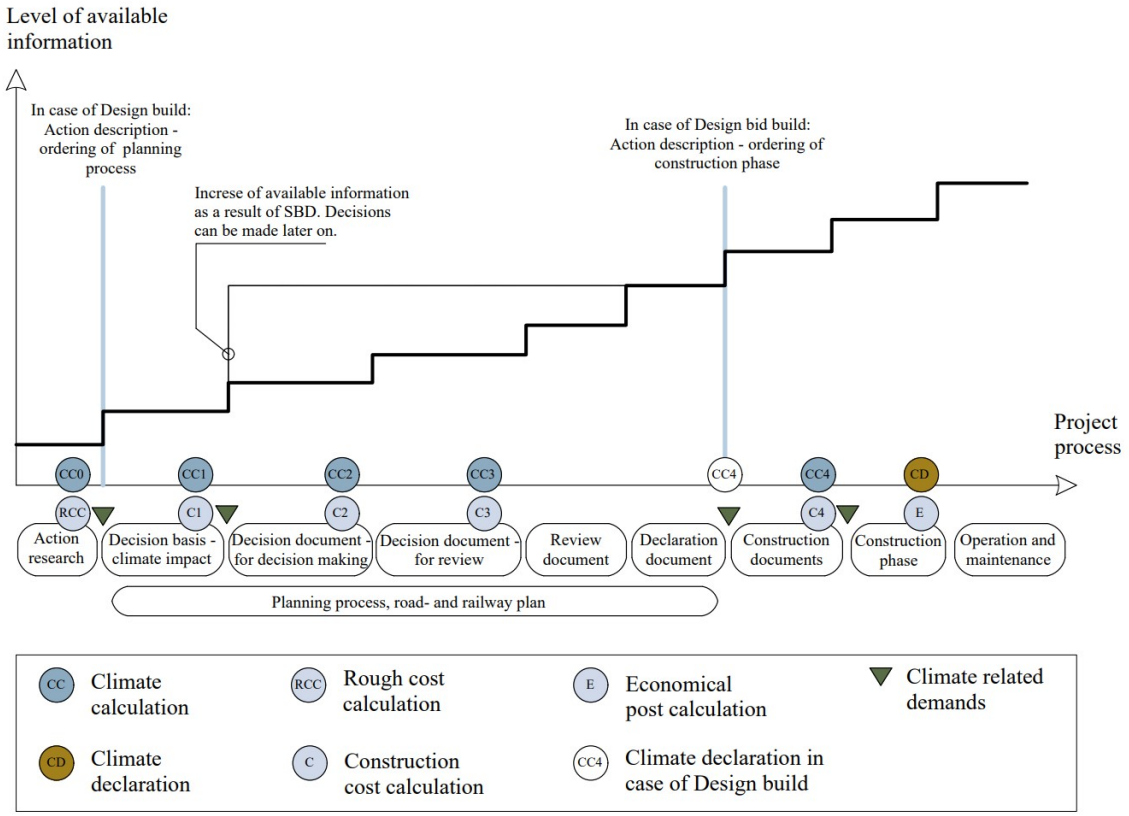

Figure 2.5: Principle figure och information increase during the project planning process, according to Miliutenko (2022).

An infrastructural project can be decomposed into nine main phases according to the working procedure implemented by the Swedish Transport Administration, visualised in Figure 2.5 (Miliutenko, 2022). During the first phase, *Action research*, an initial investigation is performed in order to concretize the main purpose of the project and the different demands giving rise to the need for a new infrastructural investment. This phase is carried out in close communication with the municipalities and the country council, to ensure an action plan where all demands have been brought to light, to ultimately reach synergy within the infrastructural system (Trafikverket, 2018). The first phase is completed by delivering a rough estimation of costs and a climate calculation indicating the anticipated energy use and climate impact from a complete life cycle perspective of the construction that is to be built (Trafikverket, 2022a).

The succeeding phases, two to six, specifically describe the planning process. The second phase, *Decision basis - climate impact*, involves collecting information about the predicted magnitude of climate impact, which is to be used as basis for the following decision performed by the country board (*Samrådsunderlag*, 2022). This phase is also concluded by performing a climate calculation and a cost calculation. Consecutively, phase three and four, *Decision document - for decision making* and *Decision document - for review*, involve presenting localisation alternatives and the corresponding environmental impacts. In the case of planning for an

extensive infrastructural investment, the alternatives are presented to the Swedish government, performing the final decision making. The chosen alternative is then further developed, creating documentation to be subjected to a final review (*Nya vägar och järnvägar - Så här planerar vi*, 2013). Each of the two phases are concluded by performing additional cost- and climate calculations. During phase five, *Review document*, the submitted documentation is exposed to the opinion of the public. The project proposal is available for review at the Swedish Transport Administration, but information is also spread in the prevailing area in order to get feedback from the people affected (*Vägplan, granskningshandling:Plan-och miljöbeskrivning*, 2022). During phase six, *Declaration document*, the final decision is established by the Swedish Transport Administration and the project plan becomes legally binding (*Samrådsredogörelse: Göteborg-Borås, en del av nya stambanor*, 2021).

Finally, construction documents are produced and delivered during phase seven, *Construction documents*, concluded by conducting the final cost- and climate calculations. Furthermore, the process continues with the *Construction* phase, phase eight, which is wrapped up by producing a climate declaration and a cost calculation for the finalized infrastructural project. The last and ninth phase is the *Operation and maintenance* phase.

Throughout the complete process, the demands set on climate impact need to be met, more specifically during phase one, two, six and seven. As previously stated, the planning process introduced by the Swedish Transport Administration was implemented in order to contribute to achieving net zero emissions by 2045. By constantly performing new and more detailed cost- and climate calculations as the project proceeds and more information is known, the goals of climate and environmental sustainability are mitigated. The presumption for more detailed calculations is the gain of additional information along the project timeline, being an important factor when trying to optimize factors related to sustainability.

A parallel can be drawn between the project process, as described by the Swedish Transport Administration, and the implementation of SBD. Figure 2.5 demonstrates the gradual information gain throughout the project process, in connection to the aforementioned phases one through nine. As new information is gained, decisions are made, resulting in progress. SBD drastically increases the degree of available information in the early design phases, leaving time to ensure that all requirements are met before the final decision is made later on, facilitating an interdisciplinary cooperation between stakeholders (Rempling et al., 2015). Figure 2.5 shows how SBD can increase the level of available information in the preliminary design phase, which enables including aspects such as buildability earlier in the project, without the need to make a decision earlier. Thus, the design space can be kept open during a larger portion of the project.

2.3 Slab frame bridges

Slab frame bridges are commonly used for span lengths up to 20-25 meters (Almén, 2016) and constitute around 46% of all the shorter span bridges in Sweden (*Klimatoptimerat byggande av betongbroar - Råd och vägledning*, 2017). To carry longer spans, up to 35 meters, prestressing can be implemented but is seldom economically feasible. The slab frame bridge enables a quick construction procedure and minimal maintenance throughout the service life (Solat Yavari et al., 2017), making it a suitable option for pedestrian/bike- and road crossings. Due to its frequent occurrence in Sweden, there are economical and environmental gains to be made by optimizing the structural performance of the slab frame bridge construction.

The structural elements of a slab frame bridge are wing walls, edge beams, frame legs, haunches, bridge deck and foundation, as seen in Figure 2.6.

The structural performance and the preliminary design procedure of slab frame bridges are presented in the following sections.

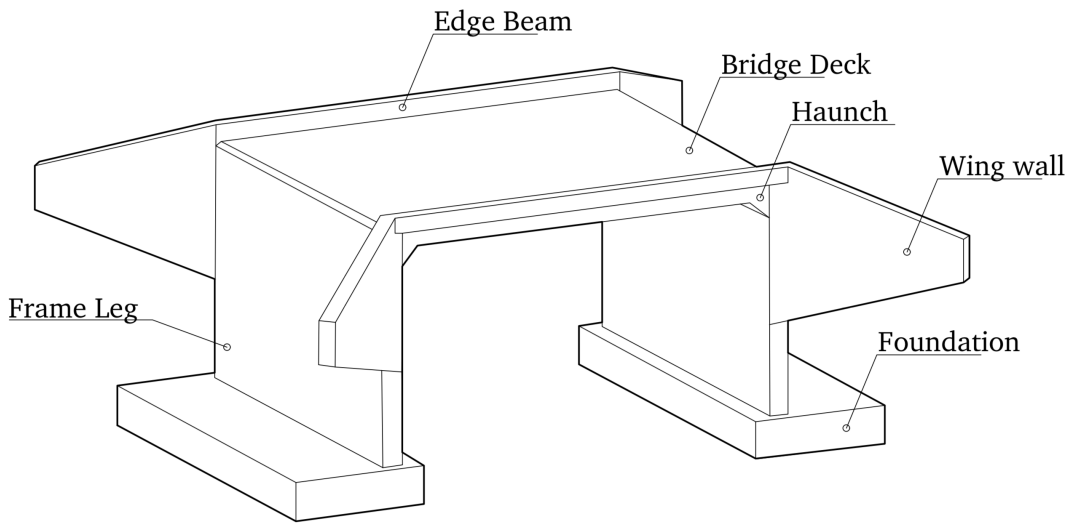

Figure 2.6: The general structural elements of a slab frame bridge.

2.3.1 Structural performance

As a system, the slab frame bridge acts as a rigid framework with varying connection degree to the ground, spanning from pinned to fixed connection. The bridge structure is, due to its moment rigid frame corner connections, statically indeterminate, meaning that sectional forces cannot be solved directly from equilibrium as compatibility conditions and constitutive relations are needed in addition.

The structural behavior of the bridge deck is dependent of the loading conditions. The frame legs carrying the bridge deck contribute to a one-way action, meaning that loads are transferred between the supporting edges with beam action. However, the horizontal width of the deck allows for load transfer across the main direction, creating a two-way plate action.

The frame legs carry the bridge deck in moment rigid connections that contribute to a moment stiff frame. Furthermore, the frame legs are subjected to the transversal earth pressure and surcharge load coming from the abutting ground, which counteracts horizontal loading on the bridge. Thereby, the bridge is stabilized by utilizing the ground as a support. The frame legs are connected to slabs, which in turn transfer the loads to the foundation.

In the corners between the bridge deck and the frame legs, angled haunches may be integrated in order to transfer sectional forces, both shear and moment. In particular, the haunches enhance the shear capacity, which can lessen the need for shear reinforcement. The specific angle of the haunches depends on the span of the bridge and is commonly decreased with increasing span lengths

In conjunction to the frame legs, wing walls are integrated in the slab frame bridge, keeping the soil in control whilst increasing the rigidity of the structure. Additionally, the wing walls contribute to stabilizing the structure against transversal horizontal loads (Alhede & Beskow, 2020).

2.3.2 Conventional design procedure of slab frame bridges

The preliminary design practice of concrete structures is to a large extent based on a trial and error approach, where design solutions are decided through assumptions and verifications in an iterative manner. In addition to being inefficient, this type of manual design approach makes it difficult to seek optimized solutions (Solat Yavari et al., 2016).

To facilitate the design process, graphs based on existing bridge structures were provided by Vägverket(1996) to be used for preliminary design of slab frame bridges, according to Figure 2.7. The graphs were published in a manual for bridge engineering back in 1996, but are considered to be somewhat too outdated to be used in today's design practice.

To further clarify the conventional preliminary design procedure used for slab frame bridges dialogues were held with a structural engineer specialist, having great insight on the matter. He stated that the preliminary design of commonly used bridge types, such as the slab frame bridge, usually is carried out based on previous experiences and reference projects. He further emphasized the use of reference projects in the tendering process, where rough dimensions can be obtained using past examples as basis for the design. In a later stage, when the tendering is decided, a more detailed

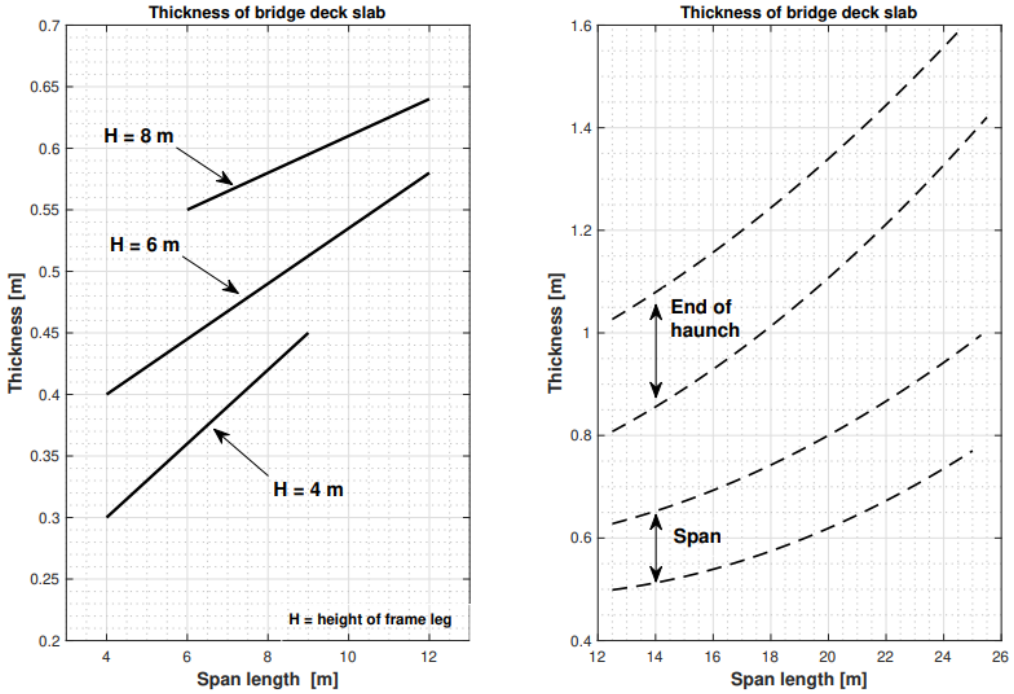

Figure 2.7: Preliminary design graphs for slab frame bridges (Vägverket, 1996).

evaluation of the amount of concrete and reinforcement is commonly carried out followed by minor adjustments of dimensions. He further explained the gradual transition from implementing the more traditional meter strip-method for the final design on slab frame bridges, to utilizing the new technologies of FEM-software. The meter strip-method involves performing a 2D-analysis on a one meter wide strip of the construction, along the bridge span. Recent additions to the Swedish legislation prohibits the use of the meter strip-method for the design of new constructions, though it is still occasionally used in projects where it is not considered economically feasible to perform extensive FE-modelling. One such example could be the case where an already existing slab frame bridge is to be widened due to an increase in traffic flow.

2.4 Parametric optimization

This chapter presents an overview of the theory behind parametric design and optimization problems. Different optimization- and gradient descent models are explained in order to concretize the theoretical background to such a problem. Furthermore, possible definitions of optimization criteria and constraints related to economy, environmental sustainability and buildability are presented, according to definitions used in previous research.

2.4.1 Parametric design

Parametric design describes design methods controlled by a set of variables, facilitating the generation of design alternatives. An essential characteristic of parametric design is that a change in individual parameters results in an automatic update of all the succeeding design steps. Consequently, parametric methods entail less manual and thereby repetitive work, which facilitates innovation or development of creative solutions (Lee & Ostwald, 2020). By creating parametric models there is a potential for rapid generation of design solutions, as variables are altered and combined. The generation of designs can subsequently be implemented as a design space in an optimization algorithm.

2.4.2 Optimization

Optimization is a general term for procedures that produce and compare alternative solutions in order to find the most suitable - optimal - one based on set criteria. Every optimization model is in principal built upon three parameters, being the *objective*, the *decision variables* and the *constraints* (Mathern et al., 2021), according to:

- The *objective* is the aspect that the model will maximize or minimize depending on the formulation of the problem. Within construction the objective could be minimized carbon dioxide emissions or maximized utilization ratio of a structural member.

- The *constraints* make up certain conditions that the algorithm must fulfill in order to be considered a valid solution to the problem. Within construction one constraint could be design verifications (ULS- and SLS- checks) or the maximum allowable number of reinforcement layers due to buildability reasons.

- The *decision variables* are the unknown variables, for which the algorithm is solved. They are defined by a domain called the *decision space* containing all values that the variables could possibly adopt. Within construction the cross-sectional dimensions of a structural element could be the decision variables.

To summarize, an optimization problem can be described mathematically according to Equation 2.1. The basic principles of such a problem, with the feasible region due to constraints is further shown in Figure 2.8.

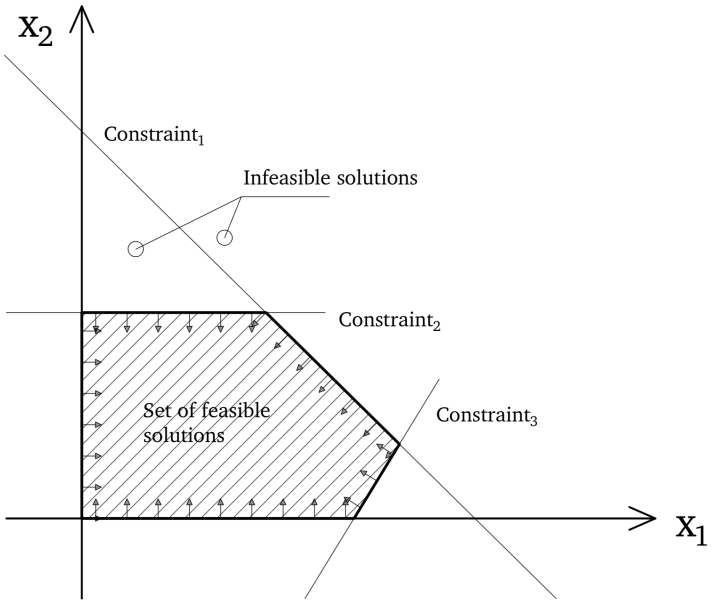

Figure 2.8: Visual representation of an optimization problem, showing the feasible region due to certain constraints, with the two parameters x_1 and x_2.

$$\begin{aligned} &\text{maximize/minimize } F(x) \\ &\text{subjected to:} \\ &g_i(x) \leq 0,\ i = 1, 2, ..., m \\ &h_j(x) = 0,\ j = 1, 2, ..., r \\ &x \in \mathcal{D} \end{aligned} \tag{2.1}$$

Where:

- x is the decision variable,
- $F(x)$ is the objective function,
- $g_i(x)$ and $h_j(x)$ are the constraints set on x, and
- $\mathcal{D}$ is the decision space of x.

2.4.2.1 Optimization models

There is a wide range of optimization models, all applicable depending on the problem to be analysed. The types of optimization problems can be divided into categories and subcategories, as described according to the tree structure in Figure 2.9.

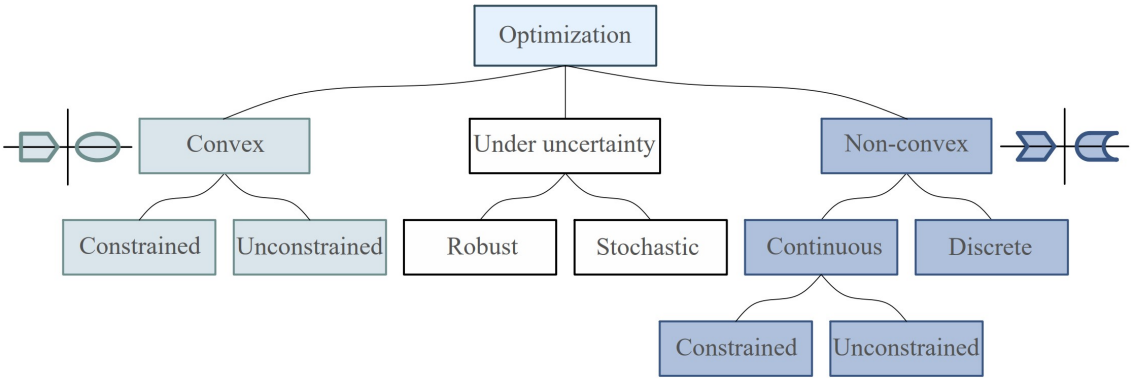

Figure 2.9: A tree structure showing different categories of optimization models together with a visualisation of a convex and a non-convex optimization problem.

Optimization algorithms can initially be classified into *convex* problems, *non-convex* problems or *optimization under uncertainty*. The latter is applicable in cases when there is an uncertainty related to the information used in the optimization algorithm, due to human errors or when the model is used to make predictions about the future (often used within economy). The uncertainty factor can be considered by either implementing probabilistic randomized variables into the algorithm (stochastic optimization) or by implementing a deterministic variability of the variables and the solution (robust optimization). The convex problems have one solution to the max/min problem, are quick to perform and can easily check large ranges of input data. The outcome of the optimization algorithm is visually represented by a convex region, being the junction of the separate convex constraint functions. Non-convex problems can instead demonstrate multiple local max/min solutions to the optimization problem and are more computationally demanding. The outcome of non-convex optimization problems is a non-convex region, being the junction of the separate non-convex constraint functions (Frontline Systems, 2023). A visual representation of the two problem types is found in Figure 2.9.

Furthermore, the category of non-convex problems can be divided into *discrete* or *continuous* optimization models. The decision variables within a discrete optimization problem can only be assigned specific values defined within a given set. An example within construction could be the diameter of the reinforcement, which is limited to specific values due to production standards. The decision variables in a continuous optimization problem can instead be assigned any real value within a specified range. One such example could be the cross-sectional dimensions of a structural member (Neos, 2022).

The models can be further categorised into *unconstrained* or *constrained* problems. Within unconstrained problems the variables can take on any value, with no exception. On the contrary, within constrained problems the outcome of the algorithm is limited due to restrictions put on the variables, where the variables have to relate to stated equalities or inequalities in the problem definition (Neos, 2022).

2.4.2.2 Gradient descent models

To find the minimum of an objective function different *gradient-based optimizers* can be applied, such as the *batch gradient descent*, *stochastic gradient descent* or *mini batch gradient descent* (Goyal, 2021). The differences between the three gradient descent models are visualized in Figure 2.10.

For the batch gradient descent method, the minimum is found by constantly evaluating the gradient of the objective function and adjusting the step size or the learning function according to Equation 2.2. The method is easy to grasp and to implement, but may sometimes find the local instead of the global minimum. Additionally, the method requires large sets of data to be stored since the gradient of the objective function is calculated for all decision variables, followed by one step at the end.

$$\theta = \theta - \alpha \nabla F(\theta) \tag{2.2}$$

Where:

- α describes the learning rate,
- F is the objective function to be minimized,
- ∇ is the gradient, and
- θ is the continuously updated decision variable.

The stochastic gradient descent method may be implemented in order to reduce the storage memory required to perform the optimization algorithm. The minimum is found by computing the derivative of each decision variable, followed by a revision of the model parameters. Hence the method takes one step per training example, eliminating the need of storing previous gradients. An additional advantage is the possibility of finding other local minima, without being trapped in the one found first. The method can be further explained according to Equation 2.3.

$$\theta = \theta - \alpha \nabla F(\theta; x(i); y(i)) \tag{2.3}$$

Where:

- α describes the learning rate,
- F is the objective function to be minimized,
- ∇ is the gradient,
- θ is the continuously updated decision variable, and
- $x(i)$ and $y(i)$ are the training examples.

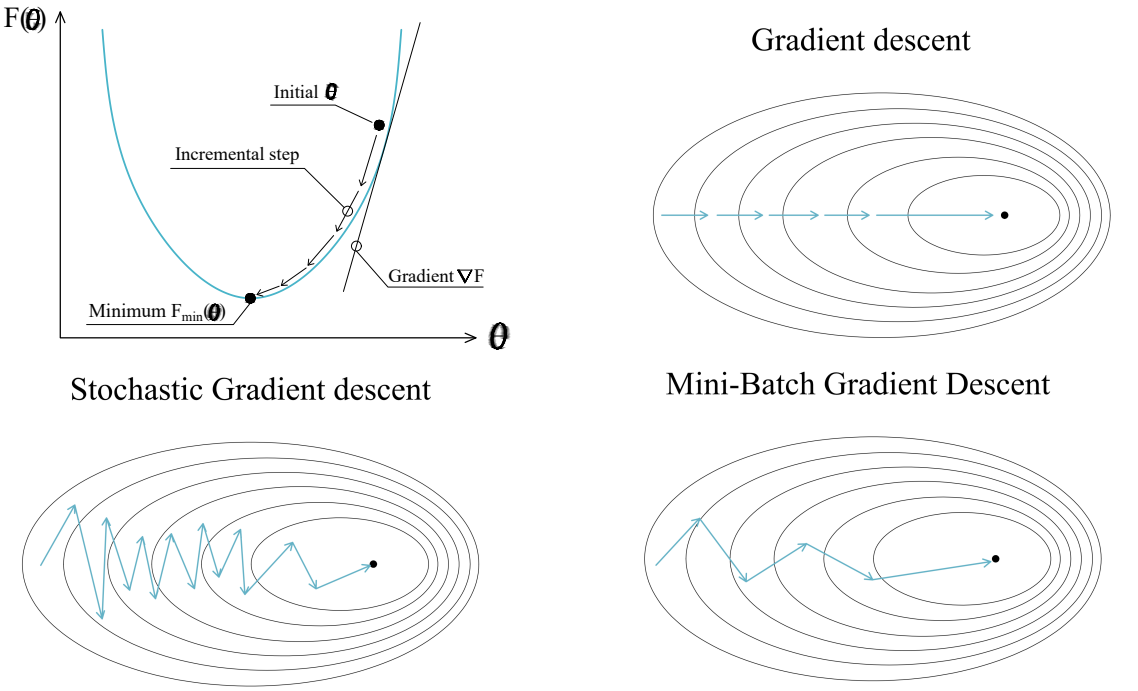

Figure 2.10: Visual representation of gradient descent models.

The mini-batch gradient descent method is a combination of the two previously explained methods, calculating the derivatives of a sub set or batch of the decision variable domain and updates the model parameters after each set has been analyzed. The method is further explained by Equation 2.4. This method requires a reasonable amount of memory to store the gradients of each batch of decision variables but might, as the Batch Gradient Descent method, also get stuck in local minima.

$$\theta = \theta - \alpha \nabla F(\theta; B(i)) \tag{2.4}$$

Where:

- α describes the learning rate,
- F is the objective function to be minimized,
- ∇ is the gradient,
- θ is the continuously updated decision variable, and
- $B(i)$ are the sub sets of the decision variable domain, a batch of training examples.

2.4.2.3 Multi-objective optimization

Many situations leave a demand for optimizing on multiple criteria all at once, e.g. multiple sustainability related criteria (Ek et al., 2019). In such cases a

multi-objective optimization method can be implemented, considering several contradictory objectives simultaneously. Such a problem is mathematically described according to Equation 2.5 (Martí et al., 2016):

$$\begin{aligned} &\text{maximize/minimize } F(x) = f_1(x), ..., f_M(x) \\ &\text{subjected to:} \\ &g_i(x) \leq 0,\ i = 1, 2, ..., m \\ &h_j(x) = 0,\ j = 1, 2, ..., r \\ &x \in \mathcal{D} \end{aligned} \tag{2.5}$$

Where:

- x is the decision variable,
- $F(x) = f_1(x), ..., f_M(x)$ are the objective functions,
- $g_i(x)$ and $h_j(x)$ are the constraints set on x, and
- $\mathcal{D}$ is the decision space of x.

One way to approach such a problem is by identifying the Pareto front, representing a subset of the possible solutions where two objectives have reached their optimum value considering both of the conflicting objectives. When the Pareto front has been found a minor improvement of one objective would result in the retrogression of one or more of the remaining objectives, thus giving a non-optimized solution (Sánchez-Silva & Gómez, 2013). Hence, in a situation where two objective functions (f_1 and f_2) are to be minimized simultaneously a set of feasible solutions can be detected, as shown in Figure 2.11.

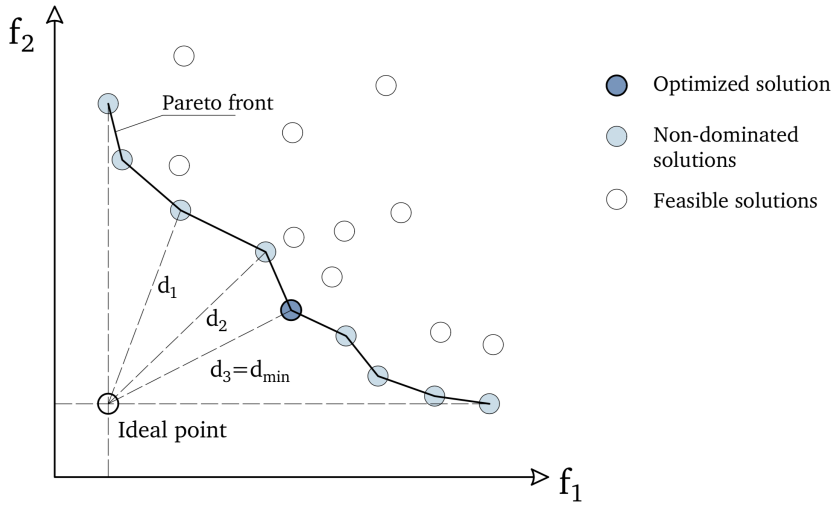

Figure 2.11: The Pareto front showing the optimal solution to a multi-objective optimization problem.

The Pareto-optimal set can be identified, containing multiple non-dominated solutions in addition to the optimal one. The optimal solution is the point within the Pareto-optimal set which lies closest to the ideal point, representing the lower threshold of the problem. Thus, all solutions within the Pareto front are valid and optimized solutions to the problem, but of differing characteristics, which can be used for negotiation during tendering procedures as previously mentioned.

In opposition to the Pareto front method, another way of concluding the impact that different criteria have on the outcome of the algorithm would be to conduct a sensitivity analysis. The analysis is performed by fixating one of the objectives (i.e making it into a constraint within the algorithm) to be able to observe how changes within the model affect the remaining objectives. By doing so, the outcomes of possible changes are known and conclusions can be drawn in terms of how the objectives are relating to one another (Sánchez-Silva & Gómez, 2013).

2.4.2.4 Termination criteria

When creating an optimization model it must include a pre-definition of when to terminate the iterative process, i.e include *termination criteria*. The termination criteria can be divided into two main categories, *local criteria* and *global criteria*. The former only has access to the data computed within the current iteration loop and compares the outcome of the specific iteration to a presumed optimal value. The drawback is hence that the predefined sought value has to be known in beforehand. The latter has access to the data produced in all iterations and can judge the progress of the optimization algorithm in a more global and stable manner. Additionally, this method is more redundant towards finding local max-/min- solutions since the results are continuously compared to all the previous iterations (Martí et al., 2016).

In general, the termination criteria are meant to minimize computational costs and abort the procedure in situations when (Martí et al., 2016):

- an optimal solution has been found,
- the solution is not the optimal one, but reaching an improved solution by further iterations is improbable,
- there is no viable solution to the problem, or
- the solution has converged and further iterations are illogical.

When dealing with multi-objective optimization problems the global stopping criteria approach has to be utilized, where all partial results are compared to previous iterations. The reason behind this is that the solution is given by a set of optimal points, making it impossible to compare to a threshold value. The consequence of applying such a method is the high computational costs coming from constantly monitoring the global progress of the algorithm in order to implement a termination criteria (Martí et al., 2016).

2.4.3 Optimization criteria

Bridge engineers generally aim to optimize structural designs by introducing objective functions related to costs and environmental impact, whilst considering the contradictory criteria of buildability. The ultimate goal is to find a solution which demonstrates a satisfactory behaviour regarding all criteria simultaneously. This chapter aims at exploring possible definitions and quantifications of the criteria of cost, environmental impact and buildability, to be used as basis for the optimization algorithm.

2.4.3.1 Defining investment cost criteria

Regarding optimization towards economic criteria, a sub categorization can be made into costs related to e.g. initial investment, manufacturing, transportation, maintenance and demolition. An algorithm which considers all the sub-criteria simultaneously would be very extensive, leaving a requirement to specify a somewhat simplified definition of the cost-criterion. The most common cost definition is in terms of labor- and/or material costs related to the initial investment made.

A previous research project distinctly focused on the investment costs related to the construction of slab frame bridges, i.e. material-, formwork- and procurement costs. The specific prices implemented within the research are further concretized in Appendix A.1 (Solat Yavari et al., 2016). The cost objective function was then defined according to Equation 2.6:

$$F(x) = Cost_{\text{concrete}} + Cost_{\text{formwork}} + \alpha_{reb} \cdot Cost_{\text{reinforcement}} \tag{2.6}$$

Where:

- $F(x)$ is the objective function of overall material- and labor costs
- $\text{Cost}_{\text{concrete}}$ is the material- and labor costs related to concrete,
- $\text{Cost}_{\text{formwork}}$ is the material- and labor costs related to formwork,
- $\text{Cost}_{\text{reinforcement}}$ is the material- and labor costs related to reinforcement, and
- α_{reb} is a factor accounting for additional costs associated with increased reinforcement amounts due to anchorage lengths and detailing.

When including the labor-aspect within the cost definition, there is a possibility to quantify buildability aspects in terms of additional costs related to a prolonged production process, as described in Section 2.4.3.3. Other research projects limited the cost definition to only consider material costs (Rempling et al., 2019), hence the opportunity of implementing buildability in terms of additional labor costs vanishes.

2.4.3.2 Defining environmental impact criteria

In order to optimize towards environmental criteria, its measurable quantities need to be defined. Environmental impact is a broad concept that concerns numerous aspects associated with health and natural resource deterioration. Therefore, the optimization can be facilitated by calculating a corresponding *environmental cost*. Previous research has been done, suggesting methods for calculating such equivalent

environmental costs. Additionally, optimization procedures commonly limit the definition of the criterion to one or a few specific environmental factors, such as CO_2-emissions (Ek et al., 2020).

When performing a multi-criteria optimization where environmental impact is included, the objective function for the environmental impact can be defined in terms of costs to ensure a consistent unit for all criteria. Han et al. (2014) presents a division of the environmental cost into *resource consumption cost* and *pollution control cost*, of which the latter is divided into solid particulate matter, waste water, SO_2, NO_2 and CO_2. The definitions presented in the paper were in accordance with Guidelines for Chinese Environmental and Economic Accounting (Yu et al., 2009). Similar research has been done on life cycle investment within the building construction industry, where an environmental cost is calculated based on air pollution, water pollution and solid waste pollution for different stages of the construction (Wang et al., 2020).

Regarding slab frame bridges in particular, means of calculating an equivalent environmental cost have been presented. Solat Yavari et al. (2017) have suggested an objective function for the environmental cost, based on *impact categories*, i.e. classes of environmentally harmful aspects. In the paper, each impact category was associated with a corresponding *monetary value*, i.e. an approximated environmental cost amplification factor associated to the impact category.

In the study by Solat Yavari et al. (2017), values of environmental impact were based on the ReCipe midpoint method (hierarchist), calculated using data from the life cycle inventory database Ecoinvent. The ReCipe method was presented by Goedkoop et al. (2009). Hierarchist denotes a *perspective based on scientific consensus with regard to the time frame and plausibility of impact mechanisms* (Huijbregts et al., 2016). The different impact criteria with corresponding characterization factors, brought forward by Solat Yavari et al. (2017), are further specified in Table A.4 in Appendix A.2.

Monetory values can be determined with different weighing systems, e.g. Ecovalue (SEK) or Ecotax (SEK). Ecovalue is based on willingness to pay (Du et al., 2014), wheareas Ecotax (short for ecologixal taxation) is based on taxes levied on environmentally harmful activities (Finnveden et al., 2006). Du et al. (2014) presents monetary weighting factors for the impact categories shown in Table A.4 in Appendix A.2, based on Ecovalue08 with updated Ecovalue12 and Ecotax02, (Finnveden et al., 2013; Finnveden et al., 2006; Ahlroth and Finnveden, 2011; Ahlroth et al., 2011).

The objective function formulated by Solat Yavari et al. (2017) summarizes each impact category weighed with the corresponding monetary values (Ecovalue or Ecotax weighing factors) according to Equations 2.7 and 2.8.

$$F(x) = Cost_{\text{env,concrete}} + \alpha_{reb} \cdot Cost_{\text{env,reinforcement}} \tag{2.7}$$

$$Cost_{\text{env}} = \sum_{i=1}^{num_{\text{impact,cat}}} impact_{\text{i}} \cdot monetary_{\text{i}} \tag{2.8}$$

Where:

- $F(x)$ is the objective function of the overall environmental impact for the given impact categories related to concrete and reinforcement,
- $Cost_{\text{env,concrete}}$ is the environmental cost corresponding to the given impact categories of the concrete,
- $Cost_{\text{env,reinforcement}}$ is the environmental cost corresponding to the given impact categories of the reinforcement,
- $impact_{\text{i}}$ is the i:th impact category,
- $monetary_{\text{i}}$ is the the environmental cost corresponding to the i:th impact category according to its Ecovalue or Ecotax monetary weighing factor, and
- α_{reb} is a factor accounting for additional environmental costs associated with increased reinforcement amounts due to anchorage lengths and detailing.

The objective function for environmental cost, defined in Equation 2.7, is similar to the objective function for the cost criteria, defined in Equation 2.6. However, as the formwork is able to be reused multiple times it was assumed to have negligible environmental impact, thus it was excluded from the objective function established by Solat Yavari et al. (2017).

2.4.3.3 Defining buildability criteria

Buildability is a term connecting the design to its effects on the actual construction (Chigozie Osuizugbo et al., 2022). As means to consider production feasibility in the early design stage, the buildability criterion can be included in the optimization algorithm. The term buildability differs from the often related term constructability. The two terms have been defined by the Construction Industry Research and Information Association (CIRIA) and Construction Industry Institute (CII), respectively, according to:

"**Buildability** is the extent to which the design of a building facilitates ease of construction, subject to the overall requirements for the completed building." (CIRIA, 1983)

"**Constructability** is a system for achieving optimum integration of construction knowledge in the project delivery process and balancing the various project and environmental constraints to achieve maximization of project goals and building performance." (CII, 1993)

As opposed to buildability, constructability is a broader term more centered about developing the management. Buildability, on the contrary, emphasizes techniques

and productivity to a larger extent (Cheetham & Lewis, 2001). Productivity in turn, can be defined in different ways depending on situation. In this case, productivity refers to labour productivity which can be defined as *earned to actual hours* (Shehata & El-Gohary, 2011). The similarities and differences between the two concepts are summarized in Figure 2.12.

As mentioned in the introduction, buildability is from a corporate perspective foremost a matter of cost. Efficient productions require less labour hours, which is of economic advantage. Optimization towards buildability can thus be highly economically motivated. Chigozie Osuizugbo et al. (2022) state that the economical benefits from regarding buildability are recurring in different parts of the process, concerning several stakeholders, as presented in Figure 2.13.

To further concretize the current implementation of buildability aspects within the construction field, a shift has taken place during recent years where the implementation of BIM-software (Building Information Modelling) has been widely spread to ensure buildable designs. Essentially, BIM is not only a principle of creating 3D-models, but also provides the possibility to assign attributes/information to all the structural members as a way to ease production. By adopting BIM, the user is able to foresee possible design problems, unnecessary waste products and unexpected clashes in advance to minimize unpleasant surprises on the construction site. More over, BIM-software provide the possibility of performing more extensive planning in before hand to ensure a realistic time schedule (Trimble, 2023). The transitional period of growing BIM applications has challenged the conventional design procedures, characterized by 2D-drawings. The new modelling principles leave the opportunity to deliver construction blueprints in the format of 3D models instead, showcasing many advantages. One vast advantage is that changes made within the model easily can be communicated to the construction workers to constantly ensure that the latest revision is being followed (Trimble, 2023), resulting in more efficient workmanship.

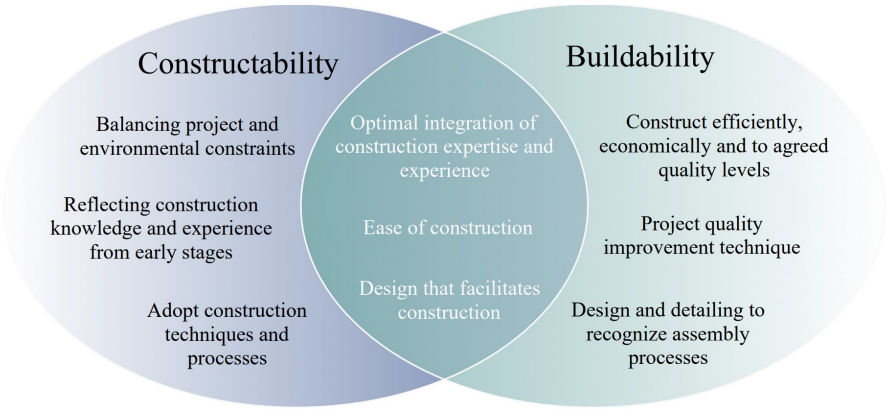

Figure 2.12: Similarities and differences between the two concepts of constructability and buildability according to Wimalaratne et al. (2021).

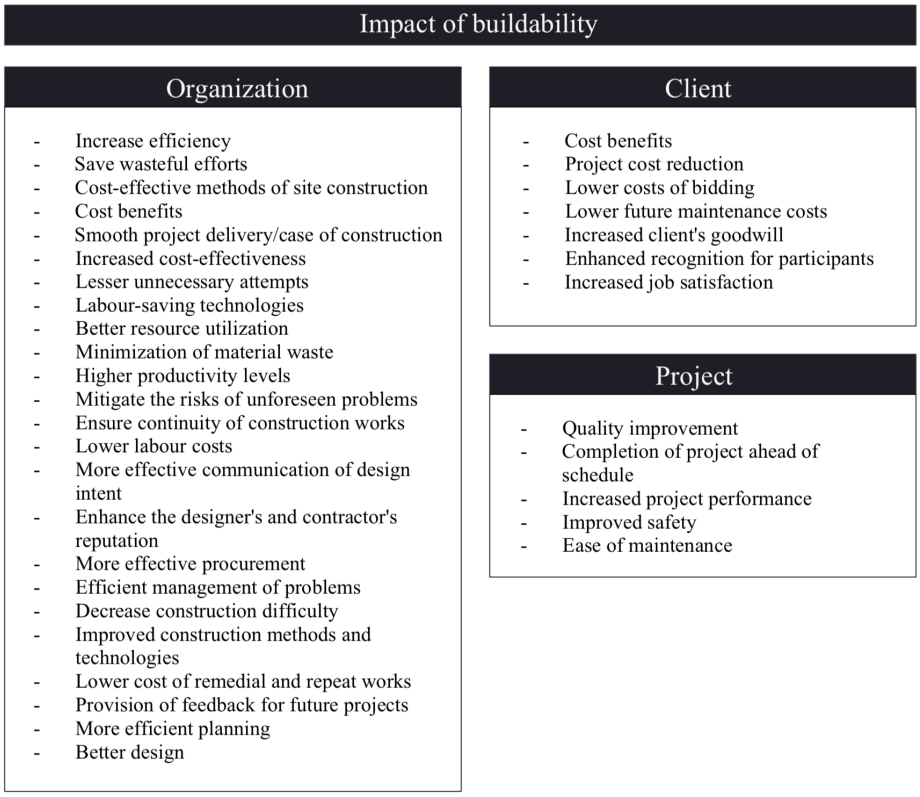

Figure 2.13: The impact of buildability optimization related to different stakeholders according to Chigozie Osuizugbo et al. (2022)

Implementing BIM is a very recent way of ensuring buildability within the field, in order to deliver cost- and time efficient projects. *Trafikplats Vega* is one of the successful pioneering projects on the subject, produced by ELU in 2018 with the Swedish Transport Administration as client, where the complete design of a traffic interchange was modelled and delivered using BIM within Tekla (ELU, 2018). Even though buildability is highly topical, there are few practical examples on how to quantify the criterion, making it a topic for further research. Further more, Sweco ensures buildability within one of their recent projects by adopting conventional design techniques when designing the first bicycle parking house in Gothenburg, relating buildability to repetition, previous experiences and time efficiency with lower costs as a second order effect (Sweco, 2022).

2.4.3.3.1 Defining measurable buildability constraints

The concept of buildability is highly situation specific and can be defined by numerous aspects concerning feasibility and efficiency of production. In order to establish its constraints within an optimization routine, the concept of buildability needs to be discretized into measurable quantities. Neither CII nor CIRIA suggest how the constructability or buildability criteria can be measured, as stated by Chigozie Osuizugbo et al. (2022).

Previous research has been performed by Solat Yavari et al. (2016) on the optimization of slab frame bridges, as mentioned in Section 2.4.3.1. The buildability aspect was considered within the research in terms of additional labor costs, as a result of specific design choices. The buildability factors considered were:

- **Slenderness**: slender structural members were assumed to require additional attention in order to ensure good quality of the reinforcement work.

- **Varying thickness**: varying thickness of structural members was assumed to increase the labor costs related to reinforcement work and formwork, in comparison to straight members.

- **Concrete class**: a higher concrete class was assumed to increase the labor costs due to further need of concrete vibration in order to ensure good quality of the concrete.

The additional labor cost factors and pure material costs, used by Solat Yavari et al. (2016), are presented in Table A.6 in Appendix A.3. Ultimately, when the algorithm was run with cost as the main objective function, the criterion of buildability was also taken into account.

With a similar fundamental idea of increasing labor costs due to decreasing buildability, another research project was performed by Khouri Chalouhi (2019) on the subject of reinforced concrete beam bridges. The study referred to three important geometrical properties, ultimately affecting the labor costs, according to:

- **Geometrical complexity**: The geometrical properties of a structural member were presumed to highly influence the procurement costs, due to more time consuming reinforcement and formwork labor (assuming constant unit volume of concrete). Geometrical complexity was defined in terms of number of changes in angles within the cross-section perimeter of a bridge deck or the shape of a bridge pier, according to Figure 2.14.

- **Kind of structural member**: The labor costs defined for a unit volume of concrete were assumed to vary depending on the type of structural member being cast. An example was given, where the labor time for producing a pier was stated to be longer than for producing a slab foundation, assuming the same unit volume of concrete. Khouri Chalouhi (2019) explained that when producing a pier, the casting has to be performed in steps where the concrete is poured, vibrated and cured in turns to avoid failure of the formwork, resulting in additional labor costs due to a prolonged production procedure.

- **Bridge height**: Additional labor costs were assumed when the distance between the bridge deck and the ground increased, to account for difficult circumstances when producing the form work.

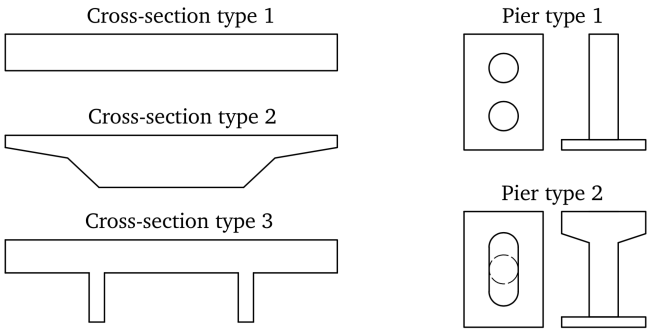

Figure 2.14: Structural member geometries of reinforced concrete beam bridges, related to buildability aspects (Khouri Chalouhi, 2019).

The specific buildability costs stated for the different bridge geometries are summarized into Tables A.7-A.9 in Appendix A.3, according to Khouri Chalouhi(2019). The final buildability costs were ultimately computed by multiplying the procurement cost for each structural member with the corresponding additional labor cost factors.

Rempling et al. (2019) adopted an alternative approach, compared to Khouri Chalouhi (2019). The buildability aspect was instead implemented by using optimization constraints, according to Section 2.4.2. Limitations were set on the allowable number or reinforcement layers, facilitating work on site. In addition, the spacing of the stirrups was rounded off and down to further ease the construction process.

Moreover, the research gap on quantifiable buildability criteria was noticed and explored by the Building and Construction Authority of Singapore in the early 2000's. The institution established a code of practise on buildable design, the *Buildable Design Appraisal System* (BDAS) published in 2005. The framework aimed to present a buildability score for construction projects, targeted on building design, where a higher score shows good prospects to achieve increased utilization of labor on the construction site. The protocol is built upon the degree of *standardisation*, *simplicity* and *single integrated elements* shown in the project design (Singapore. Building and Construction Authority., 2005). The buildability criteria were defined according to:

- **Standardisation**: the standardisation criteria covers the extent of repetition in the structural layout, detailing and dimensions of structural members.

- **Simplicity**: simplicity refers to the complexity of the structural design. Well-known construction principles, simple geometries in formwork production for in-situ casting and uncomplicated reinforcement layouts are examples on measures of simplicity.

- **Single integrated elements**: single integrated elements is a measure of the degree to which members can be pre-fabricated and/or mounted prior to arriving on the construction site. Examples such as precast walls or pre-mounted bathrooms are given in the code of practice.

The buildability score of the building was subsequently defined according to Equation 2.9 (Singapore. Building and Construction Authority., 2005):

$$\text{Buildability} = 50[S_s(A_\text{s} \cdot S_\text{s})] + 30[S_w(A_\text{w} \cdot S_\text{w})] + N \tag{2.9}$$

Where:

- 50 and 30 are weighting factors for labor costs related to structural and architectural design,
- A_s and A_w correspond to the floor/wall area of a specific structural (A_s) and architectural (A_w) design,
- S_s and S_w are indices in the range of 0.3-1 based on the structural (S_s) and architectural (S_w) system used in design, and
- N is the buildability score referring to "other design considerations" related to the extent of repetition, simplicity and possibilities of pre-fabrication.

Although the code focuses on buildings, the measurable criteria presented in the protocol can be interpreted, adjusted and applied within bridge construction likewise.

Further investigations show that the complexity of adding and anchoring shear reinforcement also increases the labor costs. Therefore, it is often of substantial advantage to avoid shear reinforcement if possible. If the shear capacity of the concrete is insufficient, it might, from an economic and buildability perspective, be more efficient to increase the cross-sectional height than to add shear reinforcement (Hendy & Smith, 2007). A structural engineer specialist at the *Bridge and infrastructure department* at Skanska was consulted in order to estimate the time consumption needed for adding shear reinforcement, based on previous experiences. He mentioned that shear reinforcement for slab frame bridges commonly is pre-frabricated, delivered to the construction site as welded reinforcement ladders. The additional labor costs related to the production of such reinforcement ladders can be implemented as additional buildability costs, see Appendix A.3 for specific buildability factors implemented in relation to stirrups.

In order to further study possible interpretations of the buildability criterion a calculation engineer, from the *Calculation department* at Skanska, was consulted on the matter. She pointed out that buildability today is taken into account by adjusting the capacities related to different tasks, ultimately adjusting the number of labor hours needed to finish certain production-procedures. Mainly, the capacities are regulated depending on which structural member is being cast,

the properties of the reinforcement, the surroundings, the climate on site and the transportation conditions. She further explained that the reinforcement diameters commonly are related to a labour capacity, meaning that certain diameters are associated with a corresponding time needed for assembly. For instance, $\phi 16$ compared to $\phi 25$ entails more hours of placement due to increased number of bars needed to reach the same unit volume of steel. The exact capacities provided can be found in Appendix A.3.

To summarize, despite the complexity of defining buildability in measurable terms, previous research presents different approaches to the problem. One way is to adjust the labor costs by factors correlating to additional construction time depending on the structural design. Another proposal is to introduce optimization constraints to facilitate the work on site. A third alternative is to define a scoring system indicating the degree of repetition, simplicity and production procedure used.

2.5 Loads

The design of concrete structures, following the European standard, should be in accordance with SS-EN 1990:2002 - *Basis of Structural Design*. When designing concrete structures, the capacity needs to fulfil requirements for ultimate limit state (ULS), meaning that the structure should withstand the design loads. Moreover, serviceability limit state (SLS) criteria should be satisfied in order to limit deflections and control cracking. Concerning cyclic loading, which traffic bridges are naturally subjected to, fatigue limit state (FLS) is also needed to be taken into consideration (SS-EN 1991-2:2003) - *Traffic Loads on Bridges*. The specific material data, load combinations and design checks are presented in Appendix B, C and D. However, due to the limited scope of this thesis, only ULS- and SLS checks were performed, concerning a limited number of main loads. See Chapter 3 for the implementation.

Load categories acting on bridge structures are further described in section 2.5.1.

2.5.1 Load categories

Loads normally acting on a slab frame bridge can be categorized into permanent and variable loads. The structure is subjected to a range of permanent loads, according to:

- **Self weight**: Constant load from the structure's weight,
- **Pavement**: Constant load from paving material on the load carrying structure,
- **Earth pressure**: Lateral pressure that the soil exerts on the structure,
- **Differential settlement**: Load emerging from movement due to uneven displacements in the foundation,
- **Creep**: Time dependent load effect due to sustained loading, resulting in a gradual increase in strain without increasing the load, and

- **Shrinkage**: Time dependent load effect emerging from the shrinkage of concrete. Creates internal and/or external restraint effects due to interaction with the reinforcement and fixation.

Furthermore, there are variable loads acting on the structure, differing in magnitude, occurrence and endurance over time and are defined according to:

- **Vertical traffic load**: Moving vertical imposed loads from traffic,
- **Accelerating/Braking forces**: In-plane imposed loads from velocity change of traffic on the bridge,
- **Counteracting passive earth pressure**: Passive earth pressure emerging as a reaction of horizontal movement of the bridge structure,
- **Centrifugal forces**: Transverse force acting radially to the axis of the carriageway,
- **Wind load**: Multi-directional action on the bridge structure due to wind loads acting on the structure itself or on passing cars,
- **Temperature induced loads**: Enforced movement due to temperature induced deformation,
- **Accidental loading**: Unintended load caused by accidental damage to the structure, and
- **Surcharge load**: Vertical load that acts on the underlying soil, creating a horizontal pressure from the embankment, acting on the bridge frame legs.

2.5.2 Traffic load models

According to SS-EN 1991-2:2003, 4.2.1, traffic load from cars, lorries and special vehicles (e.g. industrial transport), result in static and dynamic forces. In order to describe actual loading situations, different simplified load models can be applied. Bridge structures can be subjected to traffic actions from vertical loading and horizontal acceleration- and braking forces, as well as centrifugal forces from asymmetrical loading along the width of the bridge deck.

Vertical traffic loads are represented by different load models described in SS-EN 1991-2:2003, 4.3.1, according to:

- **LM1**: Concentrated and uniformly distributed loads, covering the majority of traffic load effects of lorries and cars, used for general and local verifications,
- **LM2**: Single axle load applied on specific tyre contact areas which covers the dynamic effects of the normal traffic on short structural members,
- **LM3**: A set of assemblies of axle loads representing special vehicles (e.g. industrial transport) which can travel on routes permitted for abnormal loads. It is intended for general and local verification, and
- **LM4**: Crowd loading, intended only for general verification.

In addition to the vertical traffic load models presented in SS-EN 1991-2:2003, the Swedish Transport Agency also presents vehicle models of vertical traffic load representing load effects from different types of vehicles (TSFS 2018:57, 4.2.1(1)).

Traffic also gives rise to horizontal loading, as described in SS-EN 1991-2:2003, 4.4. Braking and accelerating forces, Q_{lk}, shall be allpied as longitudinal forces acting at the surfacing level of the carriageway (SS-EN 1991-2:2003, 4.4.1), resulting in normal forces and a bending moment. Centrifugal forces, Q_{tk}, should also be applied as a transverse force acting at the finished carriageway level and radially to the axis of the carriageway (SS-EN 1991-2:2003, 4.4.2).

Moreover, fatigue loading is represented by load models, presented in SS-EN 1991-2:2003, 4.6. Fatigue refers to damage of the structure due to cyclic loading, which is relevant to consider for recurring traffic load on bridges. To examplify, fatigue load model 3 represents single vehicle loading and consists of four concentrated axle loads.

2.6 Software

Grasshopper is a parametric interface supported by the 3D modelling software *Rhino*, developed for effective generation of design alternatives (Oxman & Gu, 2015). Additionally Grasshopper can be connected to *Excel*, to manage input- or output data, and to the BIM-software *Tekla Structures* to auto-generate 3D-models based on the designs presented within the parametric interface.

Grasshopper is essentially a visual programming tool, making it user-friendly, thus suitable for people who are not previously acquainted with programming. The software was mainly used within architecture in the early years but has grown to include complex engineering applications as well. The interface is based on pre-coded *components* which can be connected in a systematic manner to perform desireable tasks. As the different components involved in the design are visibly connected, an overview of the parametric progress can be obtained. Each component is a system or a function that can take certain variables as input and deliver specific outputs.

A simple example of a Grasshopper-code creating a cylinder with given dimensions is shown in Figure 2.15a, to demonstrate the main principles of the software. In step 1, the circle component takes as input a plane of origin (the xy-plane) and a desired radius of the circle (5m). In step 2, the extrude component takes as input a base shape (the circle) and a distance in a specific direction (10m in the z-direction) and creates a tube. In step 3, the holes of the tube are capped to create the cylinder. The final product of the script is a cylinder with a radius of 5m and a total height of 10m, visualized in Rhino according to Figure 2.15b. Such a code could be used to model the geometry of a cylindrical bridge support.

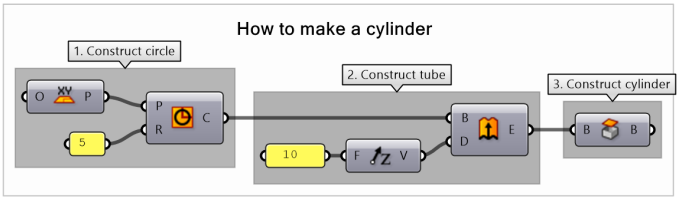

(a) Grasshopper code creating a cylinder

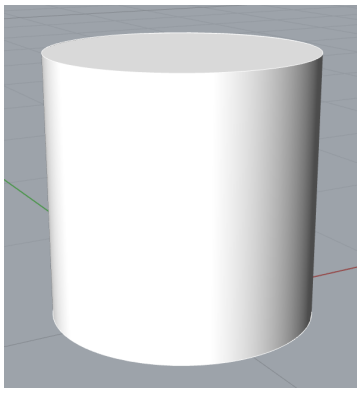

(b) Visualization in Rhino

Figure 2.15: Visual programming example on how to make a cylinder in Grasshopper.

If there is no pre-coded component available to perform a task that the user wants to execute, there are empty Python- and C# components that can be used to create project-specific functions using either of the two programming languages. The user writes the script that controls the tasks performed by the component, together with deciding its input- and output data.

To demonstrate the alternative coding-approach, the same cylinder is created using a Python-component according to Figure 2.16a. In step 1, the inputs of the component are set to be a radius and a height (integer type). In step 2, the Python-code is implemented into the component. Lastly, in step 3, a cylinder is outputted and possible error messages can be viewed. Visualisation within Rhino is showing the same result as in the previous example, according to Figure 2.16b.

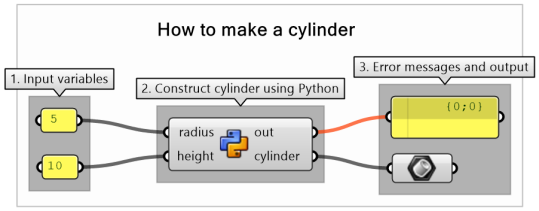

(a) Python component creating a cylinder

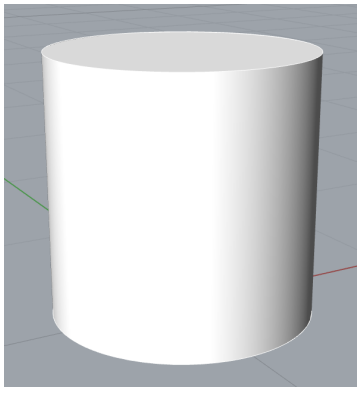

(b) Visualization in Rhino

Figure 2.16: Programming example on how to make a cylinder using the Python-component within Grasshopper.

By creating Python- or C# components, which are task specific, the code can most often be shortened and better adapted to the specific demands set within the project. When only utilizing the existing components within the Grasshopper interface the user becomes somewhat limited. Despite the extensive component library, some tasks are unavailable or demanding to perform by only using the pre-defined components. The opportunity to implement user-specified programming allows for a large freedom in controlling the parameterization.

By installing add on features to Grasshopper, the input- and output data for an algorithm can be handled via Excel, allowing for a more comprehensive overview of the variables and/or outputs. Furthermore, additional component-packages can be installed for auto-generation of designs in BIM-software, such as Tekla Structures. The vast advantage of using Grasshopper is the possibility to visualize the results in the Rhino 3D interface, and the possibility of connecting the code to other 3D modelling software. This allows for a better overview of the project, facilitates communication and provides a basis for extracting blueprints of the optimized design. A majority of alternative programming interfaces provide very poor graphical visualization of results, making Grasshopper a huge asset when the visual perspective is important.

2.7 Machine learning within structural engineering

The construction industry today is lagging behind regarding the ongoing development and utilization of methods based on automation. By implementing such methods, time could be saved from repetitive work and tedious tasks performed by structural engineers. However, the development within automation has accelerated during recent years. Research regarding *machine learning* and *artificial intelligence* (AI) has drastically increased, providing means for integrating sustainability aspects into the structural design process. Furthermore, such methods enable the interdisciplinary collaboration between stakeholders, to ensure a design that fulfills all requirements while simultaneously fulfilling the criteria of environmental-, economic- and social sustainability. Current design software are not compatible with the implementation of optimization procedures where such sustainability criteria can be fully considered and compared for multiple design alternatives in a time-efficient manner. Hence, there is great incentive for developing AI- and machine learning procedures within the construction sector (Mathern et al., 2019).

AI represents the creation of intelligent computerised systems that perform tasks that would otherwise require human resources. One branch within AI is machine learning where the system analyses immense sets of data in order to detect patterns, enabling computerised decision making. The model outputs still have to be verified by human resources before considered valid. A branch within machine learning is *deep learning*. Within deep learning, the AI model more correctly mimics the thinking process of the human brain, becoming self-sufficient. The system can then deliver well grounded decisions that do not require double checking by actual

human intelligence (Janiesch et al., 2021). The different levels of AI, machine learning and deep learning respectively, are summarized into Figure 2.17 along with their corresponding definitions.

The ultimate goal of creating a machine learning procedure within structural engineering is to imitate the work performed by structural engineers, achieved by training the models through utilizing human experiences and large data sets. Such methods enable the combination of intelligence from multiple specialists within different fields. Furthermore, once created, the procedure is disconnected from heavy optimization algorithms including extensive calculations in order to ensure that all constraints within the algorithm are met. The machie learning model is in contrast based on recognising parameters that commonly result in optimal designs, making its own decisions in order to provide design proposals without having to perform any major calculations (Mathern et al., 2019).

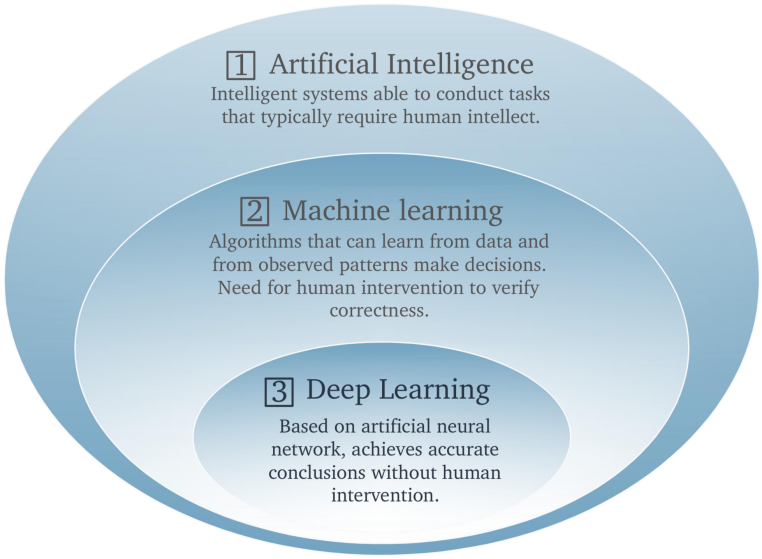

Figure 2.17: Machine learning and deep learning within artificial intelligence according to Janiesch et al. (2021).

3
Methods

The study aimed to explore the economic and environmental gains to be made by implementing parametric SBD optimization algorithms in the preliminary design phase of bridges, whilst considering the additional cost effects of buildability aspects.

The slab frame bridge, slab bridge and girder bridge were all considered suitable research subjects, being the most commonly used bridge types in Sweden (Olsson McDowell, 2021). To achieve the sought result of minimizing the climate impact and costs within the construction sector, the parametric optimization procedure implemented in this thesis was targeted at the most frequently built construction types.

Furthermore, different approaches were studied for the execution of the optimization method. One option was to utilize pre-coded optimization components within Grasshopper, such as the multi-objective evolutionary optimization component *Octopus*. Prior knowledge within programming is not needed when implementing such a method and the visual programming interface ensures a full overview of every design step. Additionally, Grasshopper offers the possibility to produce automated 3D-models in Tekla, which by extension could be used for construction blueprints. On the contrary, visual programming is limited to pre-coded components, thus sometimes demonstrating cumbersome solutions. Another alternative was to implement Python coding, either within a FEM-software, e.g., Brigade, or within the visual programming interface of Rhino/Grasshopper. The former would enable non-linear analyses using finite element method, while loosing the connection to BIM-software. However, non-linearity is seldom used in the design practice, due to extensive computation. The latter provides the possibility of extending the code into modeling the solution in Tekla, as one step towards considering buildability where design clashes can be detected in advance.

3.1 The chosen method

The chosen method for the optimization was a parametric algorithm in Python, via Grasshopper, implemented for linear elastic preliminary design of the most frequent bridge type in Sweden – slab frame bridges. Implementing the optimization method to a common bridge design type was considered of importance in order ensure a large-scale application of the method, whilst limiting the scope to a singular construction type. The structural analysis was decided to be linear, in order to

reduce the computational complexity, especially as the method was aimed for preliminary design. Thereby, greater emphasis could be put on analysing large sets of data while also mitigating the computational complexity. The choice of writing the script in Grasshopper was predominantly based on the possibility of outputting the results in a 3D environment, as well as a basis for subsequently extending the code to BIM-software.

Furthermore, a study was carried out in dialog with a specialist within bridge engineering from the *Bridge and infrastructure department* at Skanska, as basis for determining the constraints of buildability for implementation in the optimization algorithm. Another intention was to get further insight into the current preliminary design practice of slab frame bridges. The choice of employee to consult on the matters was based on experience of structural engineering and bridge design in particular. The chosen employee was regarded suitable, being able to contribute with practical understanding from the construction site and experiences related to consequences of different design choices from past projects.

To further investigate a possible interpretation of buildability in terms of additional costs, another dialogue was held with a calculation engineer from the *Calculation department* at Skanska, specialised within production costing. The aim was to establish how buildability is considered within production costing today and to get additional inputs on possible quantitative measures of buildability to be used within the optimization algorithm.

3.1.1 Social and ethical considerations

Social and ethical sustainability were additional aspects considered for the chosen method. An important dilemma arising in conjunction with automated design processes is the possible consequences of not being in control of every design step. Input parameters for the parametric model are defined by the user, followed by an output of the optimized structural design, without transparency of the process in between. This *black box - phenomenon*, where the user is not in control of the steps between the input and output, is important to consider (Kenton, 2022). A measure taken in avoiding this phenomenon was to move forward with a method solely based on Python coding, in which every design step and iteration within the optimization procedure could be followed, by the support of explanatory comments. Visual programming- and FEM-software have many advantages, but also increase the need for considering the black box phenomenon and verification of the models produced. Programming contributes to a transparency, giving the user greater control of the automated process.

In addition to the economic incentive of efficient production, designing buildable structures is also a matter of labour conditions. It is important to find a balance between optimized structural performance and the societal effects related to buildability. The labour conditions as well as urban effects from the construction site

are aspects that need to be kept in mind when developing structurally optimized designs, where the final design also needs to be feasible ("Constructability in Construction and Issues at Design and Execution", 2023). In the method applied, these societal effects were regarded by implementing buildability in the objective function.

3.2 Optimization model

The fundamental ideas of the optimization model created, derived from the principles explained in Section 2.4.2, are summarized into Equation 3.1. Here, soft constraints refers to requirements that can potentially be changed by negotiation, as opposed to hard constraints, which need to be followed according to norms.

$$\text{Optimization model} \begin{cases} \text{Decision variables} = \begin{cases} \text{Concrete class } (f_{ck}) \\ \text{Rebar diameter } (\phi) \\ \text{Number of rebars } (n_\phi) \\ \text{Cross-sectional height (h)} \end{cases} \\ \text{Constraints} = \begin{cases} \text{Hard constraints} \begin{cases} \text{ULS-verification} \\ \text{SLS-verification} \end{cases} \\ \text{Soft constraints} \end{cases} \\ \text{Objective} = \text{Equivalent cost} \begin{cases} \text{Investment cost} \\ \text{Environmental cost} \\ \text{Buildability cost} \end{cases} \end{cases} \tag{3.1}$$

Furthermore, based on the classifications presented in Section 2.4.2.1, the model created is characterized by a non-convex optimization procedure. Multiple objective functions weighed together results in numerous local max/min solutions to the problem, as illustrated by a pareto front for double objective optimization problems, according to Section 2.4.2.3. Additionally, as explained in Section 2.4.2.1, non-convex optimization commonly results in more computationally demanding algorithms, making it important to mitigate computational complexity in order to achieve time efficiency.

The general optimization problem implemented can be described mathematically according to Equation 3.2:

$$\begin{aligned} &\text{minimize } F_{eq}(x) = f_{inv}(x), f_{env}(x), f_{build}(x) \\ &\text{subjected to:} \\ &\mu_{ULS,i}(x) \leq 1,\ i = 1, 2, ..., m \\ &\mu_{SLS}(x) \leq 1 \\ &x \in \text{Design space } \mathcal{B} \end{aligned} \tag{3.2}$$

Where:

- x is one bridge design alternative,
- $F_{eq}(x) = f_{inv}(x), f_{env}(x), f_{build}(x)$ is the objective function,
- $f_{inv}(x)$ is a partial objective function (the investment cost criterion),
- $f_{env}(x)$ is a partial objective function (the environmental impact cost criterion),
- $f_{build}(x)$ is a partial objective function (the buildability cost criterion),
- $\mu_{ULS,i}(x)$ are the ULS-utilization ratio constraints set on all cross-sections $i = 1, 2, ..., m$ within one bridge design x,
- $\mu_{SLS}(x)$ is the SLS-utilization ratio constraint set on each bridge design x, and
- Design space $\mathcal{B}$ contains all possible and impossible bridge designs x.

3.2.1 Implementation of set-based design

The optimization method developed adopts SBD, as presented in Section 2.2.1, meaning that the algorithm creates a set of initial design solutions which is narrowed down along the continuation of the algorithm. In the narrowing of data sets, information is disregarded without being deleted. Figure 3.1 shows the principles of SBD, of which the dashed area represents the design spaces implemented in this study. Excluded from the implementation is the initial design space $\mathcal{A}$, consisting of all possible slab frame bridge designs, regardless of specified input. Design space $\mathcal{A}$ is narrowed down to Design space $\mathcal{B}$ (initial data set in this study) by establishing input parameters for the bridge structure, being the span length (L), structural height (H), bridge deck width (W), and boundary conditions (bc) between frame legs and foundation. Bridge designs that do not fulfill the constraints defined according to national requirements on structural performance (ULS and SLS) are disregarded, resulting in further narrowing into Design space $\mathcal{C}$. The subset of passed designs is saved for evaluation according to the objective function, ultimately yielding optimized solutions with the lowest objective function values amongst passed alternatives (Design space $\mathcal{D}$).

A broader implementation of SBD would be to start from Design space $\mathcal{A}$. Then the algorithm would generate a library of all possible bridge design solutions, regardless of the specific geometrical input of an individual bridge. The design alternatives for a particular bridge project (Design space $\mathcal{B}$) constitutes a subsection of all design solutions for any slab frame bridge structure (Design space $\mathcal{A}$). An advantage of the broader SBD approach would be the possibility to change even the

fundamental dimensions of the bridge, if changing them can be proven more optimal in the early design phase. However, the project-based SBD method, starting from Design space $\mathcal{B}$, was regarded as more closely related to today's conventional design procedure, where the specific dimensions of a construction commonly are determined in beforehand, after which the structural engineers are being involved, thus not leaving room for geometrical changes. It was considered more realistic to change the industry by means of smaller steps which can subsequently be extended to a broader adaption, which motivated the decision.

A predominant advantage of SBD is that the design space is kept wide for as long as possible, as design alternatives are deselected without being deleted. Thereby, there is a possibility of tracing solutions that were initially disregarded, based on a soft constraint, but later deemed suitable if proven optimal in some aspect. This possibility of accessing past alternatives can be beneficial during the tendering process, where the client can be presented with design alternatives that are ineligible according to functional demands, however showing e.g., a greater cost efficiency than alternatives that do fulfil all requirements. Thereby, SBD enables a negotiable design process where more optimal alternatives can be brought forward, as soft constraints can be discussed. The possibility of tracing alternatives during the design process is illustrated in Figure 3.1.

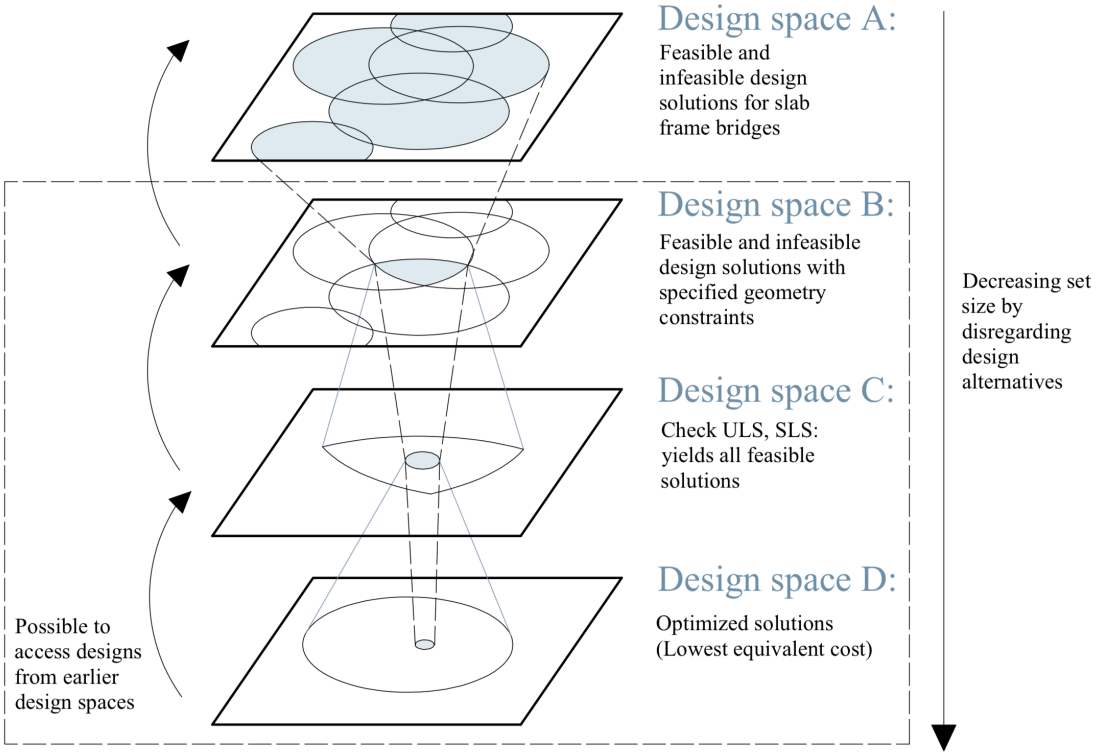

Figure 3.1: Implementation of SBD, where Design space $\mathcal{B}$ represents all bridge designs with predefined geometrical constraints (initial set within the algorithm).

3.2.2 Algorithm layout

A flowchart defining the main routines of the algorithm is here presented in terms of the optimization model explained in Section 3.2, in combination with the SBD-approach described in Section 3.2.1.

The three main routines are illustrared in Figure 3.2 where *Module 1: Decision variables* generates the initial set of alternatives (Design space $\mathcal{B}$), *Module 2: Constraints* narrows the set (Design space $\mathcal{C}$) by performing structural verifications and *Module 3: Objective* perfors the optimization procedure, further narrowing the design space (Design space $\mathcal{D}$). Each of the three modules are further explained in the following Sections 3.2.2.1-3.2.2.3.

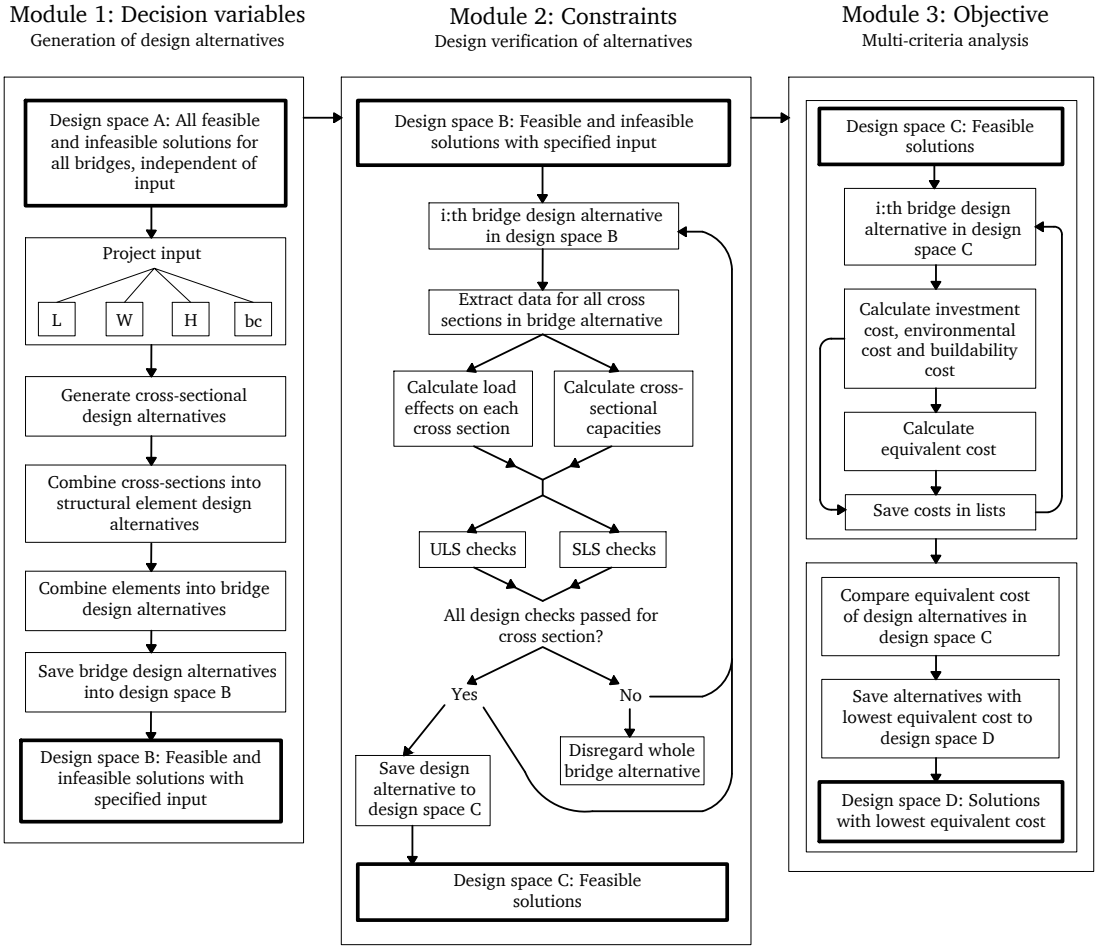

Figure 3.2: Flow chart of the algorithm.

3.2.2.1 Module 1: Decision variables

Module 1 of the algorithm was aimed at generating all possible design alternatives (feasible or not) for an arbitrary slab frame bridge, with specified input geometry (L, H, W and bc). Based on these set input parameters, design alternatives were generated with varying decision variables – concrete strength class, cross-sectional heights of structural members, tensile reinforcement diameter and the number of tensile rebars within a cross-section. Henceforth, the decision variables within the algorithm are a combination of continuous and discrete variables, according to Section 2.4.2.1. Concrete classes and reinforcement diameters are limited to specific values due to production standards, thus are distinguished as discrete values. On the contrary, the cross-sectional height of a structural member can adopt any real value within a given range of a particular step size, thus is characterized as a constrained continuous variable. All the input parameters, as well as the variable parameters are summarized into Table 3.1.

Input parameters and variable parameters	
Input parameters per design solution	**Notation**
Span length (Including supports)	L
Structural height (Including bridge deck)	H
Bridge Width (Excluding edge beams)	W
Boundary condition between frame leg and foundation slab	bc
Variable parameters per cross-section	**Notation**
Concrete strength class	f_{ck_i}
Cross-sectional height	h_i
Tensile reinforcement diameter in cross-section	ϕ_i
Number of tensile rebars in cross-section	$n_{i,j}$

Table 3.1: Input parameters and variable parameters within the algorithm, where i denotes the numbering of cross-sections and j denotes the tensile reinforcement row number within cross-section i.

In order to lessen the computational complexity, a discretization of the frame was made. The frame was divided into nine critical parts, each corresponding to one cross-sectional design determined according to the maximum load effects – shear force and bending moment – observed within the specific part of the frame. The discretization made was in accordance with previous research performed on slab frame bridges (Difs Jon & Karlsson Fredrik, 2015).

Figure 3.3 illustrates the input- and variable parameters in a global and local scale, as well as the discretization of the frame into nine critical areas, designed according to the worst case loading within each specific area, resulting in nine final cross-sectional designs.

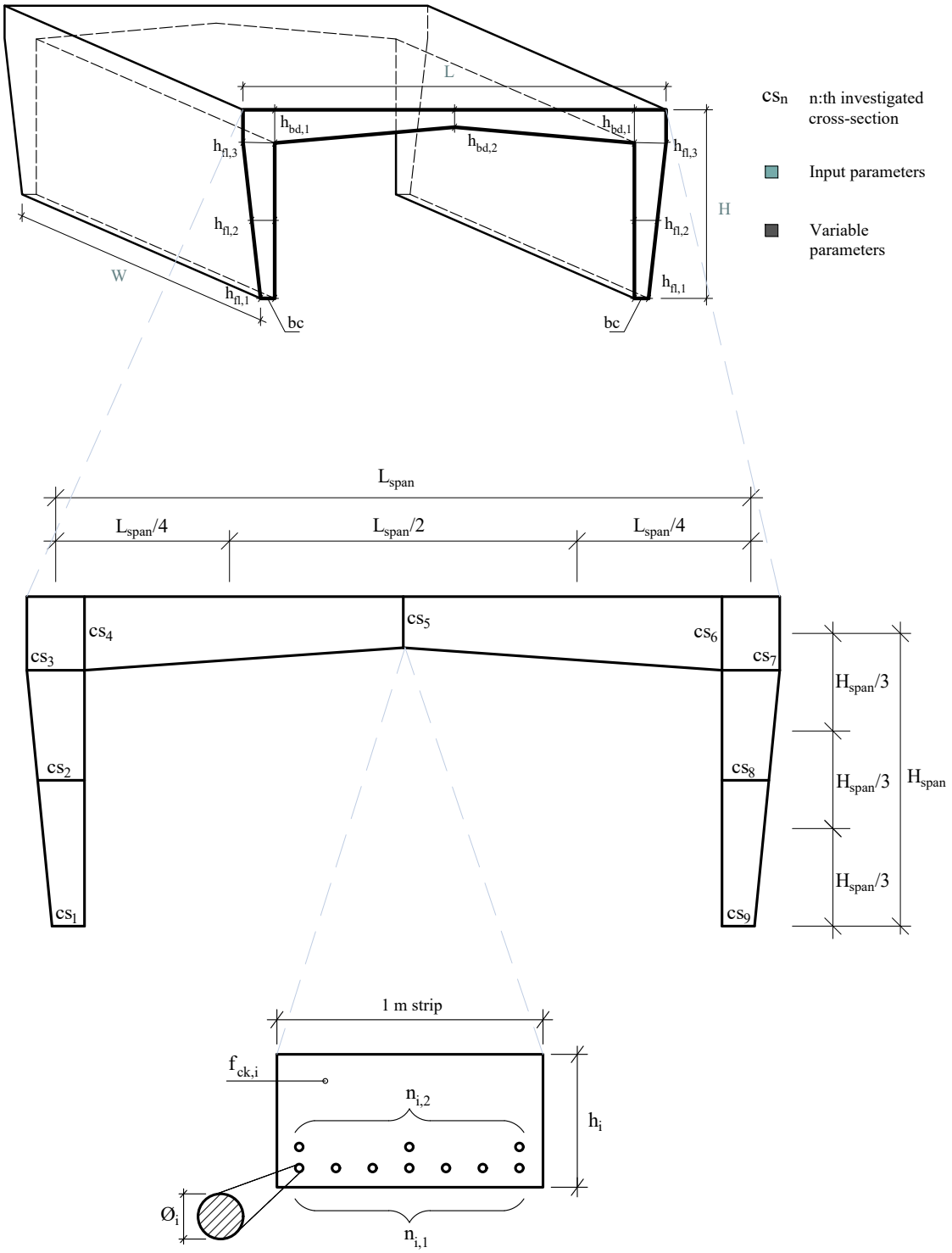

Figure 3.3: An illustration of the input- and variable geometry parameters in global scale, the discretization of the bridge frame into critical cross-sections and span lengths, and the variable parameters within each cross-section.

The frame was divided into frame legs and bridge deck, where each structural element was allowed to have varying cross-sectional heights in order to geometrically optimize the structural design. Nine cross-sections within the frame were considered critical, but the cross-sectional design was performed for five of them due to symmetry, according to Figure 3.3. Furthermore, the concrete class and tensile reinforcement diameter were kept the same for both the frame legs and the bridge deck within one generated design alternative, as means of easing the production procedure. The compressive reinforcement was disregarded as the positive contribution from compression rebars commonly is disregarded within the calculations performed by structural engineers, but instead adding them afterwards. Transverse reinforcement was also neglected.

The final generation of bridge design alternatives was performed by combining all the values for the above stated decision variables, given the specific input of L,H,W and bc, ultimately yielding Design space $\mathcal{B}$ according to Figure 3.1.

An important aspect in the generation of the initial data set of feasible and infeasible design solutions (Design space $\mathcal{B}$), was the ranges and step sizes for each parameter. The value of each parameter in the reference project was set as a reference, around which the variable values varied. The step sizes were chosen with a balance between mitigating too large computational complexity, and finding a sufficient resolution in the optimization result. Another important aspect in the generation of data sets is to set ranges large enough to capture outliers, i.e, solutions deviating considerably from the mean value of the probability density distribution.

3.2.2.2 Module 2: Constraints

Module 2 of the algorithm was aimed at implementing the optimization constraints, by performing structural design checks (ULS and SLS) on all the bridge design alternatives generated in Module 1. Hence, the set of designs was further narrowed down from Design space $\mathcal{B}$ to Design space $\mathcal{C}$ according to Figure 3.1.

A linear elastic structural analysis was performed on a 2D frame as previously mentioned, utilizing fundamental cases for frames according to Appendix C.1. The choice of a linear elastic 2D analysis was made in order to mitigate the computational complexity of the algorithm, to ultimately be able to generate and check large sets of data in a time-efficient manner. The calculations were based on the method of accounting for a 1 m wide strip of the bridge, the meter-strip method mentioned in Section 2.3.2. The choice further facilitated verification of the algorithm by comparison to a reference project utilizing the same meter-strip method.

The permanent loads applied were:

- Self-weight, and
- Earth pressure

The variable loads applied were:

- Surcharge load,
- LM1: UDL,
- LM1: TS,
- LM1: Braking/accelerating forces, and
- Counteracting earth pressure.

Load Model 1 (LM1) was implemented for the traffic loads instead of the *Vehicle Model* (VM), both explained in Section 2.5.2, as LM1 commonly is governing for shorter span bridges such as the slab frame bridge. Since the algorithm considers a one meter wide strip of the bride, the traffic loads were applied according to predefined amplitudes for lane 1, being the most conservative. The specific load calculation procedure of all the loads applied can be found in Appendix C.2.

All the load effects were computed for the nine critical cross-sections illustrated in Figure 3.3. Due to unsymmetrical loading, the load effects were compared in the corresponding positions on either side of the symmetry line (1-9, 2-8, 3-7 and 4-6) and the worst case was used in the design verifications of the five observed cross-sections. Two different load combinations were performed for ULS, Load combination 1 (dominating permanent loads) and Load combination 2 (non-dominating permanent loads), out of which the worst one was chosen for design verification. For the SLS deflection check frequent load combination was implemented, in combination with fundamental cases for frames. In each of the five cross-sections, the permanent load effects were load combined with the unfavorable variable load effects in the same position. See the procedure in Appendix C.4.

Sectional capacities in ULS (bending moment and shear) were calculated according to Appendix D, with the material properties stated in Appendix B. The allowable mid span deflection was set to L/400.

For each of the bridge design alternatives in Design space $\mathcal{B}$, the five cross-sections were checked towards the ULS constraints. If the shear capacity was not enough, stirrups were added in accordance with the applied shear force. Stirrups were thus not included as an initial design variable, but were rather added if required since optimized designs often result in slimmer constructions. Hence, it was considered important to relate buildability aspects to the need for stirrups as well. If any of the five cross-sections did not pass the checks, the whole bridge design alternative was disregarded. If all the five cross-sections passed the checks, an additional vertical SLS-deflection check was performed for the bridge deck span. Bridge designs that were verified against ULS- and SLS- constraints were added to Design space $\mathcal{C}$.

3.2.2.3 Module 3: Objective

Module 3 of the algorithm was aimed at evaluating the objective function of all the structurally verified bridge designs (Design space $\mathcal{C}$), generating the final set of the three most optimized bridge designs (Design space $\mathcal{D}$).

The module was built up as a multi-criteria optimization procedure based on three different criteria – investment cost, environmental impact and buildability. The three criteria were converted into costs to ensure a consistent unit, before being weighed together into an equivalent cost.

In addition to the equivalent cost calculation, the results were made transparent for the separate optimization criteria. Hence, spider graphs corresponding to each solution could be plotted in order to visually compare the optimized solutions on a criteria-basis . Each optimization criteria – investment cost, environmental impact and buildability – were represented by an axis on which the value for each cost category was plotted, creating a plane representing the bridge design solution. The principle behind the spider graph is further illustrated in Figure 3.4.

Three separate objective functions for the criteria were defined, together constituting an equivalent cost. Ultimately, the equivalent cost was used as the final objective function, enabling a single-objective optimization based on several criteria. Practically, Design space $\mathcal{D}$ was generated by constantly storing the three designs with the lowest equivalent cost as of yet, replacing them if more optimized solutions were found in the succeeding iterations.

For each bridge design alternative in Design space $\mathcal{C}$, the equivalent cost was calculated according to Equation 3.3, in order to compare designs to ultimately find the most optimized solutions.

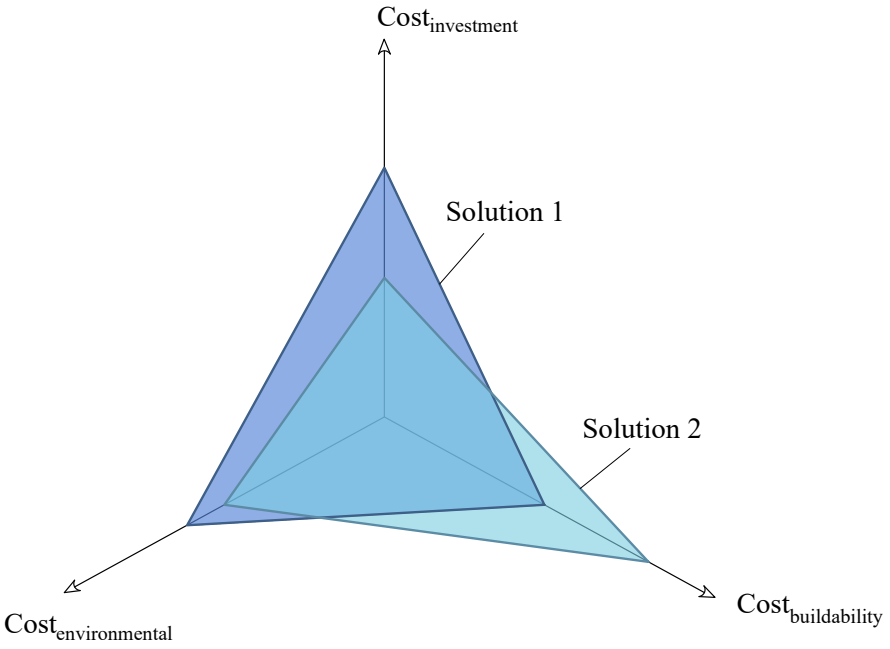

Figure 3.4: Illustration of two example solutions to the optimization problem, where the axes correspond to the three optimization criteria and the plane created by three points represents a solution.

$$cost_{eq} = cost_{inv} \cdot \psi_{inv} + cost_{env} \cdot \psi_{env} + cost_{build} \cdot \psi_{build} \tag{3.3}$$
$$0 \leq \psi_i \leq 1$$

Where ψ_i denotes the respective weighting factor per optimization criterion, enabling the choice of emphasis in the optimization. All criteria were considered to be of equal importance, thus weighted with the factor of one.

The unit volumes and unit weights of concrete and steel respectively, were calculated to subsequently be used as basis for the individual calculations of investment-, environmental- and buildability costs. Additionally, the formwork was assumed to be reused, thus not affecting the environmental impact cost.

The investment cost was defined in terms of material and labor costs related to the material amounts used. Furthermore, the environmental impact cost was defined using Ecovalue monetary values. Lastly, buildability aspects considered were factors related to geometrical complexity, material properties and the reinforcement ultimately yielding additional labor costs, according to:

- Varying thickness within structural members was assumed to increase the labor costs related to reinforcement work and formwork in comparison to straight members,
- The slenderness of structural members was assumed to affect the labor costs related to reinforcement work, since slender members require additional attention in order to ensure good quality,
- Concrete strength class C50/60 was assumed to add to the labor costs due to increased need of concrete vibration,
- The reinforcement diameter was assumed to affect the labor cost, since smaller diameters result in more ineffective reinforcing work ultimately increasing the time consumption for reinforcement work, and
- The need for shear reinforcement was assumed to increase the labor cost related to reinforcement work.

The total investment-, environmental- and buildability- costs for a bridge design were then defined according to Equations 3.4 through 3.6 respectively.

$$cost_{inv} = cost_{inv,reb} \cdot \alpha_{reb} + cost_{inv,form} + cost_{inv,conc} \tag{3.4}$$

$$cost_{env} = cost_{env,reb} \cdot \alpha_{reb} + cost_{env,conc} \tag{3.5}$$

$$cost_{build} = cost_{build,var} + cost_{build,sl} + cost_{build,conc.class+} \\ \alpha_{reb} \cdot (cost_{build,\phi} + cost_{build,stirrup}) \tag{3.6}$$

Where α_{reb} is a factor accounting for additional costs associated with increased reinforcement amounts due to anchorage lengths and detailing.

The full calculation procedure, as well as the unit prices and buildability factors implemented can be found in Appendix E.

3.2.3 Verification of optimization model

Two reference projects of existing slab frame bridges, provided by Skanska, were included in developing the algorithm, as means of verifying the calculations as well as for comparison of the results. One had been performed using 2D FE-modelling, for a bridge widening, while the second had been executed using 3D FE-modelling, for the complete construction of a new slab frame bridge. The 2D reference was solely used for verification of load effects, due to the similarities in load paths because of the two dimensional calculation model, similar to the procedures performed in the algorithm. The 3D reference was used for evaluation of the outcome of the algorithm, as a complete slab frame bridge construction was presented in the project documentation, needed as input for the optimization procedure. In order to obtain a fair evaluation of the optimization potential, the 3D reference project was inputted in the algorithm, from which the results were extracted and compared to the results provided by the optimized designs. Additionally, filtration plots were computed in order to verify the choice of initial set (Design space $\mathcal{B}$). See the following Sections 3.2.3.1-3.2.3.3.

3.2.3.1 Two-dimensional reference project

Initially, a 2D reference project was utilized as verification of cross-sectional capacities, applied loads, load combinations and load effects. In order to obtain a comparable verification, the reference project was chosen to be one calculated using 2D beam analysis in finite-element-modelling (FEM), in accordance with the algorithm developed. The reference project was performed in 2D since the client's request was to widen an existing bridge due to an increase in traffic flow, making it unnecessary to perform substantial 3D FEM. The 2D reference project was only used in order to verify load effects, but was not regarded as a reference project for verifying the effect of the algorithm due to its limited scope (bridge widening).

Additionally, the traffic loads implemented within the 2D reference project were based on Vehicle Models (VM) instead of Load Model 1 (LM1), thus made it necessary to implement the supposed governing vehicle model into the algorithm, to

facilitate the verification of results. Vehicle model n), according to Appendix C.2.6, was adopted within the simplified hand-calculations presented in the calculation documents provided by Skanska, used for verification of the FEM. Thus, the verification of the algorithm was also performed using vehicle model n). The simplified implementation of one single vehicle model was hence expected to result in some differences in load effects when verifying the algorithm against the 2D reference project. The specific dimensioning vehicle models according to the FEM-analysis, for shear and bending moment respectively, were not specifically stated in the calculation documents. A summary of the verification of load effects can be found in Appendix F.

3.2.3.2 Three-dimensional reference project

Since the provided 3D reference project dealt with the complete construction of a new slab frame bridge it was considered a suitable reference for the evaluation of the procedure created. An edge strip of the FE-model was used for comparison of values, where three-dimensional effects, such as load spread along the width of the bridge deck, are considered minimal. Due to the difference in calculation procedure, between the algorithm and the reference, minor modifications were made to the 3D reference project to account for those differences, continuously discussed in Chapter 5.2.

Input data from the 3D reference project was used as origin for defining spans of variable parameters, to be used in Module 1 of the algorithm (generation of design alternatives). Thereby, a finite initial design space (Design space $\mathcal{B}$) could be set, centered around the reference project. In addition to constituting the basis for variable parameters, the reference project was used for comparison with the optimized solutions. Running the specific reference project inputs through the code and extracting its results was a prerequisite for a fair comparison and evaluation of the procedure.

3.2.3.3 Filtration of data sets

In order to analyze the internal and external results of the design spaces, probability density distributions were plotted, being a data representation showing the solution frequency of certain solution intervals. In this case, the values on the x-axis show cost intervals, while the values on the y-axis show the probability density of each cost interval. For each design space generated by the algorithm, probability density distributions were outputted per optimization criterion. Naturally, as Design space $\mathcal{D}$ is a subset och Design space $\mathcal{C}$, which in turn is a subset of the larger domain Design space $\mathcal{B}$, their respective probability density distributions are contained within each other.

Additionally, as the optimization result was highly dependant of the choice of initial data set (Design space $\mathcal{B}$), a verification of the sets was carried out. It had

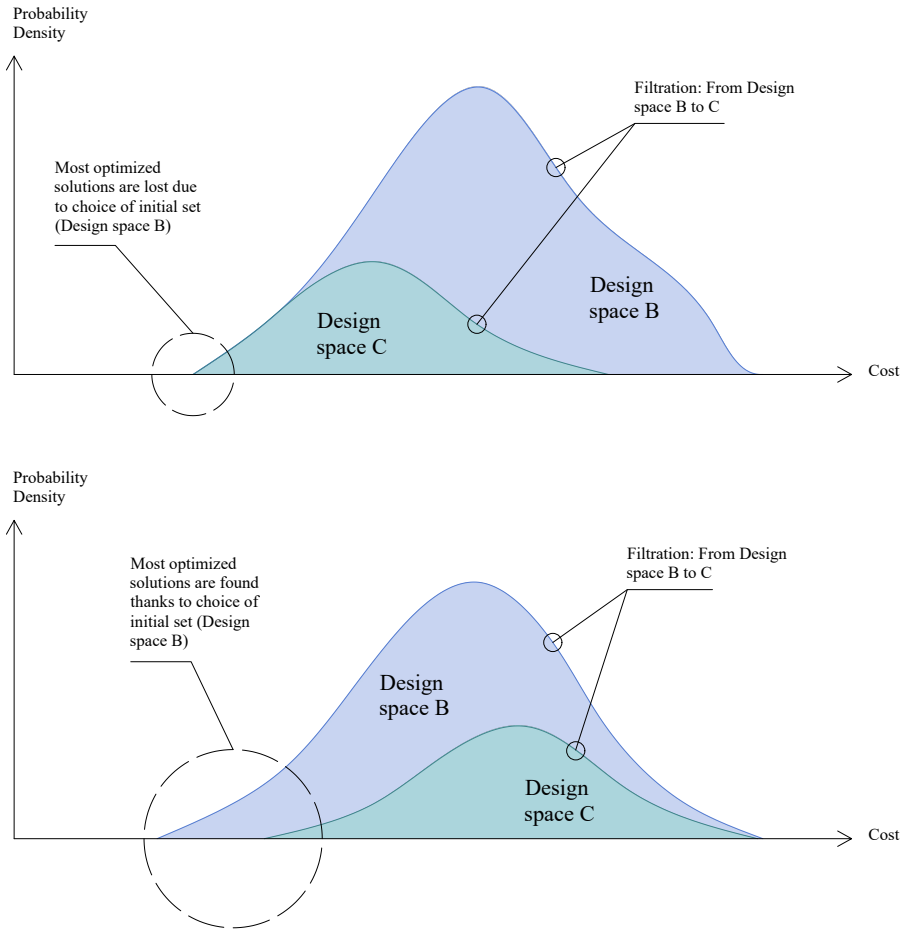

Figure 3.5: The choice of initial design space highly influences the result of the optimization procedure, illustrated by the principles of a filtering-procedure.

to be assured that Design space $\mathcal{C}$ did not share the lower domain boundary with the initial Design space $\mathcal{B}$, denoting that Design space $\mathcal{C}$ has ability of developing outliers – extreme values – with optimized results. If Design space $\mathcal{B}$ and $\mathcal{C}$ were to share the lower boundary of the domain, there would be a potential of finding more optimized designs, which were lost due to the choice of initial design space (Design space $\mathcal{B}$). The principles behind the choice of initial design space are further illustrated in Figure 3.5.

3.2.3.4 Automatic modelling of optimized solutions

The optimized design was automatically modelled in the 3D interface of Rhino as the algorithm outputted the results, as another mean of quickly verifying the results provided by the procedure. As a result of implementing an algorithm in a Python script within the parametric design software Grasshopper, the output is directly integrated in a 3D-modeling context, which is an efficient starting point for additionally connecting the algorithm to BIM. All the data that is generated within the script can be stored and re-interpreted into 3D-points ([x,y,z] or [u,v]), within the

grasshopper environment. Figure 3.6 shows an automatically updated 3D-model of the geometrical outline based on the output data for an optimized bridge. However, the modelling can be executed by parallelization for several design alternatives simultaneously, enabling effective visual comparison. Thereby, the implementation of the algorithm in Grasshopper facilitates automated modelling of the optimization result, which also constitutes a prerequisite for automatically connecting the results to BIM.

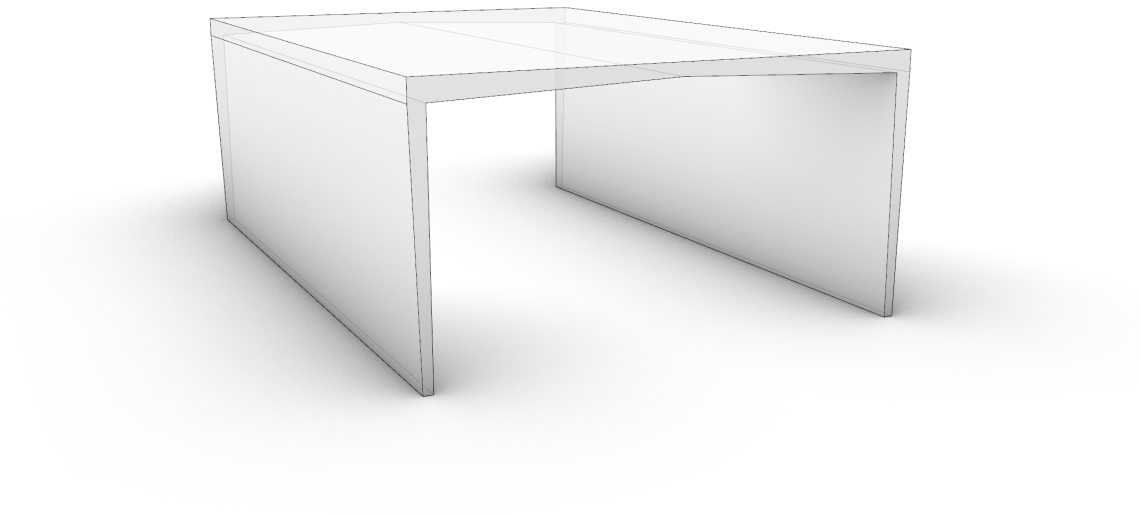

Figure 3.6: Automatic 3D model of the geometrical outline for the optimized design, generated from output data provided by the algorithm.

4

Results

The optimization procedure was performed in relation to a modified 3D reference project, as explained in Section 3.2.3.2, henceforth referred to as the reference. The input of variable ranges were decided by varying the parameters about the values observed in the reference, as explained in Chapter 3. All three optimization criteria were considered to be of equal importance, i.e., weighed with the factor $\psi_i = 1$ in the equivalent cost calculation.

Two initial sets were analysed. Set 1 sought to find the solution with the lowest equivalent cost (referred to as the optimal solution or Design 1), whereas Set 2 sought to find the design with the lowest environmental impact (referred to as the geometrically optimal solution or Design 2). The design alternatives in Set 1 were restricted to uniform members, whereas set 2 allowed for variable members. Here, *uniform* and *variable* refer to elements with constant and varying cross-sectional height, respectively. The results representing the two sets are presented in Sections 4.1 and 4.2.

4.1 Set 1: Optimized design

The initial data set called Set 1 was aimed at identifying the most optimal bridge design, considering all the optimization criteria contributions. The initial set of 104 976 bridge designs (Design space $\mathcal{B}$) was narrowed down to the three most optimized designs (Design space $\mathcal{D}$), according to Table 4.1, within a 3.8-minute running time of the algorithm.

Size of data set in each design space	
Design space	Nr. of bridge designs
$\mathcal{B}$: Initial set with fixed L, H, W and bc	104 976
$\mathcal{C}$: Set of designs that passed ULS and SLS constraints	9 371
$\mathcal{D}$: Set of optimized designs	3

Table 4.1: Number of bridge design alternatives in each design space.

4.1.1 Filtration of design spaces

To further illustrate the results, probability density functions of the design solutions were plotted for each of the optimization criteria, describing the observed outcome of all three design spaces $\mathcal{B}$ through $\mathcal{D}$. Figures 4.1-4.3 demonstrate the successive narrowing of the design spaces. Naturally, set $\mathcal{D}$ is a subset of set $\mathcal{C}$, which is turn is a subset of the larger domain $\mathcal{B}$. The choice of initial set was made in a manner allowing for finding far-left solutions in the set of feasible solutions.

Furthermore, the probability density functions related to environmental impact and investment cost exhibit a normal distribution amongst the design alternatives. Hence, very few design alternatives display a low normalized criteria cost in comparison to the rest of the design alternatives, i.e., highlighting the importance of implementing optimization procedures in order to find optimal solutions. In addition, the reference project is located in the center of the normal distribution curves of the two criteria. The two graphs also indicate on a well chosen initial set, since Design space $\mathcal{C}$ does not share the lower domain boundary with the initial set $\mathcal{B}$, denoting that all optimized designs are included within the initial set according to Section 3.2.3.3. In comparison, the probability density function representing normalized buildability costs does not show a normal distribution amongst design alternatives, since the criterion is defined in terms of a few discretely established design characteristics.

The set of optimized designs (Design space $\mathcal{D}$) was compared to the set of structurally feasible designs (Design space $\mathcal{C}$), according to Figures 4.1-4.3. The optimized designs show the lowest investment cost, an average environmental impact cost and the lowest buildability cost possible, denoting that the buildability criterion is decisive when identifying the most optimized designs.

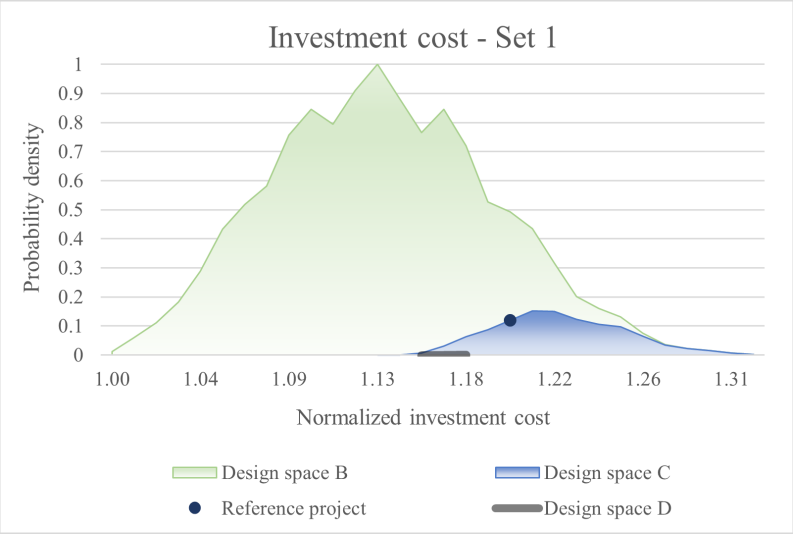

Figure 4.1: Normalized investment costs for the three design spaces observed.

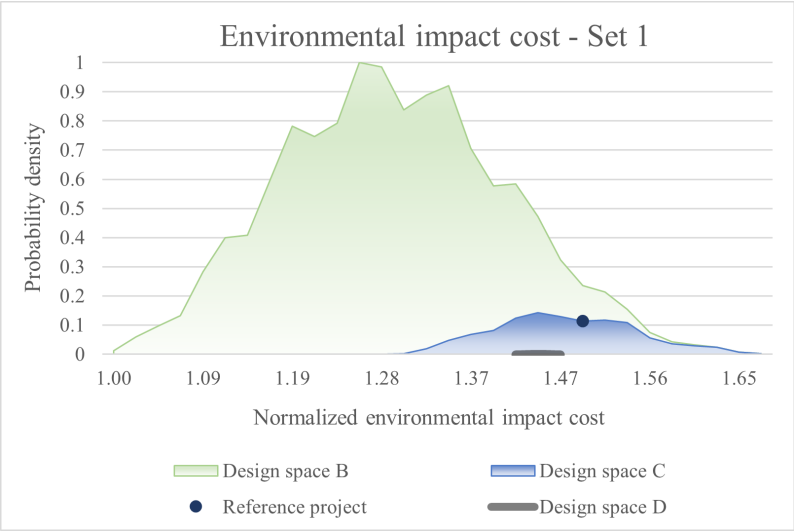

Figure 4.2: Normalized environmental impact costs for the three design spaces observed.

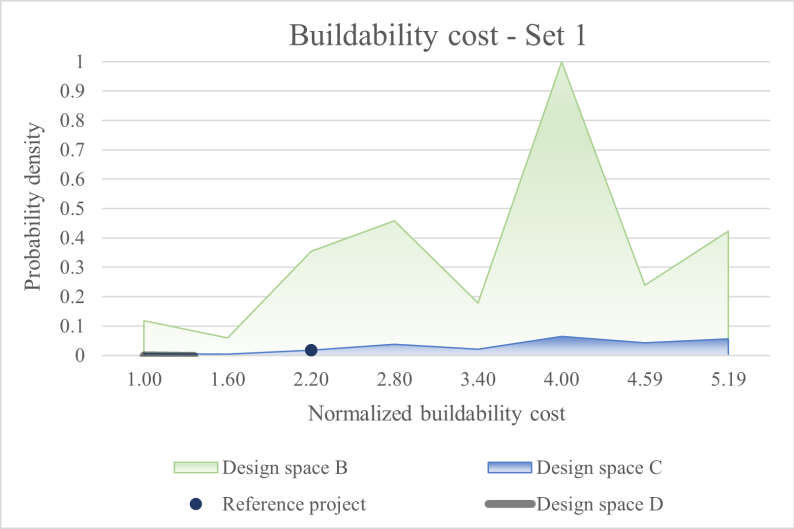

Figure 4.3: Normalized buildability costs for the three design spaces observed.

The optimized design delivered by the algorithm is further presented in Section 4.1.2.

4.1.2 Output data

The bridge design alternative displaying the lowest equivalent cost is characterized by having:

- A uniform frame, i.e., uniform frame legs and bride deck, resulting in minimized buildability costs for formwork and reinforcement labor,

- A low concrete class, resulting in minimized material costs and buildability costs, the latter due to less need for concrete vibration in order to achieve adequate concrete quality,

- Decreased cross-sectional heights with increased reinforcement amounts, due to minimized investment- and environmental impact costs.

- The largest reinforcement diameter, owing to less buildability cost additions related to reinforcement work, and

- Added shear reinforcement, which results in somewhat increased buildability costs, however enabling lessened concrete volume.

The bridge design optimized towards equivalent cost – Design 1 –, as delivered by the algorithm, is further illustrated in Figure G.1. Additionally, its corresponding costs are stated in Table 4.2.

Criteria results for Design 1			
	Reference	Optimal design	Percentage
Equivalent cost	2 417 000 SEK	2 285 000 SEK	-5.5%
Investment cost	1 856 000 SEK	1 818 000 SEK	-2.1 %
Environmental impact cost	442 000 SEK	423 000 SEK	-4.4 %
Buildability cost	119 000 SEK	44 000 SEK	-62.6 %
Total cost for client	1 975 000 SEK	1 862 000 SEK	- 5.7%

Table 4.2: Costs of the optimal design alternative in relation to the reference project.

As Table 4.2 indicates, the optimal design shows an equivalent cost decrease of 5.5 % in comparison to the reference project. When analyzed separately for the three constitutive criteria, the investment-, environmental impact- and buildability costs of this solution exhibit a decrease of 2.1%, 4.4% and 62.6% respectively. The result indicates on an overall cost gain of 5.7% for material and labor cost including additional buildability costs, i.e., costs relevant for the client.

In order to further clarify the algorithm's choice of optimal design, the contributions from the three constitutive criteria were further investigated. The environmental impact criterion is predominantly governed by the material volume. Similarly, the investment cost is generally mitigated by more slender designs. In contrast, the buildability cost tends to increase as slim designs are associated with additional need for labor work due to need for stirrups, larger amounts of reinforcement and higher concrete class. As previously mentioned in Section 4.1.1, the buildability criterion is the determinant factor for identifying optimized designs. The importance of the buildability criterion is further established as the chosen alternative has a uniform frame, i.e., minimized buildability costs resulting in somewhat higher investment

costs. The complex interaction between lowered investment costs and additional buildability costs (costs that the client needs to pay for), were further investigated and the results are described in Section 4.1.3.

4.1.3 Interaction between investment- and buildability costs

The optimization procedure indicated conflicting results regarding investment costs and buildability costs, thus resulting in a constant balancing between the two criteria contributions. Since these two criteria, as opposed to the environmental impact, are determinant in the actual cost affecting the client, it is of interest to compare their internal balance. Figure 4.4 shows the interaction between investment costs – material- and labour costs – and buildability costs for three design alternatives: the ones with the lowest, mean and highest equivalent cost, all of which are compared to the reference project. Proportions of the internal cost contributions of the investment cost and the buildability cost, respectively, are shown in order to deduce governing factors of high costs.

According to Figure 4.4, the investment cost is predominantly governed by the formwork labor cost and the material cost for concrete. The major contribution to the buildability criterion is in terms of additional formwork labor costs due to having structural elements of varying thickness. A difference between the investment costs of Design 1 and the reference is that Design 1 has reduced the amount of concrete material, however gained a comparable amount of reinforcement material- and labour. For the most optimized solution, the largest contribution to the buildability cost emerges from additional reinforcement work from having slender structural elements, while the buildability costs related to varying cross-sectional heights are mitigated.

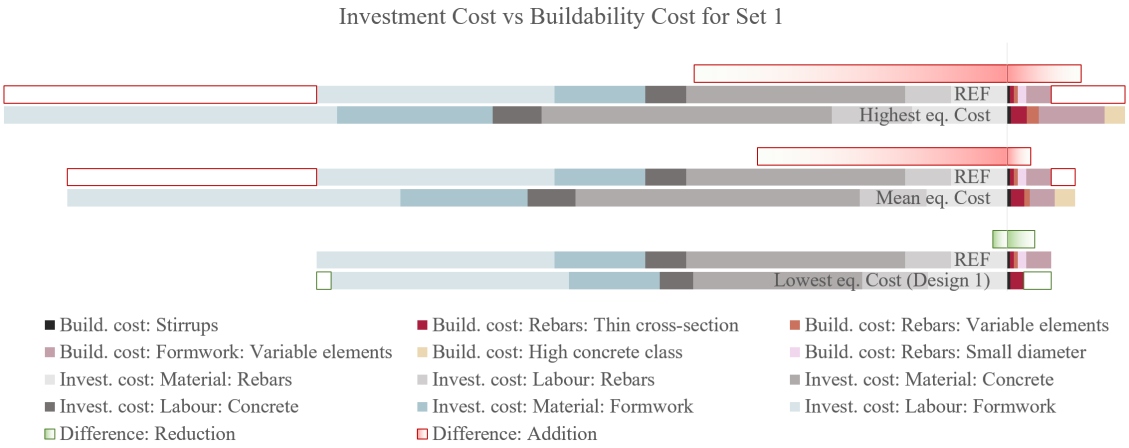

Figure 4.4: Comparative bar chart showing investment cost (material cost + labour cost) in relation to different buildability cost aspects, for the solution with the highest, mean and lowest equivalent cost in Set 1, all compared to the reference project.

The material- and labor costs related to formwork represent a major part of the initial investment costs and are rather constant for all bridge design alternatives, optimized or not, as shown in Figure 4.4. In order to describe the outcome of the optimization of the construction materials more fairly, additional results were extracted without considering criteria related to formwork, thus providing a more representative outcome of the investment- and environmental impact- cost gains due to minimized material volumes (concrete and reinforcement). The results are presented in Table 4.3.

Criteria results for Design 1 excl. formwork			
	Reference	Optimal design	Percentage
Equivalent cost	1 467 000 SEK	1 401 000 SEK	-4.5%
Investment cost	973 000 SEK	934 000 SEK	-4.0 %
Environmental impact cost	442 000 SEK	423 000 SEK	-4.4 %
Buildability cost	120 000 SEK	52 000 SEK	-14.8 %
Total cost for client	1 025 000 SEK	978 000 SEK	-4.5%

Table 4.3: Costs of the optimal design alternative in relation to the reference project, excluding formwork.

As seen in Table 4.3, the same solution exhibits an equivalent cost reduction of -4.5%. The constitutive criteria representing investment-, environmental impact- and buildability costs demonstrate decreases of 4.0%, 4.4% and 14.8% respectively, when excluding formwork from the criteria calculations. The environmental cost is unaffected of the inclusion of formwork as formwork is not included in the environmental cost criterion, being considered recyclable. The cost which the client is responsible for paying is decreased by 4.5%. Thus, clarifying the adverse impact of including formwork in the criteria calculations.

In order to further explore the impact of formwork related criteria, the algorithm was run a second time for the same initial set (Set 1), but completely ignoring costs related to formwork. The ultimate goal was to identify if the algorithm would still consider Design 1 as the optimal design. A completely different optimal bridge design was instead delivered by the algorithm, one with structural elements of varying thickness, i.e. an alternative which is more geometrically optimized (more material efficient).

As the algorithm is highly controlled by the buildability criterion, which is governed by additional labor costs related to varying thickness of structural members, the optimal design according to Set 1 is presented as a uniform frame, as long as formwork is included. In order to identify geometrically optimized designs (lowest environmental impact), another initial set (Set 2) was analysed where all design alternatives exhibit varying thickness of structural members, thus ignoring possible solutions of uniform frames. The results representing the most geometrically optimized designs are further presented in the following Section 4.2.

4.2 Set 2: Geometrically optimized design

Set 2 was aimed at identifying the most geometrically optimal bridge designs, considering all the optimization criteria contributions, while only allowing structural elements of varying thickness. The initial set of 104 976 bridge designs (Design space $\mathcal{B}$) was subsequently narrowed down to the three most optimized designs (Design space $\mathcal{D}$), according to Table 4.4, within a 3.8-minute running time of the algorithm.

Size of data set in each design space	
Design space	Nr. of bridge designs
$\mathcal{B}$: Initial set with fixed L, H, W and bc	104 976
$\mathcal{C}$: Set of designs that passed ULS and SLS constraints	9866
$\mathcal{D}$: Set of optimized designs	3

Table 4.4: Number of bridge design alternatives in each design space.

4.2.1 Filtration of design spaces

Probability density functions representing the successive narrowing of the second initial set are presented in Figures 4.5 - 4.7. When comparing the set of geometrically optimized designs (Design space $\mathcal{D}$) to the set of structurally feasible designs (Design space $\mathcal{C}$), the optimized designs are characterized by the lowest investment-, environmental impact- and buildability costs possible for the initial set containing only variable bridge frames, thus minimizing all the criteria simultaneously. Noteworthy is the absence of a reference project indicator within Figure 4.7. Since Set 2 only contains bridge frames of varying thickness, i.e. very high buildability costs, the correlating cost for the reference project lies outside the buildability cost range presented in the graph, thus is not indicated.

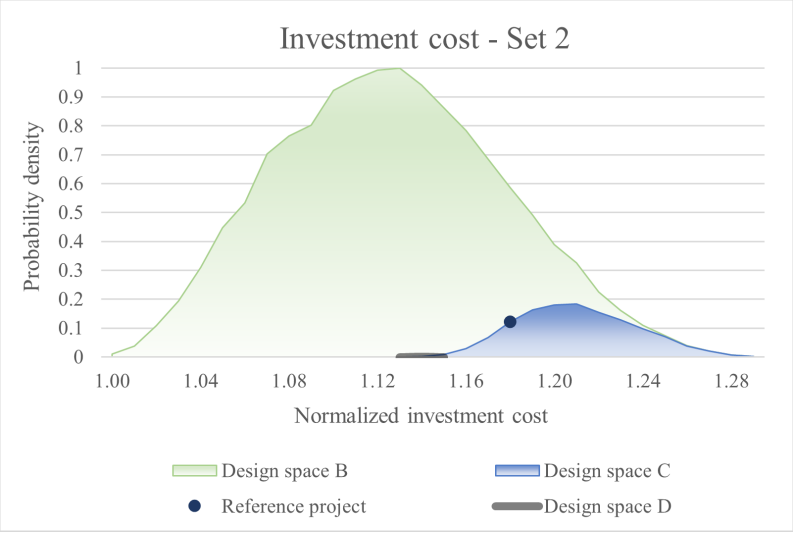

Figure 4.5: Normalized investment costs for the three design spaces observed.

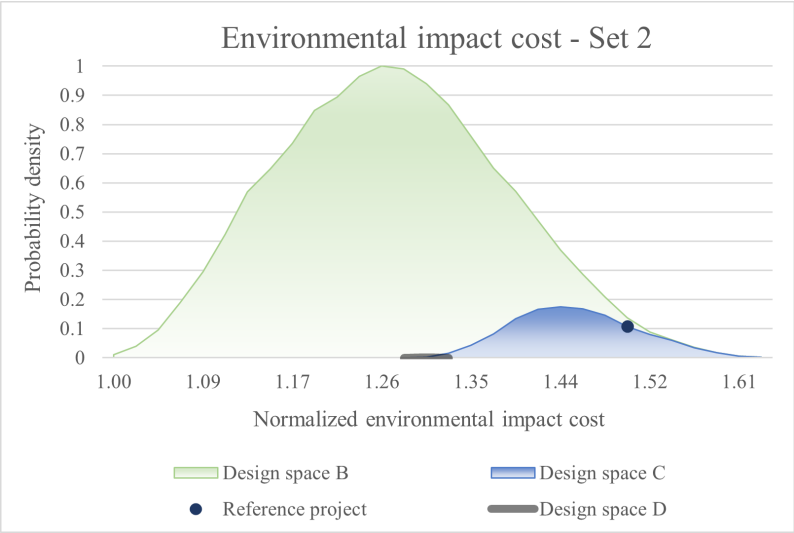

Figure 4.6: Normalized environmental impact costs for the three design spaces observed.

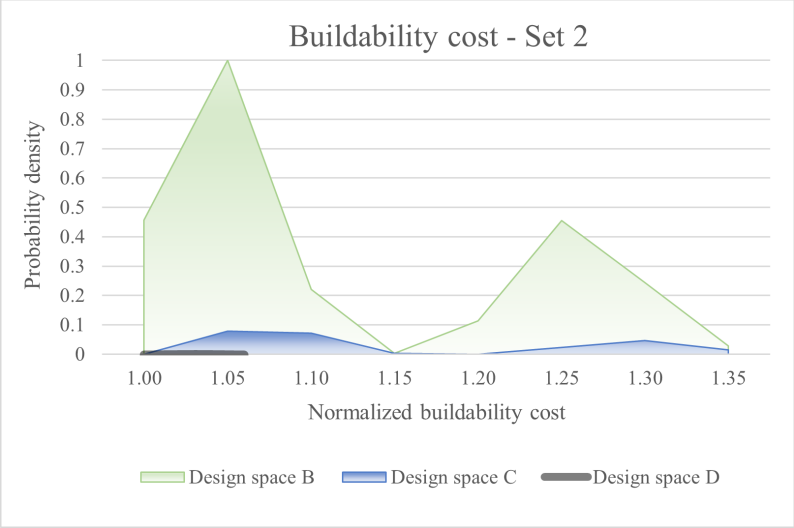

Figure 4.7: Normalized buildability costs for the three design spaces observed.

The geometrically optimized design delivered by the algorithm is further presented in Section 4.2.2.

4.2.2 Output data

The geometrically optimized bridge design alternative, displaying the lowest environmental cost, is characterized by having:

- A non-uniform frame, i.e., variable thickness of frame legs and bride deck, resulting in minimized environmental- and investment- costs, but increased buildability costs,

- A low concrete class, resulting in minimized material costs and buildability costs, the latter due to less need for concrete vibration in order to achieve adequate concrete quality,

- Decreased cross-sectional heights with increased reinforcement amounts, due to minimized investment- and environmental impact costs.

- The largest reinforcement diameter, owing to less buildability cost additions related to reinforcement work, and

- Added shear reinforcement, which results in somewhat increased buildability costs, however enabling lessened concrete volume.

The geometrically optimal bridge design, Design 2, as delivered by the algorithm is further illustrated in Appendix G. Additionally, the corresponding costs are stated in Table 4.5. Noteworthy is that the geometrically optimized design delivered by running Set 2 is the same optimal design as provided by the algorithm when running Set 1 without formwork, again highlighting the importance of the buildability criterion when finding optimal bridge designs.

Criteria results for Design 2			
	Reference	Optimal design	Percentage
Equivalent cost	2 417 000 SEK	2 401 000 SEK	-0.7%
Investment cost	1 856 000 SEK	1 781 000 SEK	-4.0%
Environmental impact cost	442 000 SEK	381 000 SEK	-13.7%
Buildability cost	119 000 SEK	238 000 SEK	+100.9%
Total cost for client	1 975 000 SEK	2 020 000 SEK	+2.3%

Table 4.5: Costs of the geometrically optimal design alternative in relation to the reference project.

As Table 4.5 indicates, the geometrically optimal design exhibits an equivalent cost decrease of 0.7% in comparison to the reference project. When analyzed separately for the three constitutive criteria, the investment- and environmental impact- costs show a decrease of 4.0% and 13.7% respectively, while the buildability cost exhibits and increase of 100.9%. The result indicates on an overall cost increase of 2.3% for material and labor cost including additional buildability costs, i.e., direct costs that the client needs to pay for. As Table 4.5 suggests, the difference in final costs is not substantial, but still noticeable. The geometrically optimized solution shows how the reduction in investment costs can be used to finance the additional buildability costs that a more environmentally optimized design entails, ultimately just increasing the price with 2.3% for a noticeably more sustainable design.

The relation between reduced investment costs and worsened buildability circumstances, for geometrically optimized designs, is further investigated in Section 4.2.3.

4.2.3 Interaction between investment- and buildability costs

As previously mentioned in Section 4.1.3, it is of interest to investigate the balance between investment cost and buildability cost, being the two criteria economically affecting the client. The optimization procedure considers the complex relationship between minimized investment costs and additional buildability costs by balancing the criteria contributions. The contradictory nature of the two criteria is best visualized by the bar chart belonging to the geometrically most optimized design presented in Figure 4.8. The graph illustrates the reallocation of costs, which has shifted from investment costs (due to non-utilized material) to buildability costs (due to complexity in geometry and material properties), ultimately yielding a bridge design of a slightly lower total cost but significantly lower environmental impact. The result clarifies the possibility of unifying economic and environmental sustainability by implementing optimization procedures.

As explained in Section 4.1.3, a more representative result for describing the investment- and environmental impact- cost gains due to minimized material volume is achieved by excluding the criteria costs related to formwork. The results are presented in Table 4.6.

The geometrically optimal bridge design demonstrates a decrease in equivalent cost of 12.3%. When looking into the three constitutive criteria, the investment- and environmental impact costs shows a reduction of 13.4% and 13.7% respectively, while the buildability criterion exhibits an increase of 19.1%. Ultimately by opting for a geometrically optimal design, the client can save 11.7% of costs excluding formwork, solely by mitigating the material usage of concrete and reinforcement.

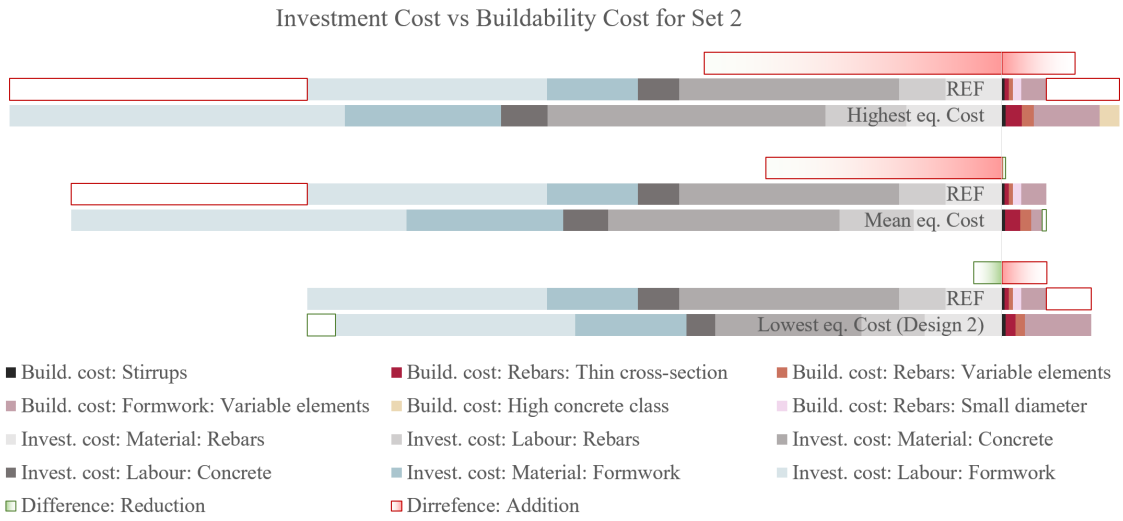

Figure 4.8: Comparative bar chart showing investment cost (material cost + labour cost) in relation to different buildability cost aspects, for the solution with the highest, mean and lowest equivalent cost in set 2, all compared to the reference project.

Criteria results for Design 2 excl. formwork			
	Reference	Optimal design	Percentage
Equivalent cost	1 467 000 SEK	1 286 000 SEK	-12.3%
Investment cost	973 000 SEK	843 000 SEK	-13.4%
Environmental impact cost	442 000 SEK	381 000 SEK	-13.7 %
Buildability cost	52 000 SEK	62 000 SEK	+19.1 %
Total cost for client	1 025 000 SEK	905 000 SEK	-11.7%

Table 4.6: Costs of the geometrically optimal design alternative in relation to the reference project, excluding formwork.

4.3 Comparison of monetary values in environmental cost

As previously explained, Ecovalue was used as the primary monetary weighing system. Additional runs were made in order to establish the impact of the chosen environmental cost definition. A comparison was made between the optimization outcome of the two discussed weighing systems for the environmental cost calculation (Ecovalue and Ecotax), where the costs implementing the Ecotax monetary system for Design 1 and 2 are presented in Tables 4.7 and 4.8 consecutively.

Criteria results for Design 1 using Ecotax monetary system			
	Reference	Optimal design	Percentage
Equivalent cost	2 073 000 SEK	1 956 000 SEK	-5.7%
Investment cost	1 856 000 SEK	1 818 000 SEK	-2.1%
Environmental impact cost	98 000 SEK	93 000 SEK	-4.4%
Buildability cost	119 000 SEK	44 000 SEK	-62.6%
Total cost for client	1 975 000 SEK	1 862 000 SEK	-5.7%

Table 4.7: Costs of the optimal design alternative in relation to the reference project, adopting the Ecotax monetary system.

Criteria results for Design 2 using Ecotax monetary system			
	Reference	Optimal design	Percentage
Equivalent cost	2 073 000 SEK	2 104 000 SEK	+1.5%
Investment cost	1 856 000 SEK	1 781 000 SEK	-4.0%
Environmental impact cost	98 000 SEK	84 000 SEK	-13.7 %
Buildability cost	119 000 SEK	238 000 SEK	-100.9 %
Total cost for client	1 975 000 SEK	2 020 000 SEK	+2.3%

Table 4.8: Costs of the geometrically optimal design alternative in relation to the reference project, adopting the Ecotax monetary system.

The monetary value solely changes the weighing of the environmental impact criterion. Using Ecotax instead of Ecovalue affects the equivalent cost, however not the respective percentage differences per criterion cost, as shown in Tables 4.7 and 4.8. For Design 1, the percentual changes in equivalent costs are observed to be -5.5% and -5.7% implementing Ecovalue and Ecotax respectively. The corresponding values observed for Design 2 are -0.7% and +1.5%. For Design 1 the two weighing systems result in similar equivalent cost decreases independent of monetary weighing system. On the contrary, for Design 2, the two systems show diverging results. When implementing Ecovalue, the final equivalent cost is assumed to decrease (-0.7%), ultimately yielding a design which is better in contrast to the reference project. When instead implementing Ecotax, the final equivalent cost increases for the optimal design(+1.5%), thus indicating on a worse solution in comparison to the reference project. Thus, the chosen definition for the environmental impact cost highly influences the interpretation of the results delivered by the algorithm, but does not affect the optimal designs delivered when running the two sets.

4.4 Summary of main results

In order to obtain an overview of all the results provided by the algorithm when run with Set 1 or Set 2, with or without the inclusion of formwork as well as with Ecovalue or Ecotax, all the cost output changes are summarized into Table 4.9.

As seen in Table 4.9, all of the aforementioned conditions result in either Design 1 or 2, where Design 1 has a uniform frame (minimized buildability costs) and Design 2 has a geometrically optimal frame with varying thickness (minimized investment and environmental costs). The previously presented contributions for investment- and buildability costs representing Design 1 and 2, in comparison to the reference project, are subplotted in Figure 4.9 for comparison of the costs affecting the client. The dominating cost contribution in Design 2 emerges from the variable elements, both affecting the reinforcing - and formwork buildability cost. As demonstrated by the cost difference bars, the additional buildability costs in Design 2, compared to the reference, dominate over the corresponding investment cost reduction, ultimately yielding a slight cost addition in total. Design 1 on the contrary, only consisting of uniform elements, demonstrate zero contributions from variable elements related to formwork- and reinforcement buildability costs. Consequently, Design 1 reduces both investment- and buildability costs in relation to the reference. Design 1 and 2 in comparison to the reference project can be found in Appendix G.

In order to visually represent the main results spider diagrams are presented in Figure 4.10, indicating the internal normalized amplitudes of each criteria for the most optimized design in Set 1 (Design 1) and Set 2 (Design 2) in comparison to the reference project. The internal contributions to each criteria can further be identified in Figure 4.9.

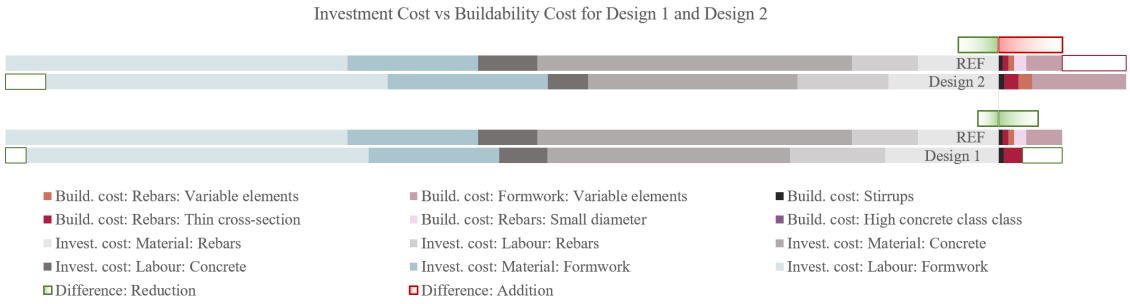

Figure 4.9: Comparative bar chart showing investment cost (material cost + labour cost) in relation to different buildability cost aspects, for Design 1 and Design 2 compared to the reference project.

Summary of percentual cost changes for optimal designs						
Input	Equiv. cost	Invest. cost	Envir. cost	Build. cost	Client cost	Optimal design
Set 1 Formwork Ecovalue	-5.5%	-2.1%	-4.4%	-62.6%	-5.7%	Design 1
Set 1 Formwork Ecotax	-5.7%	-2.1%	-4.4%	-62.6%	-5.7%	Design 1
Set 1 No formwork Ecovalue	-4.5%	-4.0%	-4.4%	-14.8%	-4.5%	Design 2
Set 2 Formwork Ecovalue	-0.7%	-4.0%	-13.7%	+100.9%	+2.3%	Design 2
Set 2 Formwork Ecotax	+1.5%	-4.0%	-13.7%	+100.9%	+2.3%	Design 2
Set 2 No formwork Ecovalue	-12.3%	-13.4%	-13.7%	+19.1%	-11.7%	Design 2

Table 4.9: Difference in cost between optimal designs provided by the algorithm considering different criteria, and the reference project.

As seen in figure 4.10a, the inclusion of formwork results in major discrepancies in buildability costs between the design alternatives, as the designs have varying numbers of uniform structural elements, being the main criteria contribution. Additionally, the investment costs are similar for all three designs due to major, almost constant, additions from formwork material- and labor- costs. Furthermore, the investment - and environmental costs are closely correlating as both are based on material volumes, while the buildability criterion is inversely related to those criteria. As material volumes are mitigated, the buildability cost is simultaneously increased.

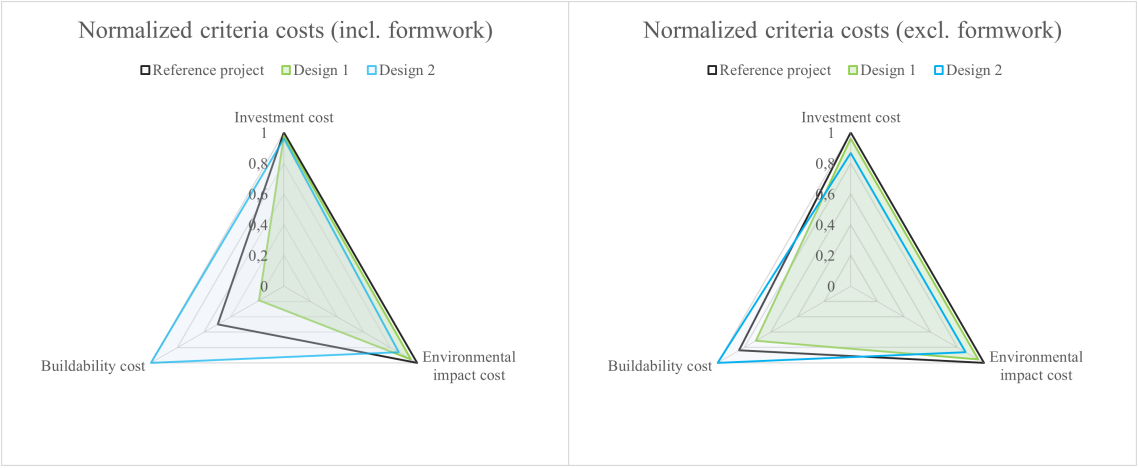

(a) Formwork, Ecovalue **(b)** No formwork, Ecovalue

Figure 4.10: Criteria costs for comparison between reference project, Design 1 and Design 2, normalized for each criterion.

Figure 4.10b instead shows the normalized criteria costs when formwork is excluded from the analysis, resulting in smaller differences in buildability costs and larger differences in investment costs. The environmental impact criterion is independent of the inclusion of formwork, being considered recyclable, hence no discrepancies are observed in the environmental when comparing the two spider plots. As seen in Figure 4.10b, the internal hierarchy of buildability cost observed between the three designs is remained when excluding the formwork, however with different proportions. The difference between Design 1 and the reference project is a result of additional labor costs due to small reinforcement diameters used within the reference project, dominating over the additional reinforcement work of thin cross-sections in Design 1, as observed in Figure 4.9. Furthermore, when comparing Design 2 to the reference, the cost contributions from additional stirrups, thin cross-sections and reinforcing work for variable elements in Design 2 dominate over the small rebar diameters in the reference, as observed in Figure 4.9.

4.5 Long term effects

The long term effects of implementing the algorithm into the preliminary design phase of slab frame bridges can be concretized in relation to forthcoming construction projects in Sweden. Solely within the ongoing project *Norrbotniabanan*, with the purpose of constructing a 270 kilometer long railway between Umeå and Luleå, approximately 250 bridges are planned (Trafikverket, 2022b).

The bridge types most suitable for coming construction projects are decided in the early stages of the planning process, partly with respect to LCC-analyses (Life

Cycle Cost), thus making it impossible to specify the number of slab frame bridges that are to be built during the coming years. In order to perform an accurate estimation on the amount, the Swedish Transport Administration was consulted. A representative working at the agency (Olsson, 2023) provided information about the number of bridges built during the time period of 2016-2020 according to Table 4.10. The information was subsequently used as basis for making reasonable predictions about the future.

Number of bridges built during 2016-2020		
Year	Total number of bridges	Number of slab frame bridges
2020	134	45
2019	95	18
2018	111	29
2017	90	21
2016	112	25

Table 4.10: The number of bridges built by the Swedish Transport Administration during the time period of 2016-2020.

As presented in Table 4.10, 542 bridges were built by the Swedish Transport Administration during 2016-2020, out of which 138 were slab frame bridges. In order to predict the effect of implementing the optimization procedure, an approximation of 140 slab frame bridges were assumed to be constructed during the forthcoming five years. The estimation further assumed the approximate dimensions of those 140 bridges to be similar to the reference project implemented within the algorithm. The potential savings of implementing the optimization algorithm, in terms of CO_2 emissions and costs are summarized into Table 4.11.

Costs and CO_2 emissions of 140 slab frame bridges				
	CO_2 eq	ΔCO_2 eq	Client cost	Δ Client cost
140 x Reference project	21 720 ton		276.5M SEK	
140 x Design 1	20 770 ton	-955 ton	260.7M SEK	-15.8M SEK
140 x Design 2	18 740 ton	-2 980 ton	282.8M SEK	+6.3M SEK

Table 4.11: Effects of implementing the optimization algorithm in the preliminary design phase of slab frame bridges, during the next five year time period based on approximations from the Swedish Transport Administration.

Consequently, as Table 4.11 infers, large savings could be made by implementing the procedure in order to identify optimal designs. Choosing Design 1 would result in 15.8M SEK in cost savings for the client while only lowering the CO_2 emissions with 955 tons. Choosing Design 2 would instead result in a decrease on 2 980 tons in CO_2 emissions for an increased cost of 6.3M SEK. For context, 2 980 tons of CO_2 emissions correspond to the average annual carbon footprint of approximately 745

people (The Nature Conservancy, 2023). Hence, there is a possibility for substantial environmental impact mitigation by implementing the optimization procedure on *one* type of bridge construction during a *five* year time period, being a considerable incentive for implementing similar procedures for other commonly built concrete structures in the future as well.

5

Discussion

This thesis sought to evaluate the possibilities of implementing a set-based multi-criteria optimization procedure in the preliminary design phase of slab frame bridges, with respect to investment cost, environmental impact and buildability. A main concern of the work was to find means of implementing buildability as a measurable quantity, in order to consider additional labour costs early in the planning process. Additionally, the research was aimed at exploring the relations between the three optimization criteria observed, as well as governing parameters within each criterion. Lastly, the possibilities of generating large data sets, as well as the future prospects of applying the algorithm, were examined.

In evaluating the output of the algorithm, two chief initial sets were analyzed (Set 1 and Set 2), combined with different means of computing the objective function. These differences were based on inclusion of formwork and choice of monetary value for the environmental impact criterion, which markedly influenced the optimization result. Two optimal designs were found based on Set 1 and Set 2, the former solely containing uniform elements, and the latter allowing for variable elements. When including formwork, Design 1 showed the lowest equivalent cost, whereas Design 2 exhibited the lowest environmental impact cost whilst slightly increasing the client's costs (investment- and buildability costs). In the case of excluding formwork, Design 2 instead demonstrated the lowest equivalent cost. Hence, the results indicated a complex relationship between investment cost and additional buildability costs, as well as a pronounced impact of costs related to the formwork. A primary observation was that the procedure demonstrated diverging results when optimizing towards the equivalent cost, and towards environmental sustainability. In the case of Design 2, a resource distribution has been made, where costs are relocated from material usage to labour. Thus, the client effectively pays for a more environmentally sustainable design, leaving a decision based on priorities.

Observations made regarding the different optimization criteria, together with differences between the optimal solutions are discussed in the following Section 5.1. Limitations and sources of error, as well as possible further developments are discussed in the successive Sections 5.2 and 5.3.

5.1 Discussion of results

When investigating the probability density distributions with respect to each optimization criterion, following the filtration of design spaces $\mathcal{B}$ trough $\mathcal{D}$, it was observed that the investment- and environmental impact criteria demonstrate a normal distribution amongst design alternatives, see Figures 4.1, 4.2, 4.5 and 4.6. Moreover, the modified reference project lies more centered in the probability density graphs of the investment cost- and environmental criteria, in relation to the most optimal designs occurring in the lower cost domains. The observation highlights the importance of implementing optimization procedures in order to identify outliers of solution alternatives – optimal designs. The probability of finding outliers when implementing traditional PBD, adopted by structural engineers today, is considerably lower than of finding solutions near the mean value of a normal distribution.

As opposed to the investment- and environmental cost, the probability density distributions related to the buildability criterion do not demonstrate a normal distribution amongst design alternatives. The distributions do not concentrate towards one pronounced peak, instead several local maxima and minima can be observed. The explanation to this irregular distribution lies within the buildability cost definition, resulting from several discrete, of one another independent, aspects with diverging effects on the criterion. Furthermore, when comparing the buildability distribution for Set 1 and 2, according to Figures 4.3 and 4.7, major differences can be observed. Set 2 exhibits fewer local maxima, as a result of the chosen initial set, only containing bridge designs of non-uniform frames, thus assures the additional buildability costs related to varying thickness of structural members.

The spider diagrams in Figure 4.10 demonstrate the relation between the optimization criteria for the two optimal designs compared to the reference, while also emphasizing the influence of formwork. A key finding was that the optimized solution, Design 1, and the geometrically optimized solution, Design 2, together with the reference exhibited a general inverse correlation between buildability and the other two criteria. When comparing the two diagrams in Figure 4.10, the formwork markedly constitutes a substantial portion of the investment cost- and buildability criteria. The investment cost from formwork is rather constant for different design solutions, as formwork costs are based on the surface area of each bridge element respectively, which is approximately the same for all design alternatives due to fixed initial dimensions of the bridges within Design space $\mathcal{B}$.

The results observed regarding the different criteria costs can be viewed in the context of today's tendering processes. Today, the effective cost of a project, i.e., the cost that the client needs to pay for, does not include the environmental impact. Within this research, the environmental impact is interpreted as a hypothetical cost. Therefore, considering today's decision basis, it is of interest to investigate the costs influencing the cost relevant for the client, i.e., investment- and buildability costs. The comparative chart diagrams, as seen in Figures 4.4 and 4.8, demonstrate

a balance between investment cost and buildability cost. When comparing the two initial data sets, it was observed that Design 2, being more materially efficient but less buildable than Design 1, did not reduce the investment cost sufficiently in relation to its increased buildability cost. Design 1, on the contrary demonstrates a significantly more buildable solution, however less materially optimized. The balance observed further motivates the need for implementing buildability in structural optimization as means of detecting costly surcharges early in the planning process.

Despite today's exclusion of environmental impact as an actual cost in tendering processes, a discussion can be brought forward regarding the future of this topic. As previously stated, tendering processes of infrastructural projects are currently governed by economical aspects by adopting the *Lowest price-* or *Lowest total cost-method*. In some cases, the *Most economically advantageous- method* is utilized, where additional profits are given to the contractor delivering a tendering proposal which considers sustainability on different societal levels. Further emphasis on environmental sustainability within tendering processes could be a necessary change in the work towards the environmental goals added to the Swedish legislation during 2018, emerging from the Paris agreement. The action plan *Färdplan för fossilfri konkurrenskraft* was developed in order to present approaches in line with realizing those changes, as explained in section 2.1. The action plan highly emphasizes the importance of the preliminary design phase, where the possibility of influencing the end product is large in relation to the cost. Additional proposals presented call for major adjustments within the tendering procedure, where it has to be profitable for contractors to present designs with high environmental awareness. The set-based optimization procedure presented shows how the level of available information can be drastically increased in the early stages of design, ensuring well informed decisions throughout the project time line. Furthermore, the algorithm enables the comparison of design solutions which are the most economically feasible to those that showcase the lowest environmental impact, further facilitating the decision of opting for a design rooted in environmental awareness. Hence, the algorithm is a possible tool to be used for negotiation during tendering procedures.

As formerly mentioned, in today's construction industry the environmental impact of a project is not an actual direct cost that any stakeholder is economically responsible for the resulting GHG emissions. Swedish construction companies are only responsible for performing and submitting a final climate declaration at the completion of a construction project according to the planning process implemented by the Swedish Transport Administration, presented in Figure 2.5. The climate declaration transparently acknowledges the impact of the already built construction, without resulting in major consequences related to the outcome. Despite that fact, the criterion of environmental impact has been included in the optimization procedure as a cost addition as means of identifying optimal designs, as it is highly topical considering the drastically increasing environmental awareness. Considering the development of sustainability focus within the industry sector, it is possible that the environmental impact will be progressively interpreted as an actual cost

in the future. This potential future economical aspect of environmental impact, together with its correlation with investment cost in structural optimization, provides an economic incentive for companies to work actively towards minimizing the environmental impact.

Continually focusing on the implementation of the environmental impact criterion, a comparison was made for the two monetary value systems considered, Ecotax and Ecovalue. Naturally, Ecovalue – corresponding to a higher monetary value – weighs the GWP contribution to the equivalent cost higher than Ecotax does. A chief distinction between the monetary systems lies within their respective definitions. Ecotax is calibrated after environmental taxes, whereas Ecovalue is based on society's willingness to pay. An interpretation can then be made that society is willing to pay for sustainable solutions weighs heavier than what is represented in the taxation system. Therefore, Ecovalue was chosen as monetary value in the main environmental cost calculations, as it was considered to reflect society's demand for environmentally optimal designs. For comparison, additional calculations were performed using the Ecotax value, showing that the algorithm delivers the same optimal designs. Nevertheless, as especially observed for initial Set 2 in Table 4.9, the choice of monetary system affected the instinctive perception of the outcome. When implementing the Ecovalue monetary system for Set 2, the equivalent cost was decreased by 0.7%, while the equivalent cost was increased by 1.5% when adopting the Ecotax-system. Thus, even though both monetary value methods delivered the same optimal design, the final results point in opposite directions, one indicating an improvement and the other on a deterioration in comparison to the reference. Ultimately, both monetary systems present a GHG emission decrease of 13.7%. In other words, the use of Ecovalue or Ecotax foremost impacts the internal weighing of criteria into the equivalent cost representing the aggregated outcome of the design solution.

Finally, the computational complexity of the algorithm, as well as the chosen method of implementing the Python code within the Grasshopper software, have been evaluated throughout the completion of the project. The computational complexity of the procedure was successfully mitigated by opting for linear elastic 2D frame analysis, with no connections to FEM software. The algorithm generated, verified and evaluated an initial set of around 100 000 bridge designs in a matter of around 4 minutes. Creating a procedure which could easily be incorporated into the preliminary design procedures performed by structural engineers was a prerequisite. The algorithm was meant to identify plausible optimal designs in a time efficient manner, guiding the engineers in the right direction when deciding for the initial design, as that primary choice is highly important for achieving a sustainable final design. As the preliminary design of slab frame bridges today simply is based on previous reference projects and experiences, the implementation of extensive FEM-analyses for identifying optimal designs in such an early stage would most likely meet resistance if introduced to structural engineers. Hence, the eventual incorporation of an optimization procedure has to be eased in order to be well received.

Python as a programming language was efficient in generating and storing data, as well as performing all routines within the optimization. The Grasshopper software was considered an applicable environment for integrating the script, however demonstrating some drawbacks. An advantage of grasshopper is its possibility of instant visualization of results within the visual programming interface. By extension, the output can be connected to BIM-software, such as Tekla, automatically creating blueprints of the optimized solution. However, not all Python libraries are accessible within Grasshopper. Secondly, since the algorithm was observed to run around 100 000 bridge designs in a matter of minutes, it was assumed that it could cover a larger initial set if allowed to run over a longer time. Unexpectedly, the running time was highly disproportional to the data size. As the initial set was increased (above 150 000 designs), the code was unable to run. Multiple attempts were made but the algorithm kept processing until eventually crashing, showing a sensibility to data sizes above a certain threshold value. Nevertheless, further studies on the reason behind this were not performed since an initial set of 100 000 bridge designs was considered enough for the scope of the thesis. Furthermore, the Python-component does not successively present the progression of the current run, making it difficult to follow the procedure after startup. Lastly, the software does not allow multiple-users working within the same file, making the work rather tedious and non-interactive. Although Grasshopper demonstrated some drawbacks, the project utility is independent of the programming host, making Python-programming a very adaptable method for optimization procedures in general.

To finalize, the optimization tool created is meant to help structural engineers make well grounded decisions early on in the planning process, considering sustainability on multiple societal levels. When completely relying on experience during the preliminary design procedure, which is often the case today, such nuanced criteria are generally being overlooked. Due to the complex relationships between the optimization criteria – investment cost, environmental impact and buildability – and the great impact of formwork and material volumes, the same design approach can not be used for each individual project, as the dimensions and circumstances differ. Such distinguished relationships require computational intelligence. For each individual project, the tool can help engineers make an initial decision on the type of frame to be used (uniform/variable), cross-sectional heights, rebar diameters and rebar layouts. Looking forward, as the development of computerized systems within structural engineering is drastically increasing, the tool is meant to be further developed to include an automatic modelling of the design in BIM-software. The 3D model could then be used for the extraction of blueprints, to be used for tendering proposals. The tool has many possibilities for future development, as further presented in Section 5.3.

5.2 Possible sources of error

The algorithm contains a number of simplifications and limitations in the execution of the structural analysis as well as in the optimization model, which influenced the outcome of the procedure.

The algorithm solely considered the frame legs and the bridge deck and discretized the frame into nine critical cross-sections. The bridge was simplified into a 2D projection, where the structural verification was performed using linear-elastic frame analysis. Transverse reinforcement was disregarded due to the 2D simplification of the frame, and compressive reinforcement was excluded as the positive contribution from compression rebars commonly is disregarded within the calculations performed by structural engineers. Furthermore, only governing loads were incorporated, a limited set of commonly governing load combinations were accounted for and the traffic load model (LM1) was placed in discrete positions in order to provide maximum load effects. Time dependant effects, such as creep and shrinkage were disregarded. ULS-checks were performed w.r.t shear force and bending moment, while SLS-verifications were performed solely w.r.t lateral deflection of the mid cross-section in the bridge deck. FLS was disregarded.

Further sources of error, highly affecting the result, are the definitions of the environmental impact- and buildability criteria. The environmental impact criterion was limited to only consider GHG emissions through implementing CO_2 equivalents, but additional contributions could be accounted for as explained in section 2.4.3.2. Additionally, the exact magnitudes of the buildability factors are highly relevant and are rather difficult to define in a feasible manner, thus affecting the outcome of the procedure.

Furthermore, the outcome of the optimization algorithm was compared to only one reference project (in addition to the 2D reference project used for load verification), thus highly influencing the proclaimed effect of the procedure. In order to obtain a more distinct and reliable result, it would be required to implement a number of reference projects. Furthermore, as mentioned in Section 3.2.3.1, slight modifications were made to the reference project as means of compensating for differences in load distributions, as the 3D-calculated design was converted into a 2D reference project within the optimization analysis, thus loosing the positive 3D effects of the load transfer. A significant difference between the 2D analysis performed within the algorithm and the 3D analysis carried out within the reference project is the load distribution occurring in the transverse direction. The traffic load effects within the algorithm were calculated conservatively, based on lane 1 as previously explained. However, concentrating worst case loading on the investigated strip results in higher load effects than those resulting from the 3D-FEM performed for the reference project. The reason for that is that positive 3D effects of transverse load distribution were not considered within the algorithm. Additionally the algorithm was based on linear-elastic design theory, further resulting in minor differences. Therefore, the reference project was slightly calibrated according to the

inequalities. As means of making the 2D analysis performed in the algorithm as comparable as possible to the 3D reference, the most representative segment of the FE-model was sought. Therefore, comparisons were executed for an edge strip of the bridge where three-dimensional effects, such as load spread along the width of the bridge deck, are considered minimal. In summary, the optimization procedure calculated load effects conservatively and minor modifications were made to the 3D reference in order to ensure a fair comparison of results, nevertheless resulting in a possible source of error.

Continuing on the subject, the internal weighing of the investment- and builability cost within the equivalent cost is highly reliant of the specific material volumes, i.e. project specific. Ultimately, the procedure will deliver optimal designs of different characters depending on the span lengths, widths and heights of the bridge, as the volumes differ between projects. Thus, the characteristics of the optimal designs presented within this research can not automatically be assumed to describe the optimal designs of bridges with differing geometrical properties. To exemplify, a uniform frame can not always be assumed to yield the lowest equivalent cost and being the most optimal design. Hence, a parametric optimization model is highly effective for identifying optimal designs as the bridge input data easily can be adjusted between projects.

Furthermore, the result highly depends upon the chosen initial set of bridge designs, as explained in Section 4.1.1. A larger initial set with broad parameter ranges entails a higher probability of finding outliers showing an exceptionally optimized solution. Specific relevant ranges were decided for each decision variable as to cover relevant design alternatives in order to somewhat limit the size of Design space B. The choice of initial design space highly influences the outcome of the procedure, but a limitation was necessary to mitigate the number of repetitions performed by the algorithm, as too large data sets could not be handled (above 150 000 bridge designs). In order to ensure a reliable result, a verification of the initial set was performed, as explained in Section 3.2.3.3. Undeniably, the choice somewhat affected the outcome of the procedure presented in this research.

Additional aspects affecting the outcome of the procedure are the specific material unit costs implemented within the algorithm. The prices used correspond to the values observed prior to Covid-19 and the war in Europe, on the conservative side. Since February 2020, i.e., immediately before the pandemic outbreak, the unit prices for steel and iron have increased by 56%, while the corresponding increase for concrete is 28% (Obando, 2023). On the contrary, buildability aspects, directly dependent on labour costs are relatively unaffected by the material prices. Thus, if adopting the current material unit prices, the investment cost criterion would have a substantially greater impact on the output of the algorithm. Consequently, the optimization procedure would prioritize geometrically optimized designs to a greater extent, rather than buildability optimized designs, as the possible reduction in material volumes would have a marked impact on the final equivalent cost. Therefore, the complex balance between reduced investment costs and additional buildability

costs would be of a different character, resulting in a slight shift of focus. Also, the equivalent cost difference between the reference and the optimized design would appear to be greater when implementing larger material costs. Thus, the percentual gains of implementing an optimization procedure are presented conservatively when adopting the lower material prices observed prior to Covid-19 and the war in Europe. Thus, the actual material prices impact the optimization result to a large extent. As conditions are constantly changing, an automated optimization procedure with updated information is a way of ensuring that all aspects are taken into consideration when aiming for more sustainable designs, in an ever changing society.

5.3 Further developments

A main field of development within the research of this thesis would be to extend the SBD implementation to a broader interpretation containing Design space $\mathcal{A}$. Effectively, this extension implies running the algorithm for all potential slab frame bridges, creating a database containing all possible designs regardless of the specific input parameters (Mathern et al., 2019). Once the database has been created, the generation of design alternatives does not need to be repeated within the optimization algorithm, as all the information generated is stored in the data base. In the context of this paper, a subset of such a database has been developed, as the input geometries and boundary conditions constitute one bridge project (Design space $\mathcal{B}$) among all possible slab frame bridges (Design space $\mathcal{A}$).

A further development would then be to analyze the most optimized bridge designs' governing parameters and their respective impact on each criterion. By extension, a tree regression model could be created by implementing machine learning, based on the conclusions drawn on governing parameters. Thus, the result presented in this paper constitutes the potential learning input for such a machine learning procedure. Once created, the tree regression model can automatically identify optimized designs independently from the original optimization algorithm. A prerequisite for using the optimization solutions' distribution as a basis for a reliable tree regression model is to have statistical significance, which requires large data sets. The primary measure taken for mitigating the complexity and thereby maximizing the data sets was, in this study, the use of linear elastic 2D analysis. The principles of a tree regression model are demonstrated in Figure 5.1. Each level corresponds to a condition $P_n \in C_n$, i.e., that the n:th parameter fulfills the n:th criterion.

To further develop the algorithm and minimize the number of iterations needed, gradient descent models can be implemented as explained in Section 2.4.2.2. By constantly evaluating the outcome of one iteration in relation to the decision variables used, the algorithm can create a learning function in order to adjust the decision variables to be used in the next iteration. In such a case, where the initial decision variables are not pre-defined but rather calculated based on learning functions, termination criteria have to be implemented according to Section 2.4.2.4.

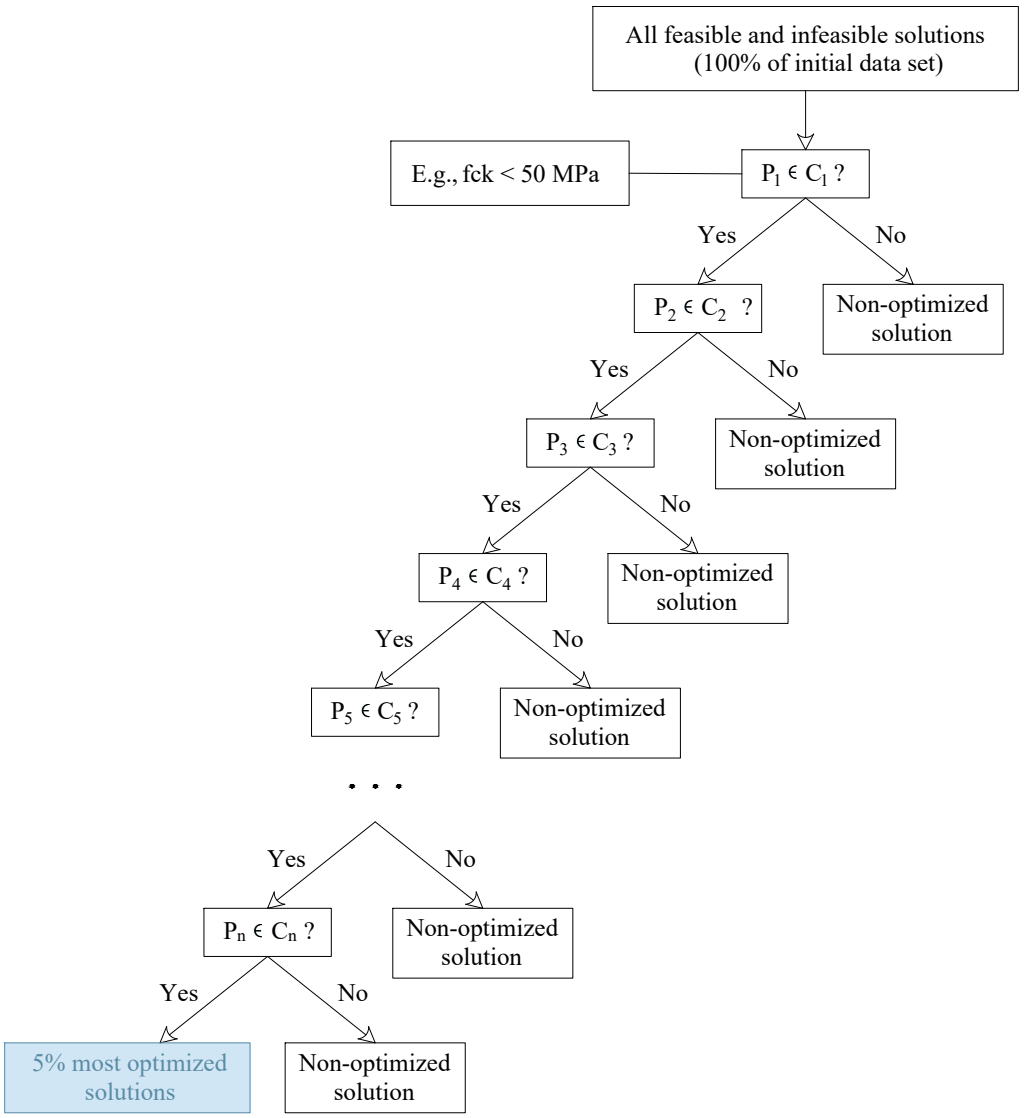

Figure 5.1: Principles of a tree regression model, where P_n denotes the n:th parameter, and C_n denotes the n:th criterion.

Additional amendments to the code could be done, where the algorithm also considers the possibility of having a frame of non-rectangular cross-sections, as explored in Section 2.4.3.3.1. More optimal slab frame bridge designs could then possibly be found, as the material volumes are further reduced. If implementing such design options, additional buildability aspects related to complex cross-sectional geometries would have to be implemented. In that case, large emphasis has to be put on the balance between reductions in investment costs and additional buildability costs, as means of correctly evaluating the economical attainability of such complex geometries.

6
Conclusion

A chief conclusion drawn from the study was that set-based multi-criteria optimization procedures have a significant potential of finding solutions optimized towards investment cost, environmental impact and buildability. The procedure identified solutions in the far-left domains of the probability density functions for each criterion. With an exception for the buildability cost of the data set aiming for environmental optimization, the reference appeared towards the center of the probability density distributions. Thus, the procedure managed to deliver solutions within low frequent intervals, as the optimized designs located in domains of considerably higher solution frequency compared to the reference. Consequently, following traditional PBD methods, the probability of identifying outliers with highly optimized performance is substantially lower than of solutions close to the reference, being a strong incentive for adopting automated SBD procedures. Furthermore, applying SBD creates a basis for negotiation of requirements, provided that solutions conflicting with soft requirements may be found to be highly optimized.

It was concluded that the implementation of a 2D linear-elastic analysis, excluding an extensive FEM analysis, provided reasonable results and reduced the computational complexity to an extent that enabled generation and storing of large data sets. Therefore, the simplification into a 2D linear-elastic analysis was considered applicable for this implementation of preliminary design optimization. By extension, the ultimate goal is for the observations of governing parameters in the optimization to be used as basis for a machine-learning procedure automatically identifying optimal designs. A prerequisite for such procedure is statistical significance in its learning data, hence the importance of large data sets generated by the optimization routine. Continually, the implementation of Python-scripting within Grasshopper functioned well considering the scope of this thesis, although Grasshopper as a host demonstrated limitations of running data sizes above a threshold value as well as limited access of importing Python packages. Nonetheless, Python as language was efficient in storing information and performing iterative operations.

Moreover, the study highlighted the importance of implementing buildability in early stage design optimization, considering its conflicting relation to investment cost and environmental impact. A correlation between minimized material use and lowered cost together with reduced environmental impact was observed. On the contrary, the buildability criterion displayed a more complex and discontinuous effect on the optimization outcome. The results indicated a large influence of

the formwork, foremost regarding additional buildability costs emerging from variable elements thicknesses. Another governing parameter in the buildability cost was additional costs related to thin cross-sections, emerging from need for shear reinforcement, additional reinforcing work or higher concrete strength class. Consequently, geometrically optimized solutions, i.e., designs minimizing the material together with related basic construction labour, were associated with increased buildability costs. Ultimately, due to these high cost surcharges, the buildability criterion was of significant magnitude in the objective function. Thus, finding buildable solutions in an early design stage can mitigate risks of unforeseen costs later in the planning process.

Furthermore, the outcome of the multi-criteria optimization emphasized the importance of integrating environmental impact in total cost optimization, in order to identify climate effective solutions that do not conflict markedly with the client's cost. A conclusion drawn was that optimizing towards the three criteria is to a large extent a matter of resource redistribution, where the client pays for additional labour associated with minimized material, ultimately resulting in a more climate effective design. The possibility of predicting and mitigating additional buildability costs from environmentally optimized designs can encourage a larger scale of environmental optimization within the construction industry. Provided that future tendering processes will be governed by environmental impact to a greater extent than today, there is even larger economical incentive of finding geometrically optimized solutions, which can be done by means of using a multi-criteria optimization as performed in this study. Increasing the extent of involving environmental optimization early in design processes is a measure for working actively towards the climate neutrality goal by 2045 set by the Swedish legislation in 2018.

6.1 Further studies

This research brought forward a number of further topics of development within the field of set-based multi-criteria optimization in general, as well as its implementation for slab frame bridges in particular:

- Application to other bridge types than slab frame bridges,
- Further development regarding simplifications made on the structural analysis, including more structural elements, fatigue, long-term effects, restraining effects, crack widths and additional placements of traffic load,
- Connecting the output directly to BIM
- Expansion of initial data set, being independent of project-specific input. This would generate a data base in which one specific bridge is a sub set, and
- Further extension of the algorithm to a machine learning procedure following identified parameters' influence of the optimization result.

Bibliography

(SFS2021:787). (n.d.).

Ahlroth, S., & Finnveden, G. (2011). Ecovalue08-A new valuation set for environmental systems analysis tools. *Journal of Cleaner Production*, *19*(17-18). https://doi.org/10.1016/j.jclepro.2011.06.005

Ahlroth, S., Nilsson, M., Finnveden, G., Hjelm, O., & Hochschorner, E. (2011). Weighting and valuation in selected environmental systems analysis tools - Suggestions for further developments. *Journal of Cleaner Production*, *19*(2-3). https://doi.org/10.1016/j.jclepro.2010.04.016

Al-Emrani, M., Engström, B., Johansson, M., & Johansson. Peter. (2013). *Bärande konstruktioner part 1*. Chalmers University of Technology.

Alhede, A., & Beskow, K. (2020). *Parameter Study and Optimization of Slab Frame Bridges* (Doctoral dissertation). Chalmers University of Technology. Gothenburg.

Almén, R. (2016). *Investigation of cracking due to restraint forces in Swedish concrete slab frame bridges* (tech. rep.). Lunds tekniska högskola, Division of structural engineering. Lund.

Anand, P. (2013). CO2 emissions from cement production. https://civildigital.com/co2-emissions-from-cement-production/

Andersson, M., & Karlsson, E. (2006). Brolaster enligt Eurocode, 3–6.

Boverket. (2022a). Tendering process. https://www.boverket.se/en/start/building-in-sweden/developer/tendering-process/

Boverket. (2022b). Types of contract and procurement. https://www.boverket.se/en/start/building-in-sweden/developer/rfq-documentation/types-of-contract/

BRE Group. (2023). Human Toxicity.

Cheetham, D. W., & Lewis, J. (2001). Productivity, Buildability and Constructability: Is Work Study the Missing Link? *Association of Researchers in Construction Management*, *1*(September).

Chigozie Osuizugbo, I., Chuks Okolie, K., Shamsideen Oshodi, O., & Olanrewaju Oyeyipo, O. (2022). *Buildability in the construction industry: a systematic review* (tech. rep.).

CII. (1993). *Australian Constructability Principles File* (tech. rep.). Construction Industry Institute. Adelaide.

CIRIA. (1983). *Buildability: an assessment (Special Publication 26)* (tech. rep.). Construction Industry Research and Information Association. London.

Constructability in Construction and Issues at Design and Execution. (2023). https://theconstructor.org/construction/constructability-in-construction-issues-design-execution/17405/

Cosentino, I., Liendo, F., Arduino, M., Restuccia, L., Bensaid, S., Deorsola, F., & Ferro, G. A. (2020). Nano CaCO3 particles in cement mortars towards developing a circular economy in the cement industry. *Procedia Structural Integrity*, *26*. https://doi.org/10.1016/j.prostr.2020.06.019

Difs Jon & Karlsson Fredrik. (2015). *Preliminärdimensionering av plattrambroar Med parallelliserade FEM-analyser enligt SBD* (Doctoral dissertation). Chalmers University of Technology. Gothenburg.

Du, G., Safi, M., Pettersson, L., & Karoumi, R. (2014). Life cycle assessment as a decision support tool for bridge procurement: environmental impact comparison among five bridge designs. *International Journal of Life Cycle Assessment*, *19*(12). https://doi.org/10.1007/s11367-014-0797-z

Ek, K., Mathern, A., Rempling, R., Brinkhoff, P., Karlsson, M., & Norin, M. (2020). Life cycle sustainability performance assessment method for comparison of civil engineering works design concepts: Case study of a bridge. *International Journal of Environmental Research and Public Health*, *17*(21), 1–34. https://doi.org/10.3390/ijerph17217909

Ek, K., Mathern, A., Rempling, R., Rosén, L., Claeson-Jonsson, C., Brinkhoff, P., & Norin, M. (2019). Multi-criteria decision analysis methods to support sustainable infrastructure construction.

ELU. (2018). ELU vinnare i Tekla Global Awards. https://www.elu.se/aktuellt/nyheter/elu-vinnare-i-tekla-global-bim-awards/

European Environment Agency. (2015). Non-methane volatile organic compounds (NMVOC) emissions.

Färdplan cement för ett klimatneutralt betongbyggande (tech. rep.). (2018). Cementa.

Färdplan för fossilfri konkurrenskraft (tech. rep.). (n.d.). Bygg-och anläggningssektorn.

Fernández Luis Santiago & Tarazona Rams David. (2014). *Applicability of Set-Based Design on Structural Engineering* (Doctoral dissertation). Gothenburg.

Finnveden, G., Eldh, P., & Johansson, J. (2006). Weighting in LCA based on ecotaxes: Development of a mid-point method and experiences from case studies. https://doi.org/10.1065/lca2006.04.015

Finnveden, G., Håkansson, C., & Noring, M. (2013). A new set of valuation factors for LCA and LCC based on damage costs – Ecovalue 2012. *The 6th International Conference on Life Cycle Management in Gothenburg 2013*, (2011).

Frontline Systems. (2023). Optimization Problem Types. https://www.solver.com/convex-optimization

Girardet, A., & Boton, C. (2021). A parametric BIM approach to foster bridge project design and analysis. *Automation in Construction*, *126*. https://doi.org/10.1016/j.autcon.2021.103679

Goedkoop, M., Huijbregts, M., De Schryver, A., & Brakkee, K. (2009). *Characterization Factors for Global Warming in Life Cycle Assessment Based on Damages to Humans and Ecosystems* (tech. rep.). University of Nijmegen. Nijmegen.

Goyal, C. (2021). Complete Guide to Gradient-Based Optimizers in Deep Learning.

Han, W., Liu, D., Fan, Y., Hu, Y., Xu, Y., & Liu, X. (2014). Methods Research to Calculate Equivalent of Environmental Cost in Power Industry. *Journal of Power and Energy Engineering*, *02*(04). https://doi.org/10.4236/jpee.2014.24014

Hendy, C. R., & Smith, D. (2007). *Designers' Guide to EN 1992-2: Eurocode 2: Design of Concrete Structures : Part 2: Concrete Bridges*. Thomas Telford.

Huijbregts, M., Steinmann, Z. J. N., Elshout, P. M. F. M., Stam, G., Verones, F., Vieira, M. D. M., Zijp, M., & van Zelm, R. (2016). ReCiPe 2016 - A harmonized life cycle impact assessment method at midpoint and endpoint level. Report I: Characterization. *National Institute for Public Health and the Environment*.

Intergovernmental Panel on Climate Change. Working Group III & Edenhofer, O. (n.d.). *Climate change 2014 : mitigation of climate change : Working Group III contribution to the Fifth Assessment Report of the Intergovernmental Panel on Climate Change*.

Janiesch, C., Zschech, P., & Heinrich, K. (2021). Machine learning and deep learning. *Electronic Markets*, *31*, 685–695. https://doi.org/10.1007/s12525-021-00475-2/Published

Johannesson, P., & Vretblad, e. (1969). *Byggformler och tabeller* (2nd ed., Vol. 3). Esselte Herzogs.

Kenton, W. (2022). What is a Black Box Model? Definition, Uses, and Examples. https://www.investopedia.com/terms/b/blackbox.asp

Khairulzaman, H. A., & Usman, F. (2018). Automation in civil engineering design in assessing building energy efficiency. *International Journal of Engineering and Technology(UAE)*, *7*(4). https://doi.org/10.14419/ijet.v7i4.35.23096

Khouri Chalouhi, E. (2019). *Optimal design solutions of concrete bridges considering environmental impact and investment cost* (Doctoral dissertation). KTH Royal Institute of Technology. Stockholm.

Kim, T. H., Chae, C. U., Kim, G. H., & Jang, H. J. (2016). Analysis of CO2 emission characteristics of concrete used at construction sites. *Sustainability (Switzerland)*, *8*(4). https://doi.org/10.3390/su8040348

Klimatoptimerat byggande av betongbroar - Råd och vägledning (tech. rep.). (2017).

Krav Brobyggande. (n.d.).

Lea, F., & Mason, T. (2022). Cement - building material. https://www.britannica.com/technology/cement-building-material

Lee, J. H., & Ostwald, M. J. (2020). Creative decision-making processes in parametric design. *Buildings*, *10*(12). https://doi.org/10.3390/buildings10120242

Levandowski, C., Raudberget, D., & Johannesson, H. (2014). Set-Based Concurrent Engineering for early phases in platform development. *Advances in Transdisciplinary Engineering*, 564–576. https://doi.org/10.3233/978-1-61499-440-4-564

Martí, L., García, J., Berlanga, A., & Molina, J. M. (2016). A stopping criterion for multi-objective optimization evolutionary algorithms. *Information Sciences*, *367-368*, 700–718. https://doi.org/10.1016/j.ins.2016.07.025

Mathern, A. (2019). *Sustainability-, Buildability-and Performance-driven Structural Design* (tech. rep.).

Mathern, A., Ek, K., & Rempling, R. (2019). *Sustainability-driven structural design using artificial intelligence* (tech. rep.). https://research.chalmers.se,

Mathern, A., Rempling, R., Ramos, D. T., & Luis Fernández, S. (n.d.). *Applying a set-based parametric design method to structural design of bridges* (tech. rep.). https://research.chalmers.se,

Mathern, A., Steinholtz, O. S., Sjöberg, A., Önnheim, M., Ek, K., Rempling, R., Gustavsson, E., & Jirstrand, M. (2021). Multi-objective constrained Bayesian optimization for structural design. *Structural and Multidisciplinary Optimization*, *63*(2), 689–701. https://doi.org/10.1007/s00158-020-02720-2

Miliutenko, S. (2022). *Klimatkalkyl - Infrastrukturhållningens energianvändning och klimatpåverkan i ett livscykelperspektiv* (tech. rep.). Trafikverket. https://www.trafikverket.se/klimatkalkyl

Neos. (2022). Optimization Problem Types. https://neos-guide.org/guide/types/

Nya vägar och järnvägar - Så här planerar vi (tech. rep.). (2013). Trafikverket.

Obando, S. (2023). Material prices back on the rise. *Construction Dive*. https://www.constructiondive.com/news/construction-input-prices-increase-january/643031/

Olsson, F. (2023). E-mail via the Swedish Transport Administration.

Olsson McDowell, A. (2021). Sveriges vanligaste brokonstruktioner. https://www.bygging-uddemann.se/sv/sveriges-vanligaste-brokonstruktioner/

Oxman, R., & Gu, N. (2015). Theories and Models of Parametric Design Thinking. *Proceedings of the International Conference on Education and Research in Computer Aided Architectural Design in Europe*, *2*. https://doi.org/10.52842/conf.ecaade.2015.2.477

Parrish, K., Wong, J. M., Tommelein, I. D., & Stojadinovic, B. (2007). Exploration of set-based design for reinforced concrete structures. *Lean Construction: A New Paradigm for Managing Capital Projects - 15th IGLC Conference*.

Penadés-Plà, V., García-Segura, T., Martí, J. V., & Yepes, V. (2016). A review of multi-criteria decision-making methods applied to the sustainable bridge design. https://doi.org/10.3390/su8121295

Råd Brobyggande. (2016).

Rempling, R., Fall, D., & Lundgren, K. (2015). Aspects of Integrated Design of Structures: Parametric Models, Creative Space and Linked Knowledge. *Civil Engineering and Architecture*, *3*(5), 143–152. https://doi.org/10.13189/cea.2015.030507

Rempling, R., Mathern, A., Tarazona Ramos, D., & Luis Fernández, S. (2019). Automatic structural design by a set-based parametric design method. *Automation in Construction*, *108*. https://doi.org/10.1016/j.autcon.2019.102936

Samrådsredogörelse: Göteborg-Borås, en del av nya stambanor (tech. rep.). (2021). Trafikverket.

Samrådsunderlag (tech. rep.). (2022). Trafikverket.

Sánchez-Silva, M., & Gómez, C. (2013). Risk assessment and management of civil infrastructure networks: A systems approach. In *Handbook of seismic risk*

analysis and management of civil infrastructure systems (pp. 437–464). Elsevier Inc. https://doi.org/10.1533/9780857098986.4.437

Shehata, M. E., & El-Gohary, K. M. (2011). Towards improving construction labor productivity and projects' performance. *Alexandria Engineering Journal*, *50*(4). https://doi.org/10.1016/j.aej.2012.02.001

Singapore. Building and Construction Authority. (2005). *Code of practice on buildable design*. Building; Construction Authority.

Solat Yavari, M., Du, G., Pacoste, C., & Karoumi, R. (2017). Environmental Impact Optimization of Reinforced Concrete Slab Frame Bridges. *Journal of Civil Engineering and Architecture*, *11*(4). https://doi.org/10.17265/1934-7359/2017.04.001

Solat Yavari, M., Pacoste, C., & Karoumi, r. (2016). Structural Optimization of Concrete Slab Frame Bridges Considering Investment Cost. *Journal of Civil Engineering and Architecture*, *10*(9). https://doi.org/10.17265/1934-7359/2016.09.002

SS-EN 1990:2002 (tech. rep.). (n.d.). European Comittee for Standardization.

SS-EN 1991-2:2003 (tech. rep.). (n.d.). European Comittee for Standardization.

SS-EN 1992-1-1:2005 (tech. rep.). (n.d.). European Comittee for Standardization. Swedish Standard Institute.

SS-EN 1992-2:2005 (tech. rep.). (n.d.). European Comittee for Standardization.

SS-EN 1997-1:2005 (tech. rep.). (n.d.). European Comittee for Standardization.

Sweco. (2022). Nu invigs Göteborgs första parkeringshus för cyklar. https://www.sweco.se/aktuellt/nyheter/nu-invigs-goteborgs-forsta-parkeringshus-for-cyklar-2/

The Nature Conservancy. (2023). Calculate Your Carbon Footprint. https://www.nature.org/en-us/get-involved/how-to-help/carbon-footprint-calculator/

Trafikverket. (2011). *2011_047_tk_geo_11_2*. Trafikverket.

Trafikverket. (2018). Åtgärdsvalsstudie. https://bransch.trafikverket.se/for-dig-i-branschen/Planera-och-utreda/Planerings--och-analysmetoder/Atgardsval/

Trafikverket. (2022a). Klimatkalkyl - infrastrukturens klimatpåverkan och energianvändning i ett livscykelperspektiv. https://bransch.trafikverket.se/for-dig-i-branschen/miljo---for-dig-i-branschen/minskad-klimatpaverkan/Klimatkalkyl/

Trafikverket. (2022b). Norrbotniabanan.

Transportstyrelsen. (2018). *TSFS 2018:57* (tech. rep.).

Trimble. (2023). BIM för verklig byggbarhet - Bygg bättre och snabbare. https://www.tekla.com/se/resurser/artiklar/bim-for-verklig-byggbarhet-bygg-battre-och-snabbare

United Nations. (2023). The Paris Agreement. https://unfccc.int/process-and-meetings/the-paris-agreement/the-paris-agreement

Vägplan, granskningshandling:Plan-och miljöbeskrivning (tech. rep.). (2022). Trafikverket. Gothenburg.

Vägverket. (1996). *Broprojektering: en handbok*.

Wåhlin, E. (1947). *Bygg i allmänna grunder*. Tidskriften Byggmästaren förlag.

Wang, Y., Pang, B., Zhang, X., Wang, J., Liu, Y., Shi, C., & Zhou, S. (2020). Life cycle environmental costs of buildings. *Energies*, *16*(3). https://doi.org/10.3390/en13061353

Westlund, P., Brogren, M., Byman, K., Hylander, B., Kellner, J., Linden, C., Löngren, Ö., Nordling, J., Strömberg, L., & Winberg, F. (2021). *Climate impact of construction processes* (tech. rep.).

Wimalaratne, P. L., Kulathunga, U., & Gajendran, T. (2021). Comparison between the terms constructability and buildability: A systematic literature review. *World Construction Symposium*, 196–207. https://doi.org/10.31705/WCS.2021.17

Yu, F., Wang, J., & Cao, D. (2009). *Guidelines for Chinese Environmental and Economic Accounting* (tech. rep.). China EnvironmentalScience Press. Beijing.

A

Optimization Criteria Definitions

Possible definitions and quantifications of the optimization criteria related to investment cost, environmental impact and buildability, according to previous research, are presented in Sections A.1-A.3.

A.1 Investment cost criterion

Material- and labor- costs are found in Tables A.1-A.3.

Concrete material- and labor costs	
Material	**Cost**
Concrete C32/40	1700 SEK/m^3
Concrete C35/45	1800 SEK/m^3
Concrete C50/60	2000 SEK/m^3
Labor	**Cost**
Casting of wing walls	1000 SEK/m^3
Casting of frame legs	750 SEK/m^3
Casting of bridge deck	800 SEK/m^3

Table A.1: Concrete material- and labor costs as presented by Solat Yavari, M., et al. (2016).

Formwork material- and labor costs	
Material	**Cost**
Formwork for wing walls, straight	250 SEK/m^2
Formwork for wing walls, varying thickness	350 SEK/m^2
Formwork for frame legs, straight	200 SEK/m^2
Formwork for frame legs, varying thickness	300 SEK/m^2
Formwork for deck, straight	500 SEK/m^2
Formwork for deck, varying thickness	500 SEK/m^2
Labor	**Cost**
Constructing formwork	500 SEK/m^2

Table A.2: Formwork material- and labor- costs as presented by Solat Yavari, M., et al. (2016).

Reinforcement material- and labor- costs	
Material	**Cost**
Reinforcement	9 SEK/kg
Labor	**Cost**
Reinforcing wing walls, straight	17.5 SEK/kg
Reinforcing frame legs, straight	15 SEK/kg
Reinforcing bridge deck, straight	17.5 SEK/kg

Table A.3: Reinforcement material- and labor- costs as presented by Solat Yavari, M., et al. (2016).

A.2 Environmental impact criterion

All environmental impact categories and monetary values for environmental impact are specifically stated in Tables A.4 and A.5.

Environmental impact categories					
Impact category	Unit	Concrete C32/40 (m^3)	Concrete C35/45 (m^3)	Concrete C50/60 (m^3)	Reinforcement (ton)
Global warming (GWP)	$kg \cdot CO_2 \cdot eq$	344.505	352.694	383.748	2387.489
Human toxicity (HTP)	$kg \cdot 1.4\text{-}DB \cdot eq$	20.381	20.385	21.968	417.752
Photochemical oxidant formation (POFP)	$kg \cdot NMVOC$	0.969	0.989	1.051	10.060
Terrestrial acidification (TAP)	$kg \cdot SO2 \cdot eq$	0.918	0.934	0.998	9.428
Marine eutrophication (MEP)	$kg \cdot N \cdot eq$	0.052	0.036	0.038	0.243
Marine ecotoxicity (METP)	$kg \cdot 1.4\text{-}DB \cdot eq$	0.237	0.240	0.249	2.956

Table A.4: Impact categories with corresponding characterization factors, as presented by Solat Yavari, M., et al. (2017).

Here, the unit $kg \cdot 1.4\text{-}DB \cdot eq$ measures toxicity and is a reference unit of kg 1-4 dichlorobenzene equivalents (BRE Group, 2023). The unit $kg \cdot NMVOC$ refers to kg emitted non-methane volatile organic compounds (European Environment Agency, 2015).

Monetary values for environmental impact		
Impact category	Ecovalue (SEK)	Ecotax (SEK)
Global warming (GWP)	2.85	0.63
Human toxicity (HTP)	2.81	1.5
Photochemical oxidant formation (POFP)	16	156
Terrestrial acidification (TAP)	30	15
Marine eutrophication (MEP)	90	12
Marine ecotoxicity (METP)	12	0.3

Table A.5: Monetary values corresponding to each impact category, as presented by Du, G., et al. (2014).

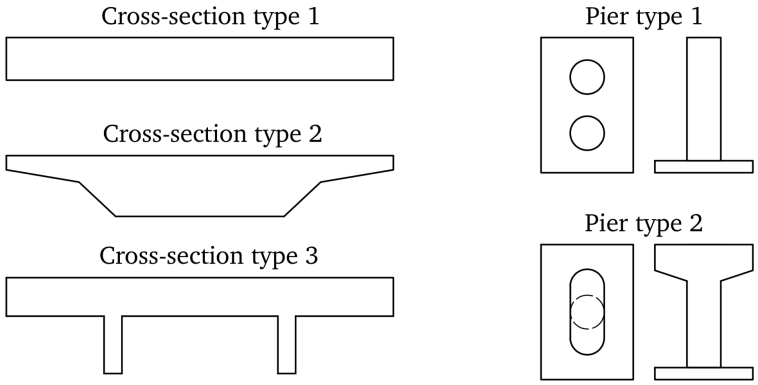

Figure A.1: Structural member geometries of reinforced concrete beam bridges (Khouri Chalouhi, 2019).

A.3 Buildability criterion

All the additional labor costs and labor cost factors related to buildability aspects are specifically stated in Table A.6 according to Solat Yavari, M., et al. (2016) and in Tables A.7-A.9 according to Khouri Chalouhi, E. et al. (2019). The values presented in Tables A.7-A.9 are related to the geometries shown in Figure A.1. Additional buildability aspects considered, provided by structural- and calcualtion-engineers at Skanska, are presented in Table A.10.

Buildability costs	
Thickness of concrete member	**Additional labor cost factor**
thickness $<$ 40cm	0.2
40cm $\leq$ thickness $<$ 60cm	0.1
60cm $\leq$ thickness	0
Reinforcing - straight/variable thickness	**Additional labor cost factor**
Reinforcing, variable thickness	0.15
Formwork - straight/variable thickness	**Additional labor cost**
Formwork for wing walls, variable thickness	500 SEK/m^2
Formwork for frame legs, variable thickness	250 SEK/m^2
Formwork for deck, variable thickness	250 SEK/m^2
Concrete class	**Additional labor cost**
Concrete C50/60	200 SEK/m^3

Table A.6: Additional buildability costs/buildability cost factors due to geometrical factors of structural members and material properties, according to Solat Yavari, M., et al. (2016).

Buildability costs for concrete		
Element	**Additional labor cost factor**	**Description**
Deck	0	cross-section type 1
Deck	0.1	cross-section type 2
Deck	0.3	cross-section type 3
Pier	0	pier type 1
Pier	1	pier type 2
Foundation slab	0	-

Table A.7: Buildability coefficients for concrete elements, where the bridge deck cross-sections and pier designs are shown in Figure A.1 (Khouri Chalouhi, 2019).

Buildability costs for reinforcement		
Element	**Additional labor cost factor**	**Description**
Deck	0	cross-section type 1
Deck	0.15	cross-section type 2
Deck	0.25	cross-section type 3
Pier	0.2	pier type 1
Pier	0.7	pier type 2
Foundation slab	0	-

Table A.8: Buildability coefficients for reinforcement, where the bridge deck cross-sections and pier designs are shown in Figure A.1 (Khouri Chalouhi, 2019).

Buildability costs for formwork		
Element	**Additional labor cost factor**	**Description**
Deck	1	distance to ground < 5 m
Deck	1.3	distance to ground 5 - 7 m
Pier	0.2	pier type 1
Pier	1.5	pier type 2
Foundation slab	0	-

Table A.9: Buildability coefficients for formwork, where the bridge deck cross-sections and pier designs are shown in Figure A.1 (Khouri Chalouhi, 2019).

Buildability costs for reinforcement		
Reinforcement diameter	**Capacity**	**Additional labor cost factor**
$\phi 16$	20 h/ton	0.25
$\phi 20$	18.22 h/ton	0.14
$\phi 25$	16 h/ton	0
Shear reinforcement	**Capacity**	**Additional labor cost factor**
If not added	0 h/ton	0
If added	25 h/ton	0.56

Table A.10: Additional buildability costs related to reinforcement diameter (from calculation engineer at Skanska) and estimated buildability costs related to shear reinforcement (from structural engineer specialist at Skanska).

B

Material Data

The optimization algorithm was based on three possible concrete strength classes, C32/40, C35/45 and C50/60 and with reinforcing steel of quality C500B. Material parameters were defined according to SS-EN 1992-1-1:2005 and SS-EN 1992-2:2005.

B.1 Concrete

γ_c=25 — Density of reinforced concrete [kN/m^3]

$\gamma_{\mathrm{psf,c}}$= 1.5 — Partial safety factor for concrete [-] (SS-EN 1992-1-1:2005, Table 2.1N)

$\alpha_{cc} = 1$ — Coefficient for long term effects on compressive strength and unfavorable affects from load application [-] (recommended value) (SS-EN 1992-1-1:2005, 3.1.6)

$\alpha_{ct} = 1$ — Coefficient for long term effects on tensile strength and unfavorable affects from load application [-] (recommended value) (SS-EN 1992-1-1:2005, 3.1.6)

$f_{cd} = \alpha_{cc} \frac{f_{ck}}{\gamma_{psf,c}}$ — Design compressive strength of concrete [MPa] (SS-EN 1992-1-1:2005, Eq 3.15)

$f_{ctd} = \alpha_{ct} \frac{f_{ctk,0.05}}{\gamma_{psf,c}}$ — Design tensile strength of concrete [MPa] (SS-EN 1992-1-1:2005, Eq 3.16)

$\epsilon_{cc} = 3.5 * 10^{-3}$ — Ultimate strain for concrete [-] (SS-EN 1992-1-1:2005, Table 3.1)

For concrete, C32/40:

$f_{ck,32}$ = Characteristic compressive strength [MPa] (SS-EN 1992-1-1:2005, Table 3.1)

$f_{ctm,32} = 3.02$ Mean tensile strength [MPa] (SS-EN 1992-1-1:2005, Table 3.1)

$f_{ctk,0.05,32} = 2.12$ 5% fractile of tensile strength [MPa] (SS-EN 1992-1-1:2005, Table 3.1)

$E_{cm,32} = 33.35$ Young's modulus [GPa] (SS-EN 1992-1-1:2005, Table 3.1)

For concrete, C35/45:

$f_{ck,35} = 35$ Characteristic compressive strength [MPa] (SS-EN 1992-1-1:2005, Table 3.1)

$f_{ctm,35} = 3.2$ Mean tensile strength [MPa] (SS-EN 1992-1-1:2005, Table 3.1)

$f_{ctk,0.05,35} = 2.2$ 5% fractile of tensile strength [MPa] (SS-EN 1992-1-1:2005, Table 3.1)

$E_{cm,35} = 34$ Young's modulus [GPa] (SS-EN 1992-1-1:2005, Table 3.1)

For concrete, C50/60:

$f_{ck,50} = 50$ Characteristic compressive strength [MPa] (SS-EN 1992-1-1:2005, Table 3.1)

$f_{ctm,50} = 4.1$ Mean tensile strength [MPa] (SS-EN 1992-1-1:2005, Table 3.1)

$f_{ctk,0.05,50} = 2.9$ 5% fractile of tensile strength [MPa] (SS-EN 1992-1-1:2005, Table 3.1)

$E_{cm,50} = 37$ Young's modulus [GPa] (SS-EN 1992-1-1:2005, Table 3.1)

B.2 Reinforcement

$\gamma_s = 7800$	Density of steel [kg/m^3]
$\gamma_{\text{psf,s}} = 1.15$	Partial safety factor for reinforcing steel [-] (SS-EN 1992-1-1:2005, Table 2.1N)
$f_{\text{yk}} = 500$	Reinforcement steel yield strength [MPa]
$E_{\text{s}} = 200$	Reinforcement steel Young's modulus [GPa]
$f_{yd} = \frac{f_{yk}}{\gamma_{psf,s}}$	Design strength of reinforcing steel [-] (SS-EN 1992-1-1:2005, Figure 3.8)
$\epsilon_{syd} = \frac{f_{yd}}{E_s}$	Yield strain for reinforcing steel [-]

B.3 Geological

$\theta = 21.8$	Angle between compression strut and the horizontal beam axis [°]
$\gamma_s = 25$	Density of surrounding soil [kN/m^3] (Brolaster enligt Eurocode)
$\phi' = 37.5$	Friction expressed as an angle tanϕ when slippage occurs in the material, according to the reference project [°]

B.4 Pavement

$\gamma_p = 23.5$	Density of pavement, according to the reference project [kN/m^3]

C

Loads and Load Combinations

C.1 Load effects

The load effects were computed based on fundamental cases for frames, presented in Section C.1.1. The fundamental cases are based on Johannesson, P., and Vretblad, e.(1969) and Wåhlin, E.(1947).

C.1.1 Fundamental cases for frames

This section presents the fundamental cases used as calculation of sectional bending moments, shear forces and deflections. The expressions are numbered according to Figure C.1, meaning that sections 1 and 9 are supports and sections 3,4,6 and 7 are corner sections.

In calculating load effects with fundamental cases on a frame, the stiffness relation between the frame legs and the bridge deck is taken into account by the factor k, according to Equation C.1.

$$k = e_I * \beta_I \tag{C.1}$$

Where e_I* and β_I are factors comparing the structural height and moment of inertia between frame legs and bridge deck, according to Equations C.3 and C.2 .

$$e_I = \frac{H}{L} \tag{C.2}$$

$$\beta_I = \frac{I_{fl,avg}}{I_{bd,avg}} \tag{C.3}$$

The sign convention follows positive sign inside of the frame structure and negative outside the frame structure, as seen in fig C.2. The load effects were calculated for pinned and fixed boundary conditions between frame legs and foundation slabs, i.e., in sections 1 and 9, as seen in C.2.

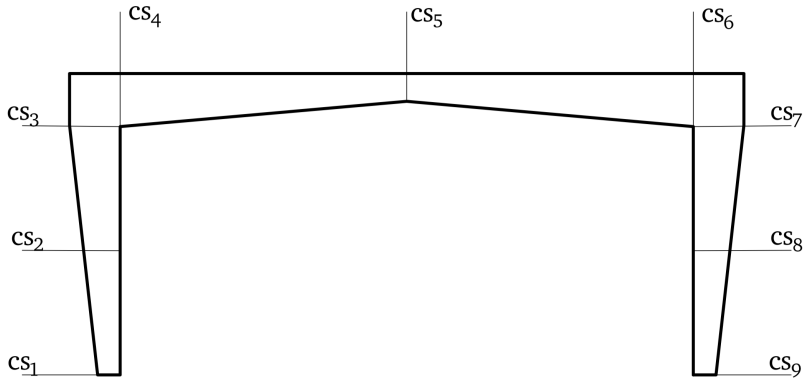

Figure C.1: Investigated cross-sections per frame structure.

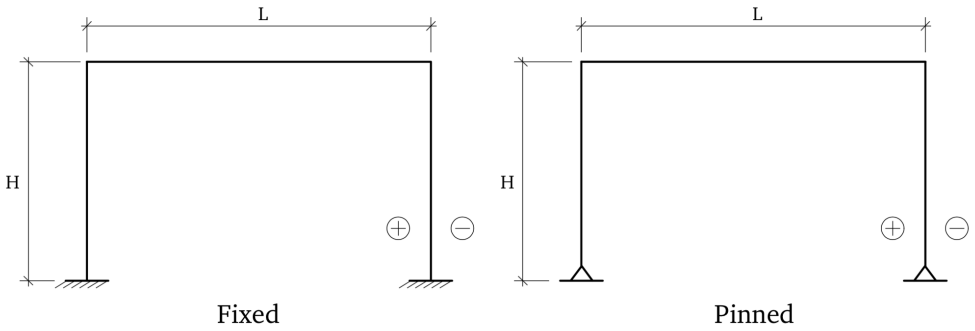

Figure C.2: Boundary conditions considered in the fundamental cases.

Tabulated equations show load effects for corners and supports. Sectional forces in intermediate sections were interpolated (for linear distributions) or calculated through equilibrium.

C.1.1.1 Bending moment

Uniformly distributed vertical load		
Section	**Fixed**	**Pinned**
M_1 (Support)	$\frac{g*L^2}{(12*(k+2))}$	0
$M_3 = M_4$ (Corner)	$-\frac{g*L^2}{(6*(k+2))}$	$-\frac{g*L^2}{4*(2*k+3)}$
$M_7 = M_6$ (Corner)	$-\frac{g*L^2}{(6*(k+2))}$	$-\frac{g*L^2}{4*(2*k+3)}$
M_9 (Support)	$\frac{g*L^2}{(12*(k+2))}$	0

Table C.1: Support-and corner moments for a frame with uniformly distributed vertical load.

Concentrated vertical load		
Section	**Fixed**	**Pinned**
M_1 (Support)	$\frac{P*a*b}{2*l} * \frac{2*\alpha*(k+2)}{(k+2)*(6*k+1)}$	0
$M_3 = M_4$ (Corner)	$-\frac{P*a*b}{2*l} * \frac{13*k+4-2*\alpha*(k+2)}{(k+2)*(6*k+1)}$	$\frac{3*P*a*b}{2*l*(2*k+3)}$
$M_7 = M_6$ (Corner)	$-\frac{P*a*b}{2*l} * \frac{11*k+2*\alpha*(k+2)}{(k+2)*(6*k+1)}$	$-\frac{3*P*a*b}{2*l*(2*k+3)}$
M_9 (Support)	$\frac{P*a*b}{2*l} * \frac{7*k+3-2*\alpha*(k+2)}{(k+2)*(6*k+1)}$	0

Table C.2: Support-and corner moments for a frame with concentrated vertical load.

Where:

- l is the element length
- a is the distance along the element length between load anchor point and end of element
- b = l-a

Concentrated horizontal load		
Section	**Fixed**	**Pinned**
M_1 (Support)	$\frac{Q*H*(3*k+1)}{2*(6*k+1)}$	0
$M_3 = M_4$ (Corner)	$-\frac{Q*H*(3*k)}{2*(6*k+1)}$	$\frac{Q*H}{2}$
$M_7 = M_6$ (Corner)	$\frac{Q*H*(3*k)}{2*(6*k+1)}$	$-\frac{Q*H}{2}$
M_9 (Support)	$-\frac{Q*H*(3*k+1)}{2*(6*k+1)}$	0

Table C.3: Support-and corner moments for a frame with concentrated horizontal load pushing on the right frame leg.

Double- sided linearly increasing distributed horizontal load		
Section	**Fixed**	**Pinned**
M_1 (Support)	$-\frac{q*H^2*(3*k+8)}{(60*(k+2))}$	0
$M_3 = M_4$ (Corner)	$-\frac{q*H^2*k}{(30*(k+2))}$	$-\frac{7*q*H^2*k}{(60*(2*k+3))}$
$M_7 = M_6$ (Corner)	$-\frac{q*H^2*k}{(30*(k+2))}$	$-\frac{7*q*H^2*k}{(60*(2*k+3))}$
M_9 (Support)	$-\frac{q*H^2*(3*k+8)}{(60*(k+2))}$	0

Table C.4: Support-and corner moments for a frame with double- sided linearly increasing distributed horizontal load.

One- sided uniformly distributed horizontal load		
Section	**Fixed**	**Pinned**
M_1 (Support)	$-\frac{q*H^2}{24}*(12-\frac{5*k+9}{k+2}-\frac{12*k}{6*k+1})$	0
$M_3 = M_4$ (Corner)	$\frac{q*H^2}{24}*(\frac{12*k}{6*k+1}-\frac{k}{k+2})$	$\frac{3*q*H^2}{8}*\frac{k+2}{2*k+3}$
$M_7 = M_6$ (Corner)	$-\frac{q*H^2}{24}*(\frac{12*k}{6*k+1}-\frac{k}{k+2})$	$-\frac{q*H^2}{8}*\frac{5*k+6}{2*k+3}$
M_9 (Support)	$\frac{q*H^2}{24}*(\frac{5*k+9}{k+2}-\frac{12*k}{6*k+1})$	0

Table C.5: Support-and corner moments for a frame with one- sided uniformly distributed horizontal load pushing on the left frame leg.

One- sided distributed horizontal load, linearly increasing towards mid depth		
Section	**Fixed**	**Pinned**
M_1 (Support)	$-\frac{q*H^2}{192}*\frac{72*k^2+323*k+63}{6*k^2+13*k+2}$	0
$M_3 = M_4$ (Corner)	$\frac{q*H^2}{192}*\frac{72*k^2+79*k}{6*k^2+13*k+2}$	$\frac{q*H^2}{64}*\frac{11*k+24}{2*k+3}$
$M_7 = M_6$ (Corner)	$-\frac{q*H^2}{192}*\frac{72*k^2+133*k}{6*k^2+13*k+2}$	$-\frac{3*q*H^2}{64}*\frac{7*k+8}{2*k+3}$
M_9 (Support)	$\frac{q*H^2}{192}*\frac{72*k^2+323*k+63}{6*k^2+13*k+2}$	0

Table C.6: Support-and corner moments for a frame with one- sided distributed horizontal load, linearly increasing towards mid depth, pushing on the left frame leg.

C.1.1.2 Shear force

Uniformly distributed vertical load		
Section	**Fixed**	**Pinned**
V_1 (Support)	$\frac{g*L^2}{4*H*(k+2)}$	$\frac{g*L^2}{4*H*(2*k+3)}$
V_3 (Corner)	$\frac{g*L^2}{4*H*(k+2)}$	$\frac{g*L^2}{4*H*(2*k+3)}$
V_7 (Corner)	$\frac{g*L^2}{4*H*(k+2)}$	$\frac{g*L^2}{4*H*(2*k+3)}$
V_9 (Support)	$\frac{g*L^2}{4*H*(k+2)}$	$\frac{g*L^2}{4*H*(2*k+3)}$

Table C.7: Support-and corner shear force for a frame with uniformly distributed vertical load.

Concentrated horizontal load		
Section	**Fixed**	**Pinned**
V_1 (Support)	Q/2	Q/2
V_3 (Corner)	Q/2	Q/2
V_7 (Corner)	-Q/	-Q/2
V_9 (Support)	-Q/2	-Q/2

Table C.8: Support-and corner shear force for a frame with concentrated horizontal load.

Double- sided linearly increasing distributed horizontal load		
Section	**Fixed**	**Pinned**
V_1 (Support)	$-0.8 * q * H/2$	$-0.6 * q * H/2$
V_3 (Corner)	$0.2 * q * H/2$	$0.4 * q * H/2$
V_7 (Corner)	$0.2 * q * H/2$	$0.4 * q * H/2$
V_9 (Support)	$-0.8 * q * H/2$	$-0.6 * q * H/2$

Table C.9: Support-and corner shear force for a frame with double- sided linearly increasing distributed horizontal load.

One- sided uniformly distributed horizontal load		
Section	**Fixed**	**Pinned**
V_1 (Support)	$-q * H * \frac{6*k+13}{8*(k+2)}$	$\frac{q*H*(5*k+6)}{8*(2*k+3)-q*H}$
V_3 (Corner)	$q * H * \frac{2*k+3}{8*(k+2)}$	$V_1 * 0.3/0.7$
V_7 (Corner)	$q * H * \frac{2*k+3}{8*(k+2)}$	$\frac{q*H*(5*k+6)}{8*(2*k+3)}$
V_9 (Support)	$q * H * \frac{2*k+3}{8*(k+2)}$	$\frac{q*H*(5*k+6)}{8*(2*k+3)}$

Table C.10: Support-and corner shear force for a frame with one- sided uniformly distributed horizontal load pushing on the left frame leg.

One- sided distributed horizontal load, linearly increasing towards mid depth		
Section	**Fixed**	**Pinned**
V_1 (Support)	$-0.8 * q * H/2$	$-0.7 * q * H/2$
V_3 (Corner)	$0.2 * q * H/2$	$0.3 * q * H/3$
V_7 (Corner)	$0.2 * q * H/2$	$0.3 * q * H/3$
V_9 (Support)	$0.2 * q * H/2$	$0.3 * q * H/3$

Table C.11: Support-and corner shear force for a frame with one- sided distributed horizontal load, linearly increasing towards mid depth, pushing on the left frame leg.

C.1.1.3 Deflection in mid section of bridge deck

Deflections of mid section in the bridge deck were calculated based on an assumption of rigid frame corners, for uniformly distributed- and concentrated vertical loads, respectively (Wåhlin, 1947).

Vertical deflection in mid section of bridge deck	
Load type	δ_v
Concentrated vertical load	$Q * \frac{a^2 * L}{48 * E_{cm} * I_{II,avg,bd}} * (3 - \frac{4a}{L})$
Distributed vertical load	$\frac{q * L^4}{384 * E_{cm} \cdot I_{II,avg,bd}}$

Table C.12: Vertical deflection in mid section of bridge deck

Where:

- a is the shortest distance between the load anchor point and the bridge deck edge.
- $I_{II,avg,bd}$ is the average moment of inertia in the bridge deck.

C.1.2 Bending moment- and shear force diagrams

Load effects (bending moment and shear force) due to all loads applied on the frame are found in Figures C.3 through C.20. For all diagrams, the sign convention is set positive inside the structure and negative outside of the structure.

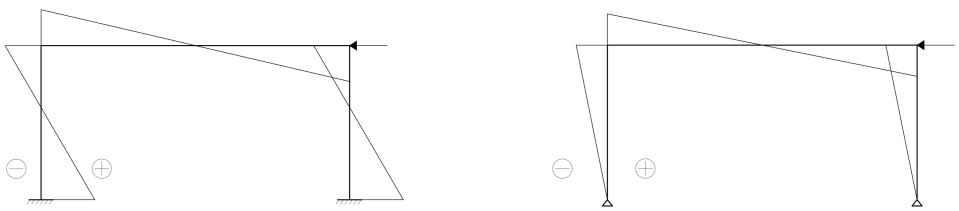

(a) Fixed connections **(b)** Pinned connections

Figure C.3: Moment diagram for braking force pushing the structure to the left

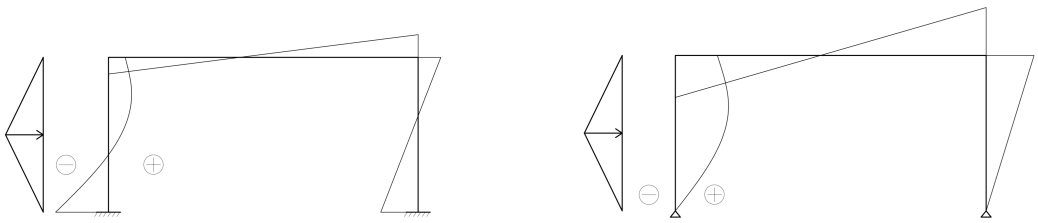

(a) Fixed connections **(b)** Pinned connections

Figure C.4: Moment diagram for counteracting passive earth pressure acting on the left frame leg.

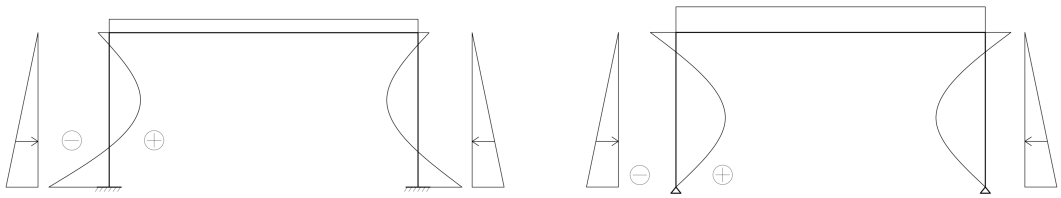

(a) Fixed connections **(b)** Pinned connections

Figure C.5: Moment diagram for earth pressure.

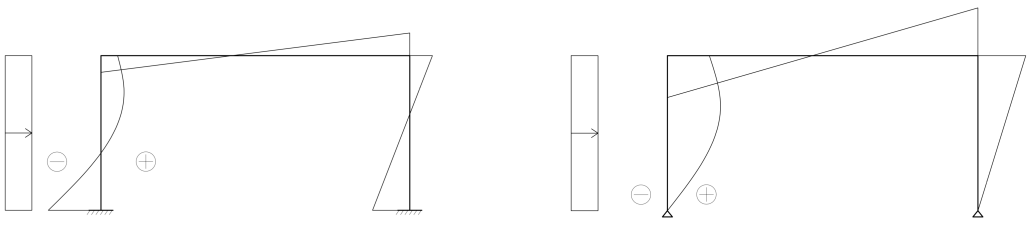

(a) Fixed connections **(b)** Pinned connections

Figure C.6: Moment diagram for surcharge load acting on the left frame leg.

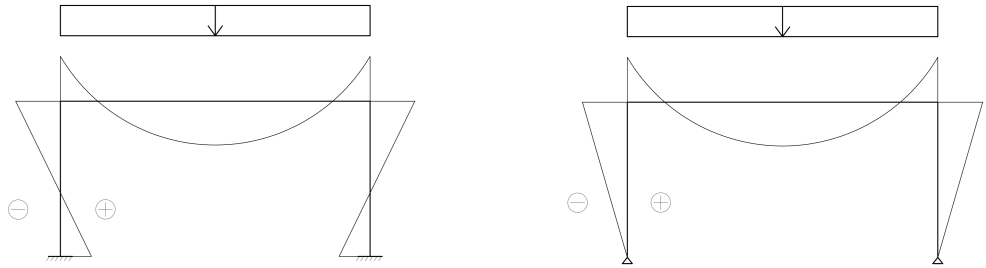

(a) Fixed connections **(b)** Pinned connections

Figure C.7: Moment diagram for self weight.

(a) Fixed connections **(b)** Pinned connections

Figure C.8: Moment diagram for LM1, first concentrated axle load per axle pair for critical position w.r.t bending moment.

(a) Fixed connections **(b)** Pinned connections

Figure C.9: Moment diagram for LM1, second concentrated axle load per axle pair for critical position w.r.t bending moment.

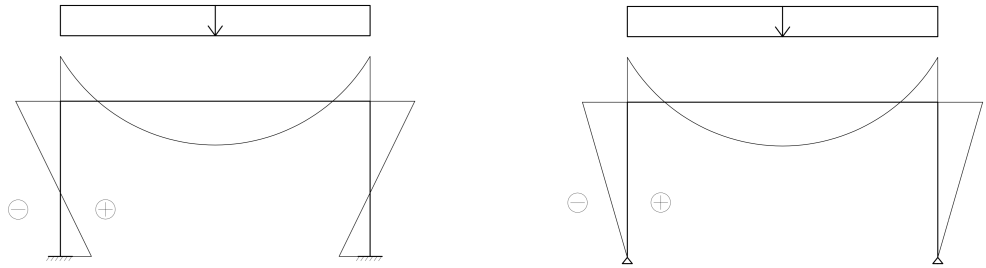

(a) Fixed connections **(b)** Pinned connections

Figure C.10: Moment diagram for LM1, uniformly distributed load.

(a) Fixed connections **(b)** Pinned connections

Figure C.11: shear force diagram for braking force pushing the structure to the left

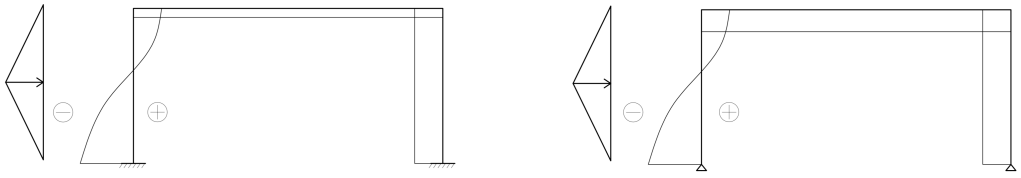

(a) Fixed connections **(b)** Pinned connections

Figure C.12: Shear force diagram for counteracting passive earth pressure acting on the left frame leg.

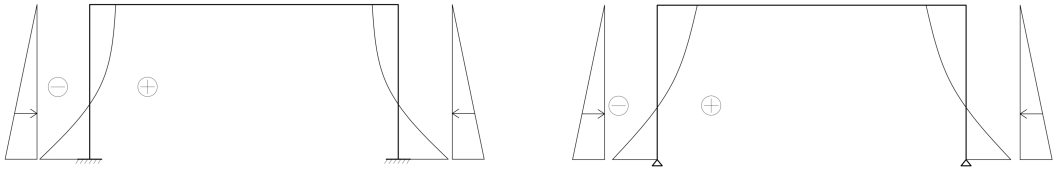

(a) Fixed connections **(b)** Pinned connections

Figure C.13: Shear force diagram for earth pressure.

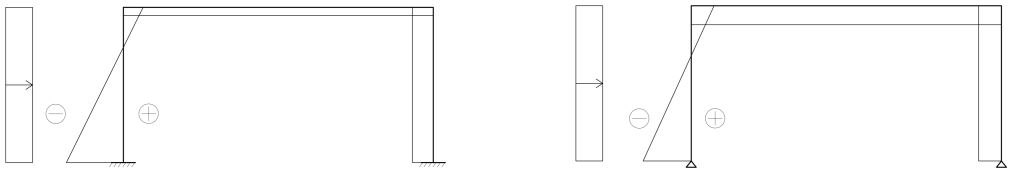

(a) Fixed connections **(b)** Pinned connections

Figure C.14: Shear force diagram for surcharge load acting on the left frame leg.

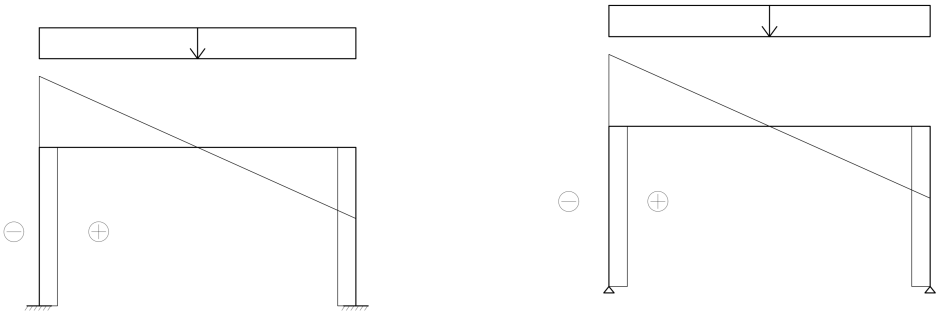

(a) Fixed connections **(b)** Pinned connections

Figure C.15: Shear force diagram for self weight.

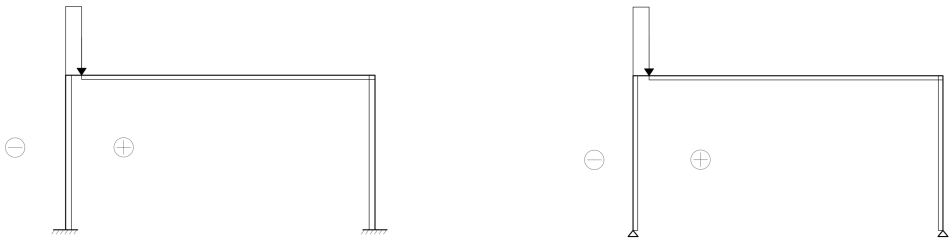

(a) Fixed connections **(b)** Pinned connections

Figure C.16: Shear force diagram for LM1, first concentrated axle load per axle pair for critical position w.r.t shear force in bridge deck.

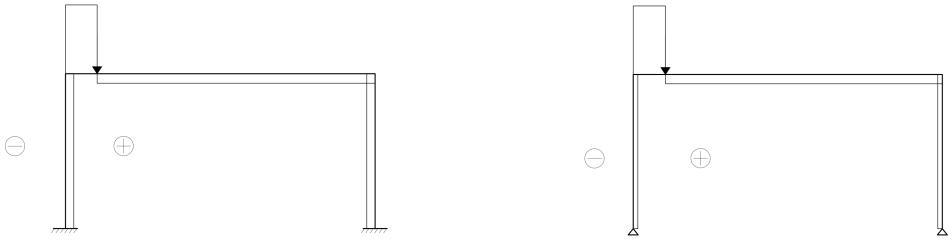

(a) Fixed connections **(b)** Pinned connections

Figure C.17: Shear force diagram for LM1, second concentrated axle load per axle pair for critical position w.r.t shear force in bridge deck.

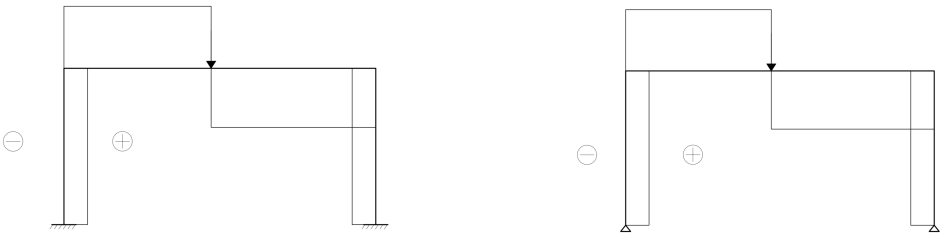

(a) Fixed connections **(b)** Pinned connections

Figure C.18: Shear force diagram for LM1, first concentrated axle load per axle pair for critical position w.r.t shear force in frame legs.

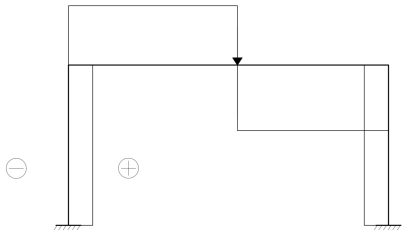

(a) Fixed connections

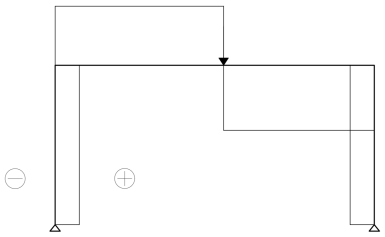

(b) Pinned connections

Figure C.19: Shear force diagram for LM1, second concentrated axle load per axle pair for critical position w.r.t shear force in frame legs.

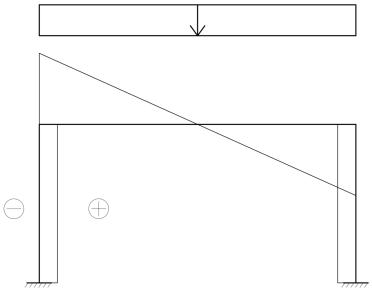

(a) Fixed connections

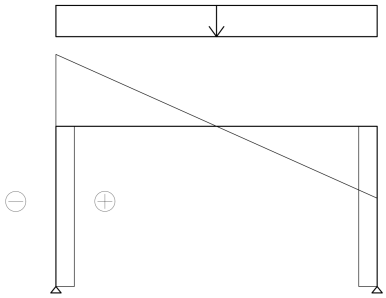

(b) Pinned connections

Figure C.20: Shear force diagram for LM1, uniformly distributed load.

C.2 Calculation of load types

C.2.1 Self weight

w	Width of cross-section
t	Thickness of cross-section
t_p	Thickness of pavement layer
$G = (\gamma_c t + \gamma_p t_p)w$	Self-weight as a line load [kN/m]

C.2.2 Earth pressure

z — Vertical distance along the depth of the ground

$K_0 = 1 - sin\phi'$ — Lateral earth pressure coefficient at rest, for friction soil/silt soil (2011_047_tk_geo_11_2, 5.2.2.2.3)

$\sigma(z) = K_0 \gamma_s z$ — Lateral earth pressure at rest (SS-EN 1997-1:2005)

C.2.3 Surcharge

$q_{sur,v} = 20$ — Vertical surcharge load [kN/m^2]

$q_{sur,h} = K_0 q_{sur,v}$ — Horizontal surcharge load [kN/m^2]

C.2.4 Counteracting passive earth pressure

H — Height of frame

c — Counteracting passive earth pressure constant (Råd Brobyggande, p.33)

$$c = \begin{cases} 300 & \text{if favorable, eg.braking forces} \\ 600 & \text{if unfavorable, eg. temperature increase in the bridge deck} \end{cases}$$

z — The vertical depth under ground

δ — The horizontal displacement of the frame corner

$\beta = \frac{\delta}{H}$ — (Råd Brobyggande, p.33)

$\Delta p = c \gamma_s z \beta$ — Counteracting earth pressure (Råd Brobyggande, p.33)

$\Delta p_{max} = (K_p - K_o)\gamma_s H$ — Available increase of counteracting earth pressure

C.2.5 Traffic load model 1 (LM1)

The following load model is found in (SS-EN 1991-2:2003, 4.3.2), together with the Swedish Transport Agency (TSFS 2018:57). LM1 is subdivided into two systems;

tandem system (TS) and uniformly distributed load system (UDL).The application of LM1 can be seen in Figure C.21. Characteristic loads, including dynamic amplification factor, in different lanes for TS and UDL are presented in Table C.13:

Characteristic values for LM1		
	TS	UDL
Location	Axle loads $Q_{ik}[kN/axle]$	$q_{ik}(orq_{rk})[kN/m^2]$
Lane num. 1	300	9
Lane num. 2	200	2.5
Lane num. 3	100	2.5
Other lanes	0	2.5
Remaining area (q_{rk})	0	2.5

Table C.13: Characteristic vales for LM1 (SS-EN 1991-2:2003, Table 4.2)

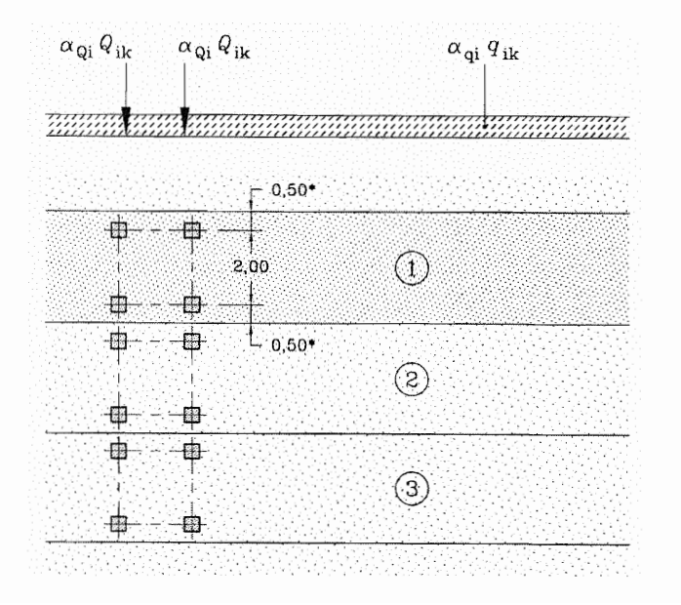

Figure C.21: Principle of application of LM1.

When verifying on a local scale, a tandem system is to be applied at the most adverse location. In case of two tandem systems on parallel notional lanes, the systems may be applied with a distance of maximum 0.5 m, as presented in Figure C.22.

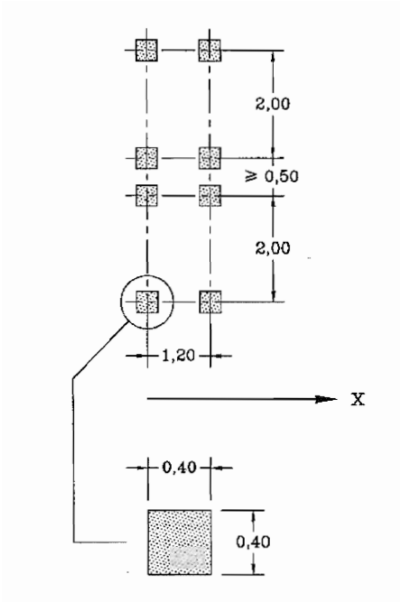

Figure C.22: Application of tandem systems for local verification.

Adjustment factors according to (SS-EN 1991-2:2003, 4.3.2) should follow the national amendments stated in the Swedish Transport Agency (TSFS 2018:57).

Adjustment factor	Value
α_{Q1}	0.9
α_{Q2}	0.9
α_{Q3}	0
α_{q1}	0.8
α_{qi}	1 for i > 1
α_{qr}	1

Table C.14: Adjustments factors based on TSFS 2018:57, 4.3.3(4)

Where i in α_{qi} denotes the lane number, and r in α_{qr} denotes remaining areas .

Design load per wheel (TS)

$Q_{id} = \frac{\alpha_{Qi} Q_{ik}}{2}$

Design load per wheel (UDL)

$q_{id} = \alpha_{Qi} q_{ik}$

Factor	Value	Description
$\alpha_q 1$	1	Adjustment factor for q_k in lane 1
$\alpha_q 2$	0.8	Adjustment factor for q_k in lane 2
$\alpha_B 1$	1	Adjustment factor for B_k in lane 1
$\alpha_B 2$	0.8	Adjustment factor for B_k in lane 2

Table C.15: Loads for different vehicle classes, according to TSFS 2018:57, 4.3.2(3) Transportstyrelsen, 2018

Design loads according to LM1, with adjustment for regulations of the Swedish Transport Administration

$B_{d1} = \frac{\alpha_{B1}\alpha_D B_k}{2}$ TS, lane 1

$q_{d1} = \alpha_{q1}\alpha_D q_k$ UDL, lane 1

$B_{d2} = \frac{\alpha_{B2}\alpha_D B_k}{2}$ TS, lane 2

$q_{d2} = \alpha_{q2}\alpha_D q_k$ UDL, lane 2

C.2.6 Traffic vehicle models

According to TSFS 2018:57(4.2.1(1)), different vehicle models can be adapted, based on different vehicle classes. Figue C.23 shows vehicle models a) through n), consisting of different sets of distributed loads and concentrated loads along the bridge span.

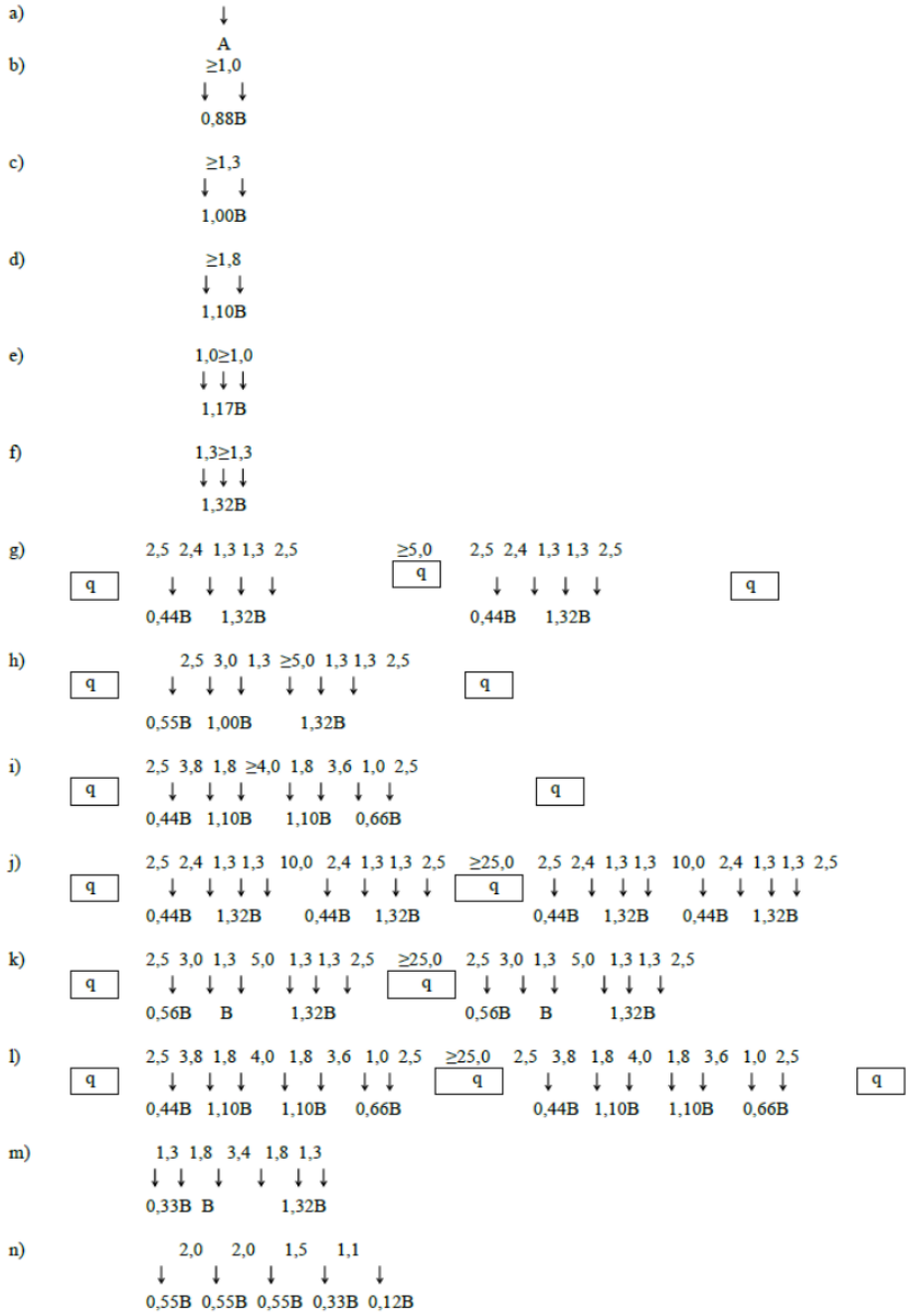

Figure C.23: Different vehicle models, according to (TSFS 2018:57, 4.2.1(1))

C.2.7 Braking and accelerating forces

A braking or accelerating force, Q_{lk}, shall be taken as a longitudinal force acting at the surfacing level of the carriageway. The Swedish transport administration states the maximum allowable the braking force should be 500 kN (TSFS 2018:57, 4.2.1(1)). Q_{lk} should be determined according to:

$$Q_{lk} = 0.6 * \alpha_{Q1} * (2 * Q_{1k}) + 0.1 * \alpha_{q1} * q_{1k} * w_l * L \qquad \text{(SS-EN 1991-2:2003, Eq 4.6)}$$
$$180 * \alpha_{q1}[kN] < Q_{lk} < 500[kN]$$

C.3 Division, location and numbering of carriageway lanes

According to SS-EN 1991-2:2003, 4.2.3, the carriageway width w is to be divided in notional lanes with width w_i according to the scheme found in Figure C.24. The location and numbering of the lanes should follow the principles presented in SS-EN 1991-2:2003, 4.2.3, as shown in Figure C.25.

Carriageway width w	Number of notional lanes	Width of a notional lane w_l	Width of the remaining area
$w < 5{,}4$ m	$n_l = 1$	3 m	w - 3 m
5,4 m $\leq w <$ 6 m	$n_l = 2$	$\frac{w}{2}$	0
6 m $\leq w$	$n_l = Int\left(\frac{w}{3}\right)$	3 m	$w - 3 \times n_l$
NOTE For example, for a carriageway width equal to 11m, $n_l = Int\left(\frac{w}{3}\right) = 3$, and the width of the remaining area is 11 - 3×3 = 2m.			

Figure C.24: Divison of carriageway into notional lane widths, (SS-EN 1991-2:2003, 4.2.3)

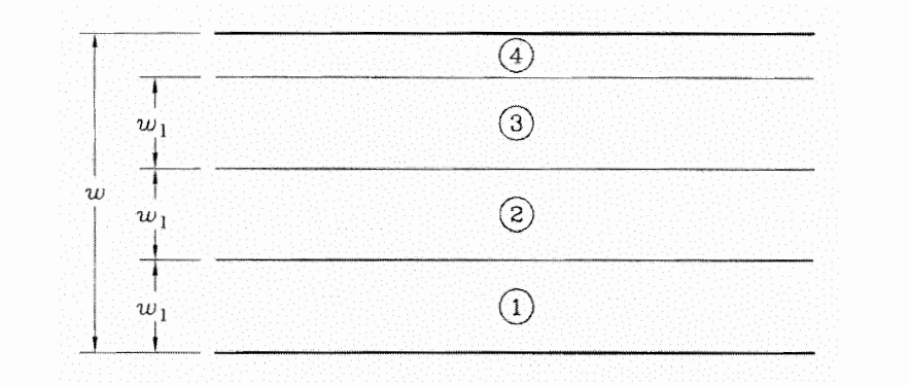

Figure C.25: Placement and numbering of lanes, (SS-EN 1991-2:2003, 4.2.4)

C.4 Load combinations

In SS-EN 1990:2002, 6.4.3, combinations of different actions on structures are presented. In ULS, permanent loads G are combined with variable loads Q, of which the most frequent is considered a main variable load whereas the others are secondary. The secondary loads are reduced with partial factors ψ. Both permanent and variable loads are multiplied with safety factors γ. Different ULS

verification are to be made in accordance with SS-EN 1990:2002, 6.4.3:

- **EQU** Loss of equilibrium.
- **STR** Internal failure of the structure.
- **GEO** Failure or excessive deformation of the ground.
- **FAT** Failure due to fatigue loading.

The load combination equation for EQU is presented in C.4. The governing load combination for STR is taken as the worst case of Equation C.4 and Equation C.5.

$$E_d = \sum_j \gamma_{G,j,sup} G_{k,j,sup} " + " \gamma_{G,j,inf} G_{k,j,inf} " + " \gamma_{Q,1} Q_{k,1} " + " \sum_i \gamma_{Q,i} \Psi_{0,i} Q_{k,i} \quad \text{(C.4)}$$

$$E_d = \begin{cases} \sum_j \gamma_{\mathrm{G,j,sup}} G_{\mathrm{k,j,sup}} " + " \gamma_{\mathrm{G,j,inf}} G_{\mathrm{k,j,inf}} " + " \gamma_{\mathrm{Q,1}} \Psi_{0,1} Q_{\mathrm{k,1}} " + " \sum_i \gamma_{\mathrm{Q,i}} \Psi_{0,\mathrm{i}} Q_{\mathrm{k,i}} \\ \sum_j \xi_j \gamma_{\mathrm{G,j,sup}} G_{\mathrm{k,j,sup}} " + " \gamma_{\mathrm{G,j,inf}} G_{\mathrm{k,j,inf}} " + " \gamma_{\mathrm{Q,1}} Q_{\mathrm{k,1}} " + " \sum_i \gamma_{\mathrm{Q,i}} \Psi_{0,\mathrm{i}} Q_{\mathrm{k,i}} \end{cases} \quad \text{(C.5)}$$

Where:

- Indices *sup* and *inf* represent unfavourable and favourable loads, respectively.
- ξ is a reduction factor for unfavourable permanent actions, which should be taken as 0.85 .

For SLS verification, characteristic, frequent and quasi-permanent combinations are included. Characteristic load combinations are to be used for irreversible serviceability limit state verification, such as for crack widths. Frequent or quasi-permanent load combinations are to be used for reversible serviceability limit state verification, such as for deflections. Load combination equations for SLS - characteristic , frequent and quasi-permanent, respectively - can be seen in Equations C.6 through C.8.

$$E_d = \sum_j G_{\mathrm{k,j}} " + " Q_{\mathrm{k,1}} " + " \sum_i \Psi_{0,\mathrm{i}} Q_{\mathrm{k,i}} \quad \text{(C.6)}$$

$$E_d = \sum_i G_{\mathrm{k,j}} " + " \Psi_{1,1} Q_{k,1} " + " \sum_i \Psi_{2,\mathrm{i}} Q_{\mathrm{k,i}} \quad \text{(C.7)}$$

$$E_d = \sum_j G_{k,j} " + " \sum_i \Psi_{2,i} Q_{k,i} \quad \text{(C.8)}$$

Depending on safety class, different γ_d-factors should be used, see Table C.16.

Safety class	Description	γ_d
2	$L \leq 15$ m	0.91
3	L $>$ 15 m	1

Table C.16: γ_d-factors based on safety class

When computing the sectional forces in each investigated cross-section, a worst-case load combination was found by looping through a set of load combinations. Load combination 1 with dominating permanent loads and Load combination 2 with non-dominating permanent loads, were implemented for ULS verifications. Factors for each of the investigated combinations, for ULS and SLS, are found in Tables C.17 and C.18.

					ULS			
					Method 1		**Method 2**	
Perm	Variation		$\gamma_{Gj,sup,B}$	$\gamma_{Gj,sup,BC}$	Sup	Inf	Sup	Inf
sw	1.0	1.0	1.35	1.0	1.23	1.0	1.09	1.0
ep	1.0	1.0	1.35	1.0	1.23	1.0	1.09	1.0
Var	Ψ_0	Ψ_1	ψ_{char}	$\gamma_{Q1,AB}$	Main	Sub	Main	Sub
sur	0.75	0.75	1.0	1.4	1.02	1.02	1.37	1.02
cep	0.7	0.7	0.6	1.4	0.57	0.57	0.82	0.57
TS	0.75	0.75	1.0	1.4	1.02	1.02	1.37	1.02
UDL	0.4	0.4	1.0	1.4	0.55	0.55	1.37	0.55
ba	0.7	0.7	0.6	1.4	0.57	0.57	0.82	0.57
VM	0.75	0.75	0.75	1.4	1.02	1.02	1.37	1.02

Table C.17: Load combination factors (ULS) for $\gamma_d = 0.91$ (safety class 2)

					SLS			
					Char		**Quasi-perm**	
Perm	Variation		$\gamma_{Gj,sup,B}$	$\gamma_{Gj,sup,BC}$	Sup	Inf	Sup	Inf
sw	1.0	1.0	1.35	1.0	1.0	1.0	1.0	1.0
ep	1.0	1.0	1.35	1.0	1.0	1.0	1.0	1.0
Var	Ψ_0	Ψ_1	ψ_{char}	$\gamma_{Q1,AB}$	Main	Sub	Main	Sub
sur	0.75	0.75	1.0	1.4	1.0	0.75	0.75	0
cep	0.7	0.7	0.6	1.4	1.0	0.75	0.75	0
TS	0.75	0.75	1.0	1.4	1.0	0.75	0.75	0
UDL	0.4	0.4	1.0	1.4	1.0	0.4	0.4	0
ba	0.7	0.7	0.6	1.4	1.0	0.75	0.75	0
VM	0.75	0.75	0.75	1.4	1.0	0.75	0.75	0

Table C.18: Load combination factors (SLS) for $\gamma_d = 0.91$ (safety class 2)

Where:

- sw denotes self weight
- ep denotes earth pressure
- sur denotes surcharge load

XXX

- cep denotes counteracting earth pressure
- TS denotes tandem system (concentrated loads) in LM1
- UDL denotes uniformely distriduted load in LM1
- ba denotes braking/accelerating
- VM denotes vehicle model

D

Capacity Verification

In narrowing down the set of feasible and infeasible solutions (Design space B) to feasible solutions (Design space C), ULS and SLS verification were performed.

D.1 Ultimate limit state

The following section presents design checks for ultimate limit state (ULS), with respect to bending moment and shear.

D.1.1 Bending moment

The following section follows the methodology given in Bärande konstruktioner part 1, B.5.2 (Single reinforced section) and B5.6 (Bending with normal force). In order to evaluate the bending moment resistance, the height of the compressive zone (location of neutral axis) is calculated for the actual sectional forces, material parameters and geometry. The calculation of the compression zone height is based on assumption of reinforcement yielding, through iteration. When the assumption is confirmed, the the tensile capacity of the reinforcement is calculated based on the calculated height of the neutral axis. The utilization ratio in bending is subsequently checked, after which the cross sectional height is updated.

Geometry

w	Bridge deck width [mm]
h	Bridge deck height [mm]
$d_1 - d_i$	Longest distance between center of gravity of tensile reinforcement layer i and cross sectional edge (Effective height) [mm]
$d'_1 - d'_i$	Longest distance between center of gravity of compression reinforcement layer i and cross sectional edge (Effective height) [mm]
$d = \frac{\sum d_i \cdot A_{si}}{\sum A_{si}}$	Average distance from tensile reinforcement to cross-sectional edge [mm]

ϕ Tensile rebar diameter [mm]

ϕ' Compression rebar diameter [mm]

$n_1 - n_i$ Number of tensile rebars in reinforcement layer i [-]

$n'_1 - n'_i$ Number of compression rebars in reinforcement layer i [-]

x Height of compression zone [mm]

e_1 Eccentricity between center of gravity in reinforcement layer 1 and center of gravity of cross section [mm]

e_2 Eccentricity between center of gravity in reinforcement layer 2 and center of gravity of cross section [mm]

$e_{N_{Ed}}$ Eccentricity between application of N_{Ed} and pivot point chosen for moment equilibrium [mm]

A_{s1} Tensile reinforcement layer 2 cross sectional area [mm^2]

A_{s2} Tensile reinforcement layer 2 cross sectional area [mm^2]

$\alpha = 0.81$ Stress block factor for simplified rectangular stress block (C12/15-C50/60) [-]

$\beta = 0.416$ Simplified stress block factor for compressive force resultant position (C12/15-C50/60) [-]

Sectional forces

M_{Ed} Design bending moment [Nmm]

N_{Ed} Design normal force [N]

The geometrical parameters, compression stress distribution and sectional forces for sectional analysis of bending moment in ULS is presented for single and double reinforced sections in in Figure D.1.

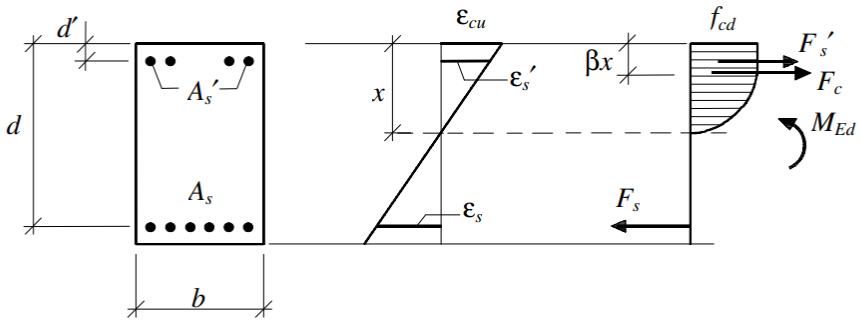

Figure D.1: Sectional forces and compressive stress distribution of double reinforced section, subjected to bending moment (Al-Emrani et al., 2013). Note that the design normal force N_{Ed} is excluded in the figure. Here, b corresponds to w

Moment equilibrium

Based on cross sectional horizontal force equilibrium, the compression zone height can be determined.

$$\alpha \cdot f_{cd} \cdot w \cdot x + \sigma_s' \cdot A_s' + N_{Ed} = \sigma_s \cdot A_s$$ Force equilibrium [N]
(Bärande konstruktioner part 1, Eq B5-23 , B5.6.2)

Deformation condition

Assuming a linear strain distribution and full interaction between concrete and reinforcement, the steel strain can be expressed in terms of the ultimate compressive strain of concrete.

$$\epsilon_s = \frac{d-x}{x}\epsilon_{cc}$$ Steel strain of tensile reinforcement [-]
(Bärande konstruktioner part 1, Eq B5-26)

$$\epsilon_s' = \frac{x-d'}{x}\epsilon_{cc}$$ Steel strain of compressive reinforcement [-]
(Bärande konstruktioner part 1, Eq B5-25)

Constitutive relation of steel

Based on the idealized stress-strain relation with horizontal upper branch:

$$\sigma_s = \begin{cases} E_s \cdot \epsilon_s, & \epsilon_s \leq \epsilon_{syd} \\ f_{yd}, & \epsilon_s \geq \epsilon_{syd} \end{cases}$$

$$\sigma_s' = \begin{cases} E_s \cdot \epsilon_s', & \epsilon_s' \leq \epsilon_{syd} \\ f_{yd}, & \epsilon_s' \geq \epsilon_{syd} \end{cases}$$

Assume that the reinforcement is yielding:

$$\begin{cases} \epsilon_s \geq \epsilon_{syd} \\ \sigma_s = f_{yd} \end{cases}$$
$$\begin{cases} \epsilon'_s \geq \epsilon_{syd} \\ \sigma'_s = f_{yd} \end{cases}$$

Calculation of Compression zone height

Based on cross sectional horizontal force equilibrium, the compression zone height can be determined.

$$x = \frac{\sigma_s \cdot A_s - \sigma'_s \cdot A'_s - N_{Ed}}{\alpha \cdot f_{cd} \cdot w}$$

Check yielding of reinforcement steel

Based on the obtained x, the steel strain can be determined using the compatibility condition:

$$\epsilon_s = \frac{d-x}{x}\epsilon_{cc}$$

$$\epsilon_s - = \frac{x-d'}{x}\epsilon_{cc}$$

If $\epsilon_s \geq \epsilon_{syd}$, the assumption of yielding in the tensile reinfrocement was correct.
If $\epsilon'_s \geq \epsilon_{syd}$, the assumption of yielding in the compressive reinforcement was correct.

If the assumption of yielding was not correct, a new x is to be calculated from the force equilibrium, assuming elastic response of the reinforcement. The steel stress can then be expressed with Hookes law:

$$\sigma_s = E_s \cdot \epsilon_s = E_s \cdot \frac{d-x}{x}\epsilon_{cc}$$
$$\sigma'_s = E_s \cdot \epsilon'_s = E_s \cdot \frac{x-d'}{x}\epsilon_{cc}$$

$$x = \frac{\sigma_s \cdot A_s - \sigma'_s \cdot A'_s - N_{Ed}}{\alpha \cdot f_{cd} \cdot w}$$

The procedure of calculating x is iterated until the assumption of the steel response (elastic or plastic) is confirmed.

Moment capacity

The moment capacity is calculated by moment equilibrium around an arbitrary point, here at the level of the tensile reinforcement.

$M_{Rd} = \alpha \cdot f_{cd} \cdot w \cdot x(d - \beta \cdot x) + \sigma'_s \cdot A'_s(d - d') - N_{Ed} \cdot e_{N_{Ed}}$ Moment equilibrium about [Nmm] F_s

(Bärande konstruktioner part 1, Eq B5-24 , B5.6.2)

Tensile reinforcement in several layers

When analysing the capacity of cross sections with more than one layer tensile reinforcement,the procedure is similar to that of one layer. In both force- and moment equilibrium, the tensile force resultant of each reinforcement layer is included. In order to set up the force equilibrium, the assumption of yielding in the reinforcement needs to be made in all reinforcement layers.With the obtained compressive height, the steel strain is checked in each layer. The iteration proceeds until all assumptions are verified. Moment equilibrium can be made about the resultant of the tensile reinforcement.

D.1.2 Shear

The shear design is performed according to SS-EN 1992-1-1:2005. In regions of the member where the applied shear is less than the capacity of the section, $V_{Ed} \leq V_{Rd,c}$, no shear reinforcement is needed, according to Section D.1.2.1. In regions where $V_{Ed} > V_{Rd,c}$ shear reinforcement has to be provided, according to Section D.1.2.2.

s	spacing of the shear reinforcement measured along the longitudinal axis of the member [mm]
b_w	The smallest width of the cross-section in the tensile area [mm]
α	Angle between shear reinforcement and the longitudinal axis [-]

D.1.2.1 No shear reinforcement

For members not requiring shear reinforcement, the procedure according to SS-EN 1992-1-1:2005 6.2.2 is followed.

d	Distance between edge and tensile reinforcement [mm]
A_{sl}	Area of the tensile reinforcement which extends l_{lb}+d beyond the section considered [mm^2]
N_{Ed}	Axial force in the cross-section due to loading or prestressing (N_{Ed}>0 for compression) [N]
A_C	Area of concrete cross-section [mm^2]
$k_1 = 0.15$	[-] (SS-EN 1992-1-1:2005, Eq 6.2b)
$\nu = 0.6[1 - \frac{f_{ck}}{250}]$	(f_{ck} in MPa) [-] (SS-EN 1992-1-1:2005, Eq 6.6N)

$k = 1 + \sqrt{\frac{200}{d}} \leq 2.0$ (d in mm)[-] (SS-EN 1992-1-1:2005, Eq 6.2b)

$\rho_1 = \frac{A_{sl}}{b_w d} \leq 0.02$ [-] (SS-EN 1992-1-1:2005, Eq 6.2b)

$v_{min} = 0.035 \cdot k^{3/2} \cdot f_{ck}^{1/2}$ [MPa] SS-EN 1992-1-1:2005, Eq 6.2b)

$\sigma_{cp} = \frac{N_{Ed}}{A_C} < 0.2 f_{cd}$ [MPa] (SS-EN 1992-1-1:2005, Eq 6.2b)

$C_{Rd,c} = \frac{0.18}{\gamma_{psf,c}}$ [-] (SS-EN 1992-1-1:2005, Eq 6.2b)

$V_{Rd,c1} = [C_{Rd,c} k (100 \rho_1 f_{ck})^{1/3} + k_1 \sigma_{cp}] b_w d$ The design value for shear resistance in concrete [N] (SS-EN 1992-1-1:2005, Eq 6.2a)

$V_{Rd,c,min} = [v_{min} + k_1 \sigma_{cp}] b_w d$ The minimum design value for shear resistance [N] (SS-EN 1992-1-1:2005, Eq 6.2b)

$V_{Rd,c} = max(V_{Rd,c1},\ V_{Rd,c,min})$ The design value for shear resistance [N] (SS-EN 1992-1-1:2005, Eq 6.2a-6.2b)

$V_{Rd,c} = min(V_{Rd,c},\ 0.5 b_w d \nu f_{cd})$ The shear force resistance [N] (SS-EN 1992-1-1:2005, Eq 6.5)

If the design value of the shear resistance in the concrete in the cross-section is insufficient, i.e., $V_{Rd,c} < V_{Ed}$, shear reinforcement is needed. The algorithm then loops over a number of s-distances until the requirement is fulfilled.

D.1.2.2 Shear reinforcement design

For members requiring shear reinforcement, the procedure follows guidelines according to SS-EN 1992-1-1:2005 (6.2.3).

z = 0.9d Internal lever arm [mm]

A_{sw} Cross-sectional area of shear reinforcement [mm^2]

$1 \leq cot(\theta) \leq 2.5$ Angle between the concrete compression strut and the beam axis perpendicular to the shear force [°]

$\nu_1 = 0.6$ Strength reduction factor for concrete cracked in shear [-] (SS-EN 1992-1-1:2005, Eq 6.10.aN)

α_{cw} Coefficient taking into account the state of the stress in the compression chord [-]
(SS-EN 1992-1-1:2005, Eq 6.11.aN-6.11.cN)

$$\alpha_{cw} = \begin{cases} 1 + \frac{\sigma_{cp}}{f_{cd}} & if \quad 0 < \sigma_{cp} \leq 0.25 f_{cd} \\ 1.25 & if \quad 0.25 f_{cd} < \sigma_{cp} \leq 0.5 f_{cd} \\ 2.5(1 - \frac{\sigma_{cp}}{f_{cd}}) & if \quad 0.5 f_{cd} < \sigma_{cp} \leq 1.0 f_{cd} \end{cases}$$

$V_{Rd,s} = \frac{A_{sw}}{s} z 0.8 f_{ywd} cot\theta$ Shear resistance [N]
(SS-EN 1992-1-1:2005, Eq 6.8)

$V_{Rd,max} = \frac{\alpha_{cw} b_w z \nu_1 f_{cd}}{cot\theta + tan\theta}$ Maximum shear resistance [N]
(SS-EN 1992-1-1:2005, Eq 6.9)

$V_{Rd} = min(V_{Rd,s}, V_{Rd,max})$ Final shear resistance [N]
(SS-EN 1992-1-1:2005, 6.2.3(3))

D.1.2.3 Minimum shear reinforcement design

For members requiring shear reinforcement, the procedure for minimum shear reinforcement follows guidelines according to SS-EN 1992-1-1:2005 (9.2.2). For members with insufficient concrete shear capacity, the shear reinforcement was taken as the one with highest shear strength of the regular shear reinforcement and the minimum shear reinforcement.

$\rho_{w,min} = \frac{0.08\sqrt{f_{ck}}}{f_{yk}}$ Minimum shear reinforcement ratio [-]
(SS-EN 1992-1-1:2005, Eq 9.5N)

$s_{l,max} = 0.75 \cdot d(1 + cot(\alpha))$ Maximum spacing of the shear reinforcement along the longitudinal axis of the member [mm]
(SS-EN 1992-1-1:2005, 9.2.2(6))

$A_{sw} = \rho_w \cdot s \cdot b_w \cdot sin(\alpha)$ Area of shear reinforcement within length s [mm^2]
(SS-EN 1992-1-1:2005, Eq 9.4)

D.2 Serviceability limit state

Together with ULS requirements, SLS was checked w.r.t deflection.

D.2.1 Deflection

This section presents SLS verification performed for vertical deflection of the mid section of the bridge deck were made for each bridge design, in accordance with

Johannesson, P., and Vretblad, e. (1969).

a The shortest distance between the concentrated load and a support [mm]

$I_{II,avg_{fl}} = \frac{I_{II_{fl,1}} + I_{II_{fl,2}} + I_{II_{fl,3}}}{3}$ Average moment of inertia for bridge deck [mm^4]

$I_{II,avg_{bd}} = \frac{I_{II_{bd,1}} + I_{II_{bd,2}}}{2}$ Average moment of inertia for frame leg [mm^4]

$\delta_{v_q} = \frac{q_{def} \cdot L^4}{384 \cdot E_{cm} \cdot I_{II,avg_{bd}}}$ Vertical deflection due to uniformly distributed load [mm]

$\delta_{v_{Q,i}} = Q_{def} \cdot (\frac{a^2 \cdot L}{48 * E_{cm} * I_{II,avg_{bd}}} \cdot (3 - 4 \cdot a/L))$ Vertical deflection due to the i:th concentrated load [mm]

$\delta_{v_Q} = \sum(\delta_{v_{Q,i}})$ Vertical deflection due to all concentrated loads [mm]

$\delta_v = \delta_{v_q} + \delta_{v_q}$ Total vertical deflection [mm]

$\delta_v < L/400$ Deflection limit [mm] (Krav Brobyggande, B.3.4.2.2)

E

Criteria Cost Calculations

This chapter presents the calculations of the equivalent cost, including the calculations of separate criterion costs. Tables E.1 through E.7 present the values implemented in the algorithm, regarding unit prices for investment-, environmental- and buildability- cost calculations. The total weighed equivalent cost for the three criteria is presented in Equation E.1.

$$\begin{aligned} cost_{eq} &= cost_{inv} \cdot \psi_{inv} + cost_{env} \cdot \psi_{env} + cost_{build} \cdot \psi_{build} \\ 0 &\leq \psi_i \leq 1 \end{aligned} \tag{E.1}$$

Where ψ_i denotes the respective weighting factor per optimization criterion, enabling the choice of emphasis in the optimization.

The calculation procedure, costs and factors related to each of the three optimization criteria are presented in the following Sections E.1-E.3.

E.1 Investment cost

The calculation procedure, as well as the costs and factors related to the investment cost criterion are presented in this section.

The investment cost for the rebars is presented in Equation E.2.

$$\begin{aligned} cost_{reb,mtrl} &= cost_{reb,mtrl,unit} \cdot V_{reb,tot} \cdot \rho_{reb} \\ cost_{reb,lab,fl} &= cost_{reb,lab,fl,unit} \cdot V_{reb,fl} \cdot \rho_{reb} \\ cost_{reb,lab,bd} &= cost_{reb,lab,bd,unit} \cdot V_{reb,bd} \cdot \rho_{reb} \\ cost_{reb} &= cost_{reb,mtrl} + cost_{reb,lab,fl} + cost_{reb,lab,bd} \end{aligned} \tag{E.2}$$

The investment cost for the concrete is presented in Equation E.3.

$$
\begin{aligned}
cost_{conc,mtrl} &= cost_{conc,mtrl,unit} \cdot V_{conc,tot} \cdot \rho_{conc} \\
cost_{conc,lab,fl} &= cost_{conc,lab,fl,unit} \cdot V_{conc,fl} \cdot \rho_{conc} \\
cost_{conc,lab,bd} &= cost_{conc,lab,bd,unit} \cdot V_{conc,bd} \cdot \rho_{conc} \\
cost_{conc} &= cost_{conc,mtrl} + cost_{conc,lab,fl} + cost_{conc,lab,bd}
\end{aligned}
\tag{E.3}
$$

The investment cost for the formwork is presented in Equation E.4.

$$
\begin{aligned}
cost_{form,lab,fl} &= cost_{form,lab,fl,unit} \cdot A_{form,fl} \\
cost_{form,lab,bd} &= cost_{form,lab,bd,unit} \cdot A_{form,bd} \\
cost_{form,material} &= cost_{form,mtrl,fl} + cost_{form,mtrl,bd} \\
cost_{form,labour} &= cost_{form,lab,fl} + cost_{form,lab,bd} \\
cost_{form} &= cost_{formwork,mtrl} + cost_{form,labour}
\end{aligned}
\tag{E.4}
$$

Where the formwork material cost for frame legs and bridge deck, depending on wheter the element is constant or varying in thickness, is calculated according to Equation E.5:

$$
\begin{aligned}
cost_{form,mtrl,fl} &= \begin{cases} cost_{form,mtrl,const,fl,unit} \cdot A_{form,fl} & \text{if const. cs-height in element} \\ cost_{form,mtrl,var,fl,unit} \cdot A_{form,fl} & \text{if varying cs-height in element} \end{cases} \\
cost_{form,mtrl,bd} &= \begin{cases} cost_{form,mtrl,const,bd,unit} \cdot A_{form,bd} & \text{if const. cs-height in element} \\ cost_{form,mtrl,var,bd,unit} \cdot A_{form,bd} & \text{if varying cs-height in element} \end{cases}
\end{aligned}
\tag{E.5}
$$

Subsequently, the total investment cost for a bridge design was calculated according to Equation E.6.

$$
cost_{inv} = cost_{form} + cost_{reb} \cdot \alpha_{reb} + cost_{conc} \tag{E.6}
$$

Material unit costs			
Concrete classes	**Symbol**	**Unit price**	**Unit**
C32/40	$cost_{conc,mtrl,unit}$	$1700 \cdot 10^{-9}$	[SEK/mm^3]
C35/45		$1800 \cdot 10^{-9}$	
C50/60		$2000 \cdot 10^{-9}$	
Rebars	**Symbol**	**Unit price**	**Unit**
General value	$cost_{reb,mtrl,unit}$	9	[SEK/kg]
Formwork (constant)	**Symbol**	**Unit price**	**Unit**
Frame legs	$cost_{form,mtrl,const,fl,unit}$	$200 \cdot 10^{-6}$	[SEK/mm^2]
Bridge deck	$cost_{form,mtrl,const,bd,unit}$	$500 \cdot 10^{-6}$	
Formwork (varying)	**Symbol**	**Unit price**	**Unit**
Frame legs	$cost_{form,mtrl,var,fl,unit}$	$300 \cdot 10^{-6}$	[SEK/mm^2]
Bridge deck	$cost_{form,mtrl,var,bd,unit}$	$500 \cdot 10^{-6}$	

Table E.1: Material unit costs.

Labour unit costs			
Concrete	**Symbol**	**Unit price**	**Unit**
Frame legs	$cost_{conc,lab,fl,unit}$	$750 \cdot 10^{-9}$	[SEK/mm^3]
Bridge deck	$cost_{conc,lab,fl,unit}$	$800 \cdot 10^{-9}$	
Rebars	**Symbol**	**Unit price**	**Unit**
Frame legs	$cost_{reb,lab,fl,unit}$	15	[SEK/kg]
Bridge deck	$cost_{reb,lab,bd,unit}$	17.5	
Formwork (constant)	**Symbol**	**Unit price**	**Unit**
Frame legs	$cost_{form,lab,fl,unit}$	$500 \cdot 10^{-6}$	[SEK/mm^2]
Bridge deck	$cost_{form,lab,bd,unit}$	$500 \cdot 10^{-6}$	

Table E.2: Labour unit costs.

E.2 Environmental cost

The calculation procedure, as well as the costs and factors related to the environmental cost criterion are presented in this section.

The environmental costs for the concrete and the rebars were calculated separately, according to Equation E.7. The environmental cost of formwork was neglected due to assumed reusability.

$$cost_{env,reb} = cost_{env,reb,unit} \cdot V_{reb} \cdot \rho_{reb} \cdot \beta_{monetary}$$
$$cost_{env,conc} = cost_{env,conc,unit} \cdot V_{reb} \cdot \beta_{monetary} \tag{E.7}$$

The total environmental cost per bridge design was thereafter caclculated according to Equation E.8.

$$cost_{env} = cost_{env,reb} \cdot \alpha_{reb} + cost_{env,conc} \tag{E.8}$$

Material unit CO_2 equivalents			
Concrete classes	**Symbol**	**Unit outlet**	**Unit**
C32/40	$cost_{env,conc,unit}$	$344.505 \cdot 10^{-9}$	[kg·CO_2· eq/mm^3]
C35/45		$352.694 \cdot 10^{-9}$	
C50/60		$383.748 \cdot 10^{-9}$	
Rebars	**Symbol**	**Unit outlet**	**Unit**
General value	$cost_{env,reb,unit}$	2.387	[kg·CO_2· eq/kg]
Monetary value	**Symbol**	**Price factor**	**Unit**
Ecotax	$\beta_{monetary}$	0.63	[SEK]
Ecovalue		2.85	

Table E.3: Environmental unit costs.

E.3 Buildability cost

The calculation procedure, as well as the costs and factors related to the buildability cost criterion are presented in this section.

Buildability cost due to small rebar diameters

In computing the buildability cost due to small reinforcement bar diameters, the most frequently occurring diameters in the frame legs and the bridge deck, were identified by the algorithm, according to Equation E.9.

$$\begin{cases} \phi_{freq,fl} = freq_{max}(\phi_{fl}) \\ \phi_{freq,bd} = freq_{max}(\phi_{bd}) \end{cases} \tag{E.9}$$

After which the buildability factor $\alpha_{build,\phi,i}$ associated with the dominating (most frequent) diameter was extracted. The values of the buildability factors are specified

in Tables E.4 trough E.7. The buildability cost associated with the rebar diameters was subsequently calculated for the frame legs and the bridge deck, based on the dominating diameter, according to Equation E.10.

$$\begin{cases} cost_{build,\phi,fl} = \alpha_{build,\phi,fl} \cdot \sum(V_{\phi,fl}) \cdot \rho_{reb} \cdot cost_{reb,lab,fl,unit} \\ cost_{build,\phi,bd} = \alpha_{\phi,bd} \cdot \sum(V_{\phi,bd}) \cdot \rho_{reb} \cdot cost_{reb,lab,bd,unit} \end{cases} \tag{E.10}$$

The total buildability cost associated with the rebar diameters, for the frame legs and the bridge deck, was subsequently calculated according to Equation E.11.

$$cost_{build,\phi} = (cost_{build,\phi,fl} + cost_{build,\phi,bd}) \cdot \alpha_{reb} \tag{E.11}$$

Buildability cost due to variable element thicknesses

An additional buildability cost was calculated for extra reinforcing- and formwork labour due to variable thickness throughout bridge elements. In case of variable thickness, an additional buidlability cost for the reinforcing work was calculated according to Equation E.12.

$$\begin{cases} cost_{build,reb,var,fl} = \alpha_{build,reb,var,fl} \cdot \sum(V_{\phi,fl}) \cdot \rho_{reb} \cdot cost_{reb,lab,fl,unit} \\ cost_{build,reb,var,bd} = \alpha_{build,reb,var,bd} \cdot \sum(V_{\phi,bd}) \cdot \rho_{reb} \cdot cost_{reb,lab,bd,unit} \end{cases} \tag{E.12}$$

After which the total buildability costs for reinforcement labour were calculated, according to Equation E.13.

$$cost_{build,reb,var} = (cost_{build,reb,var,fl} + cost_{build,reb,var,bd}) \cdot \alpha_{reb} \tag{E.13}$$

In case of variable thickness, an additional buildability cost for the formwork labour was calculated according to Equation E.14.

$$\begin{cases} cost_{build,formwork,var,fl} = \alpha_{build,formwork,var,fl} \cdot cost_{formwork,lab,fl} \\ cost_{build,formwork,var,bd} = \alpha_{build,formwork,var,bd} \cdot cost_{formwork,lab,bd} \end{cases} \tag{E.14}$$

After which the total buildability costs for formwork labour were calculated, according to Equation E.15.

$$cost_{build,formwork,var} = cost_{build,formwork,var,fl} + cost_{build,formwork,var,bd} \tag{E.15}$$

Buildability cost due to slender elements

An additional buildability cost was defined for extra reinforcing work associated with slender elements, according to Equations E.16 and E.17.

$$cost_{build,slender,fl} = \begin{cases} \alpha_{build,sl,1} \cdot \sum(V_{\phi,fl}) \cdot \rho_{reb} \cdot cost_{reb,lab,fl,unit} & \text{if} \quad h_{fl,mean} \leq 400 \\ \alpha_{build,sl,2} \cdot \sum(V_{\phi,fl}) \cdot \rho_{reb} \cdot cost_{reb,lab,fl,unit} & \text{if} 400 < h_{fl,mean} \leq 600 \\ 0 & \text{Otherwise} \end{cases} \tag{E.16}$$

$$cost_{build,slender,bd} = \begin{cases} \alpha_{build,sl,1} \cdot \sum(V_{\phi,bd}) \cdot \rho_{reb} \cdot cost_{reb,lab,bd,unit} & \text{if} \quad h_{bd,mean} \leq 400 \\ \alpha_{build,sl,2} \cdot \sum(V_{\phi,bd}) \cdot \rho_{reb} \cdot cost_{reb,lab,bd,unit} & \text{if} 400 < h_{bd,mean} \leq 600 \\ 0 & \text{Otherwise} \end{cases} \tag{E.17}$$

Subsequently, the total buildability cost for slender elements was calculated according to Equation E.18.

$$cost_{build,sl} = (cost_{build,sl,fl} + cost_{build,sl,bd}) \cdot \alpha_{reb} \tag{E.18}$$

Buildability cost due to concrete strength class $\geq C50/60$

An additional buildability cost due to required vibration work for concrete strength classes $\geq C50/60$ was calculated according to Equation E.19.

$$cost_{conc.class} = \begin{cases} cost_{build,conc,unit} \cdot V_{conc,tot} & \text{if} f_{ck} \geq 50MPa \\ 0 & \text{Otherwise} \end{cases} \tag{E.19}$$

Buildability cost due to use of shear reinforcement

A buildability cost due to extra work for shear reinforcement was calculated according to EquationE.20.

$$\begin{aligned} cost_{build,stirrup,fl} &= \alpha_{build,stirrup} \cdot V_{stirrup,fl} \cdot \rho_{reb} \cdot cost_{reb,lab,fl,unit} \\ cost_{build,stirrup,bd} &= \alpha_{build,stirrup} \cdot V_{stirrup,bd} \cdot \rho_{reb} \cdot cost_{reb,lab,bd,unit} \end{aligned} \tag{E.20}$$

Subsequently, the total buildability cost for shear reinforcement in frame legs and bridge deck was calculated, according to Equation E.21.

$$cost_{build,stirrup} = (cost_{build,stirrup,fl} + cost_{build,stirrup,bd}) \cdot \alpha_{reb} \tag{E.21}$$

Total buildability cost

A total buildability cost considering the different buildability aspects was calculated according to Equation E.22.

$$cost_{build} = cost_{build,\phi} + cost_{build,var} + cost_{build,sl} + cost_{build,conc.class} + cost_{build,stirrup} \tag{E.22}$$

Concrete - Buildability aspects			
Concrete classes	**Symbol**	**Unit price**	**Unit**
Concrete class ≥ C50/60	$cost_{build,conc,unit}$	$200 \cdot 10^{-9}$	[SEK/mm^3]

Table E.4: Buildability value due to concrete strength class.

Bending reinforcement - Buildability aspects			
Rebar diameter	**Symbol**	**Price factor**	**Unit**
ϕ16	$\alpha_{build,\phi,i}$	0.25	[-]
ϕ20		0.14	
ϕ25		0	
Variable thickness in element	**Symbol**	**Price factor**	**Unit**
Variable	$\alpha_{build,reb,var}$	0.15	[-]
Slenderness of cross-section	**Symbol**	**Price factor**	**Unit**
400<h<600 mm	$\alpha_{build,sl,i}$	0.1	[-]
h<400 mm		0.2	

Table E.5: Buildability values due to additional reinforcing labour.

Formwork - Buildability aspects			
Variable thickness in element	**Symbol**	**factor**	**Unit**
Variable	$\alpha_{build,form,var}$	0.33	[-]

Table E.6: Buildability values due to additional formwork labour.

Shear reinforcement - Buildability aspects			
Stirrups are used	**Symbol**	**Price factor**	**Unit**
Stirrups	$\alpha_{build,stirrup}$	0.56	[-]

Table E.7: Buildability values due to shear reinforcement.

F

Verification of Algorithm

The calculations of load effects within the algorithm were verified in comparison to a 2D reference project. The results are presented in Table F.1.

Comparison - 2D reference project		
	Algorithm	Reference
Distributed load, bridge deck, self-weight	20 kN/m	19 kN/m
Moment, support, ULS	42 kNm	40 kNm
Moment, frame corner, ULS	147 kNm	145 kNm
Moment, field, ULS	149 kNm	156 kNm
Shear, support, ULS	62 kN	60 kN
Shear, frame corner, frame leg, ULS	77 kN	90 kN
Shear, frame corner, bridge deck, ULS	180 kN	208 kN

Table F.1: Verification of algorithm in comparision to 2D reference project.

The load effects calculated by the algorithm generally correlate well to the load effects presented in the calculation report for the 2D reference project. Vehicle model n) (see Appendix C.2.6) was used in hand-calculations for verification of bending moments presented by the FEM-model within the calculation documents provided by Skanska. Thus, vehicle model n) was also implemented into the algorithm for verification of sectional forces. Minor differences in shear forces around the frame corners were expected, due to the choice of implementing one single vehicle model. All vehicle models could have been tested in order to identify the worst case for shear as well, but as LM1 was to be used insetad of VM for the final run of the algorithm that was regarded as unnecessary as moments has already been verified against the 2D reference project.

G

Optimized Designs

This chapter presents the cross-sectional design for Design 1 and Design 2, described in Sections 4.1 and 4.2 respectively.

G.1 Optimized design (Design 1)

Figure G.1 shows the cross-sectional design for cs_1 through cs_5 for the optimized design alternative, described in Section 4.1.

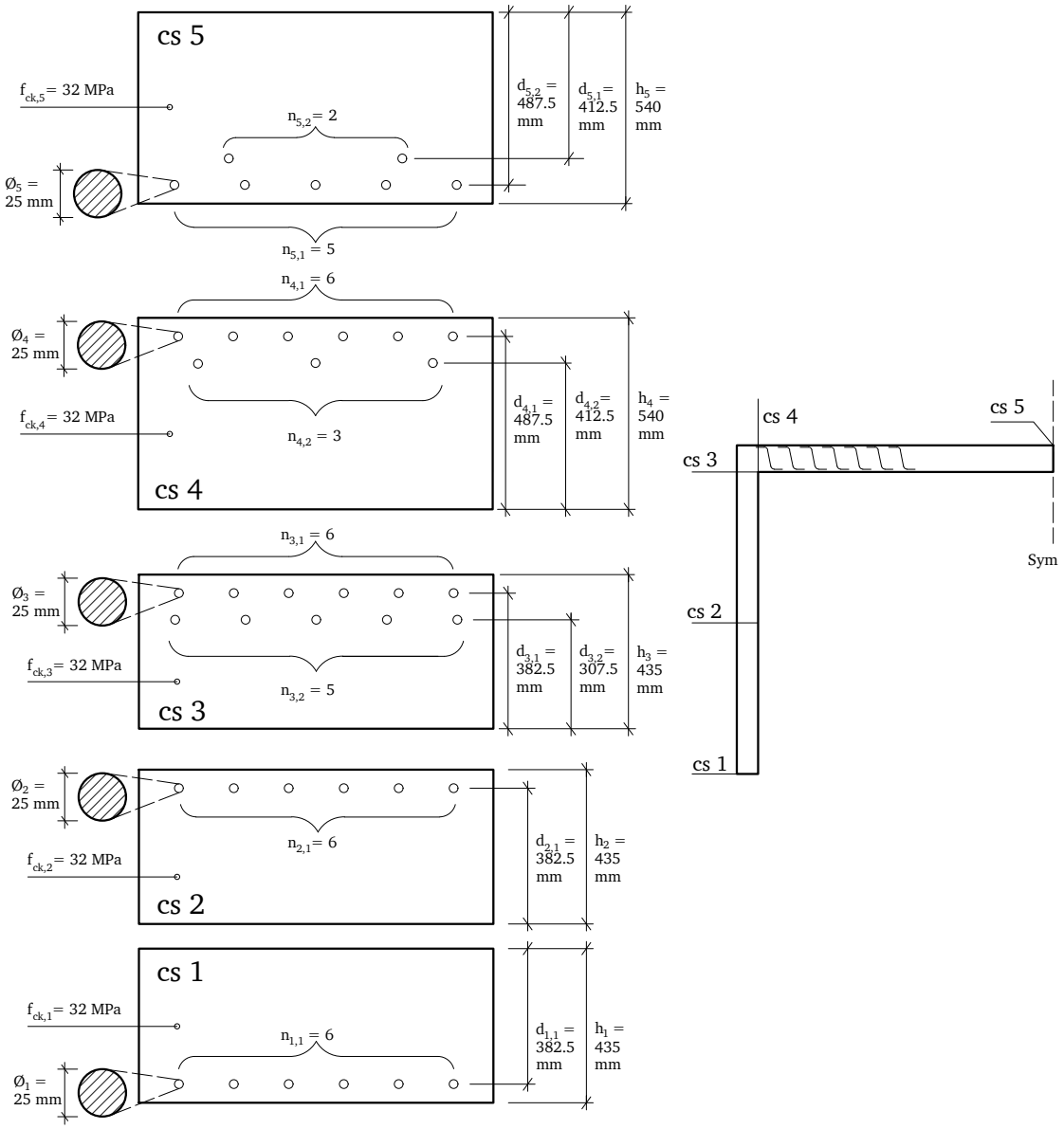

Figure G.1: Output data of 1 meter strip cross-sections in the optimized bridge design

G.2 Geometrically optimized design (Design 2)

Figure G.2 shows the cross-sectional design for cs_1 through cs_5 for the geometrically optimized design alternative, described in Section 4.2.

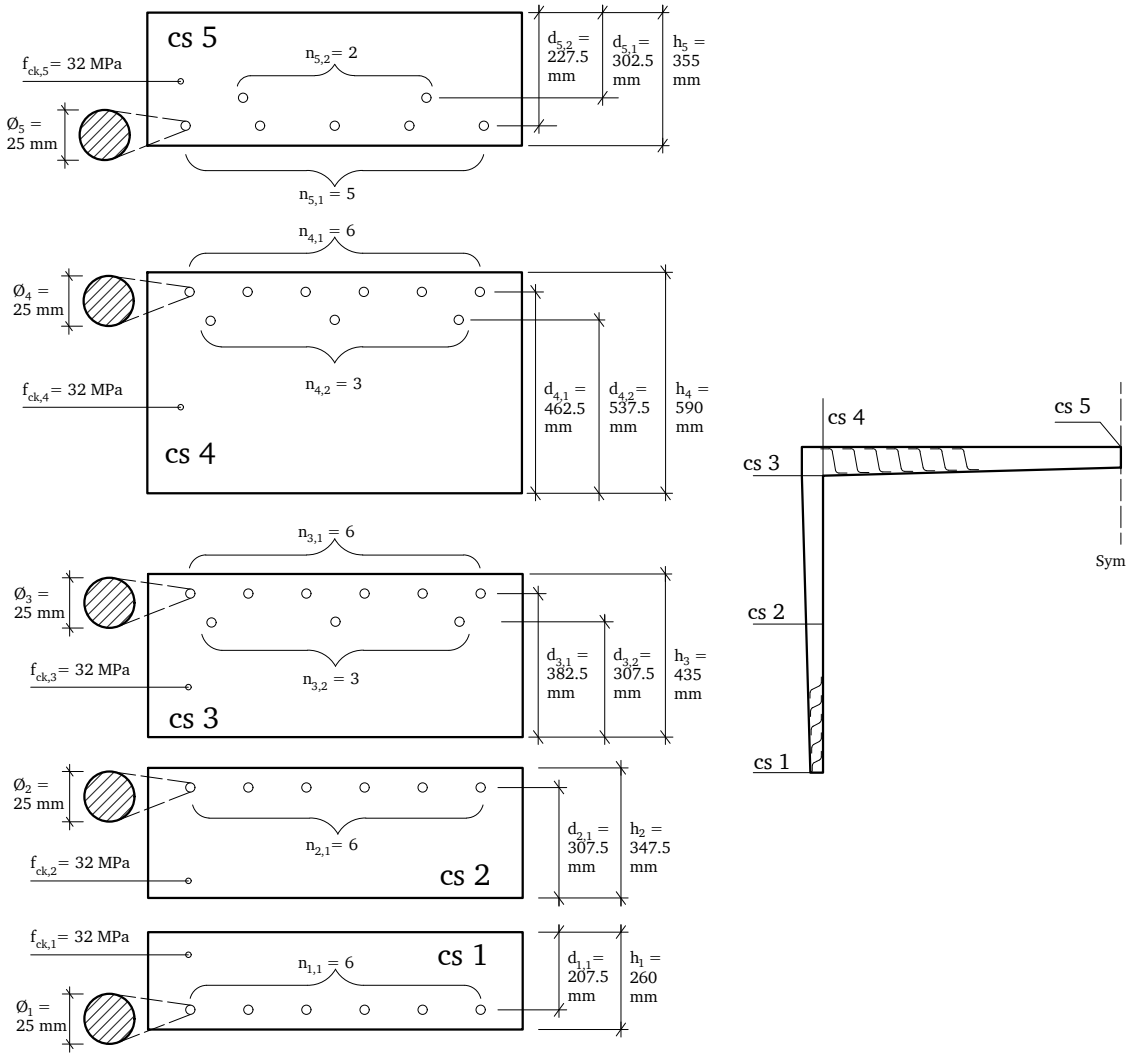

Figure G.2: Output data of 1 meter strip cross-sections in the geometrically optimized bridge design

G.3 Modified reference design

Figure G.3 shows the cross-sectional design for cs_1 through cs_5 for the modified reference project, described in Section 3.2.3.2.

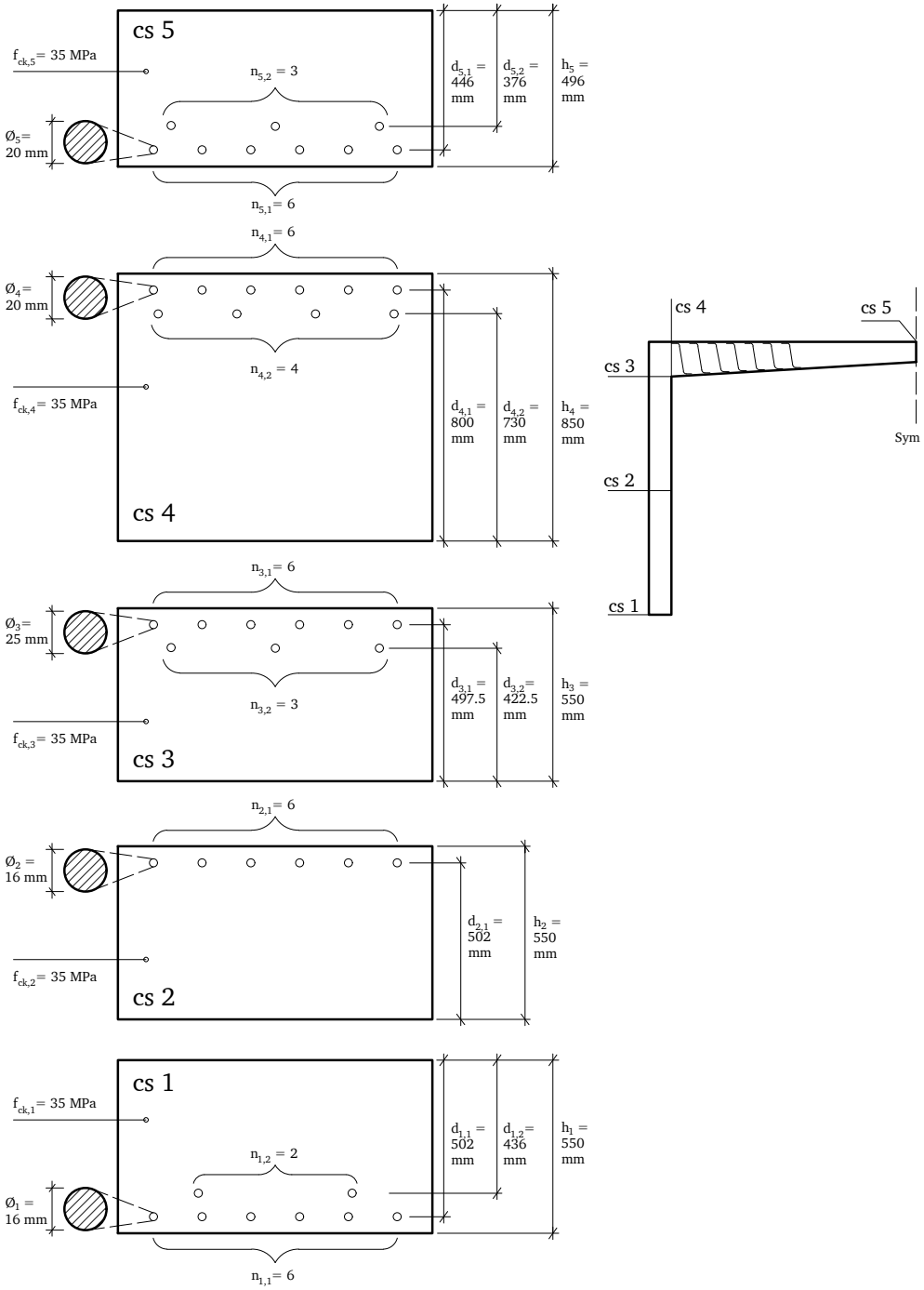

Figure G.3: Output data of 1 meter strip cross-sections in the modified reference project

H

Summary - Study

This chapter presents the studies made on possible definitions of the buildability criterion, as well as a review performed in order to clarify how the preliminary design phase of slab frame bridges is performed today. A calculation engineer familiar with cost definitions and an experienced bridge engineer, both working at Skanska, were consulted on the matters. The concluded answers from the respective dialogues are presented in Sections H.1 and H.2.

H.1 Dialogue with calculation engineer at Skanska

How is buildability considered in today's cost calculation at Skanska?

Examples of buildability aspects considered in cost calculations, that affect the price in the production of concrete bridges, are type of bridge element, complexity of geometry, the need for scaffolding, reinforcement dimensions, number of pours according to crack control, transportation conditions, availability and climate affecting the casting speed.

Detailed cost analyses are seldom conducted on comparisons of different types of cross sectional geometry. The analysis is rather based on bridge element type, such as bridge deck or foundation, as well as type of reinforcement bars. For instance, reinforcement work of edge beams require more time than that of a bridge deck assuming the same unit volume of concrete. Concerning reinforcement bars, the reinforcement work is more efficient when using bars with a larger diameter, as greater material amounts can be put in place per unit time. Similarly, straight bars entail less labour hours than bent bars. The construction site is taken into account by evaluating scaffolding costs and whether ground work or other preparations are needed. The cost calculation is partly based on a discussion with experienced construction workers familiar with production procedures. Furthermore, climate factors affecting the casting are considered in the cost calculation.

The considerations taken to buildability in today's conventional cost calculation are chiefly based on a combination of labor hours and material costs. The calculation engineer typically receives material amounts from the structural engineer. Labour costs are dependent on the capacity of the construction work, which in turn in based on element type. Ultimately, a certain bridge element type is associated with

a unit price per unit weight material. A final cost can subsequently be calculated based on the labour capacity and the material amounts related to all parts to be cast.

Do you think it is reasonable to define buildability in terms of increased labor costs due to slender elements, varying thicknesses, complex cross-sectional geometries and structural element types (according to newly explored definitions presented in previous research papers)?

The definitions used in previous research to quantify buildability are definitely reasonable interpretations. Adjustments of labor costs due to slender elements, varying thicknesses or complex cross-sectional geometries are not peformed today in that sense. The labor costs related to the kind of structural element being cast are always adjusted, since some require more work capacity than others, but no modifications are made specifically in terms of the geometrical complexity of the cross-sectional design or dimensions. It is more a matter of adjusting the price for the different structural parts of a bridge, than analysing the actual geometries.

One approach could be to define the geometrical complexity of a cross-section in terms of the required number of bending radii on the reinforcement or in terms of the number of mold surfaces necessary to achieve the required geometry. Are these feasible quantifications of buildability connected to complex geometries?

The number of required bending radii to perform a reinforcing work is never analysed today, but it could be a valid interpretation of the buildability criterion moving forward. The procurement costs related to the reinforcing work are usually considered in terms of the rebar diameters used. Assuming the same unit volume of steel is to be added, it is more advantageous and less costly to use rebars of larger dimensions, resulting in more steel volume added per unit time, ultimately making the production more efficient with decreasing production costs.

H.2 Dialogue with bridge engineer at Skanska

How can buildability be defined in relation to slab frame bridges and how is the criterion best implemented into an optimization procedure in your opinion?

It is a reasonable approach to recalculate complexity aspects in the construction work into equivalent costs, using amplifying factors for increasing difficulty. In the tendering process, unit prices per unit weight can be set based on an evaluation of the complexity in executing the design. Examples of such quantifiable aspects affecting the complexity of the labour work could be in terms of form work surface or the proportions of straight and bent bars.

We are exploring one buildability definition in terms of additional labor costs related to adding shear reinforcement. In comparison to the labor capacities needed for adding bending reinforcement, how much more time-consuming would you estimate it to be for adding shear reinforcement, based on experience?

Shear reinforcement for slab frame bridges is commonly pre-fabricated in the shape of welded reinforcement ladders, thus not resulting in any additional work on site. On the contrary, the additional labor work costs related to the welding procedure off-site can be included as buildability factors related to stirrups. The capacity needed for the procedure could be estimated to be 25% higher than the capacity needed for adding bending reinforcement of $\phi 16$ diameter.

What is the conventional design procedure for slab frame bridges today?

A large amount of the preliminary designs of commonly built bridge structures, such as the slab frame bridge, are carried out based on experience. In most cases, the preliminary design is performed using previous projects as reference. When creating a tendering proposal, rough dimensions can be obtained using old reference projects as basis. In a later stage, when the tendering is decided, a more detailed evaluation of the amounts of concrete and reinforcement is commonly carried out, as well as minor adjustments of dimensions.

Today, the final design of slab frame bridges is carried out using 3D-FEM. In some cases when such analyses are unproportional to the task, for example when working on a bridge widening, 2D-FEM can be performed instead, using the meter-strip method. Though, the meter-strip method was prohibited for new construction projects by the Swedish legislation some time ago.

Regarding the conventional production process, there are also standardized solutions of design using e.g. prefabricated reinforcement meshes for slab frame bridges, further easing the design and production procedure.

DEPARTMENT OF ARCHITECTURE AND CIVIL ENGINEERING
CHALMERS UNIVERSITY OF TECHNOLOGY
Gothenburg, Sweden
www.chalmers.se

CHALMERS
UNIVERSITY OF TECHNOLOGY